Univerzita Karlova v Praze
Přírodovědecká fakulta

Buněčná a vývojová biologie

Mgr. Tomáš Venit

Myosin 1c isoforms and their functions in the cell nucleus and in the cytoplasm

Isoformy proteínu myosin 1c a jejich funkce v buněčném jádře a v cytoplasmě

Disertační práce

Školitel: Prof. RNDr. Pavel Hozák, DrSc.

Praha, 2013

Prohlášení:

Prohlašuji, že jsem závěrečnou práci zpracoval samostatně a že jsem uvedl všechny použité informační zdroje a literaturu. Tato práce ani její podstatná část nebyla předložena k získání jiného nebo stejného akademického titulu.

V Praze, 27.03.2013

Podpis

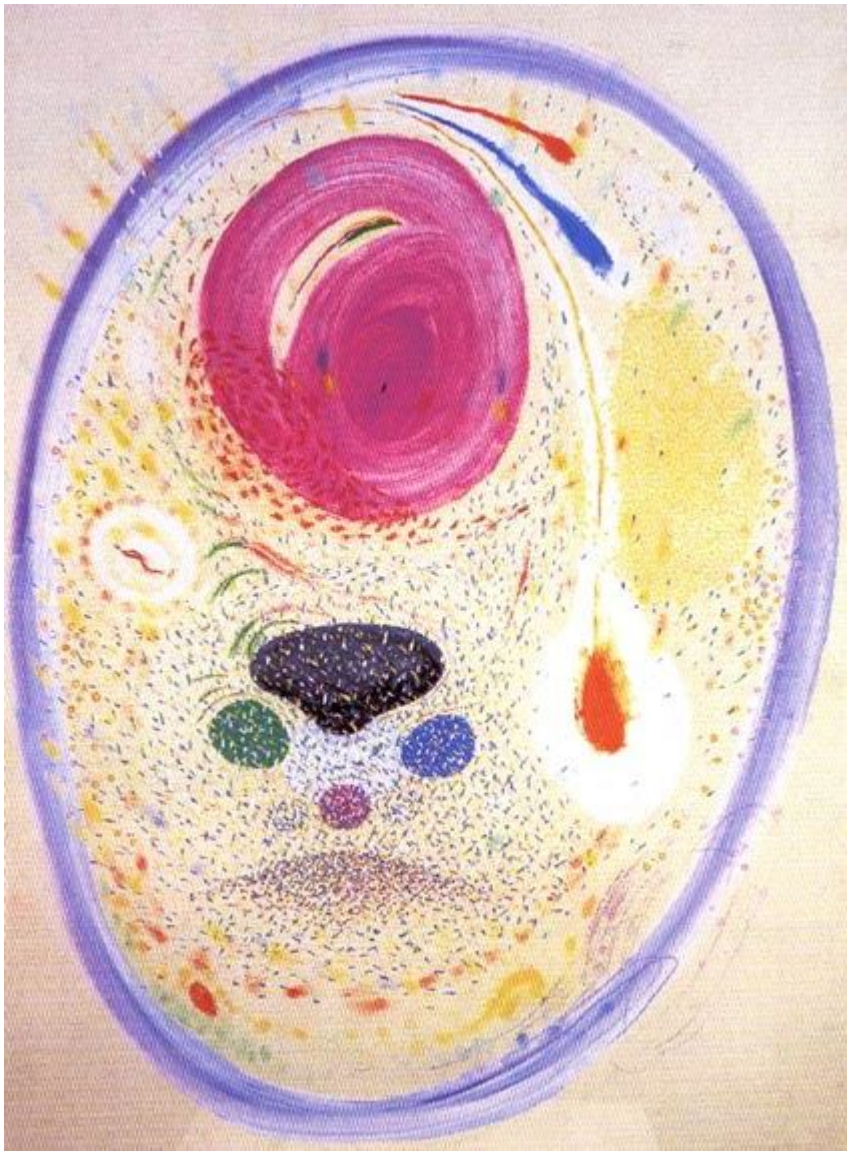

Pán Bůh připoutal člověka k zemi tím, že mu dal schopnost plodit pokračování sebe sama. Těm několika z mnohých ponechal možnost uvidět a pochopit nicotu všeho. Tuto nicotu změnil v energii, která těm, co ji spatřili a uvědomili si ji, dává možnost tvořit. V tvorbě pak na tuto nicotu chvíli zapomenou a vytvářejí svou představu o světě.

Karel Malich, 1970

Nuclear myosin I was the first myosin discovered in… I would like to thank many people who contributed to my life during last four years.

First of all, I am very thankful to my supervisor Prof. Pavel Hozák, who gave me the chance and the place to work and who taught me to be responsible for my own experiments.

My big thanks belong especially to Janka Rohožková, Betka Kalendová and Sukriye Yildirim, who were and still are nearest to my heart and mind. Nevertheless, without the LAB buffer containing a lot of 37.5% alcohol and different sugar forms, 1x Ilona, 1x Margerita, 2x Lenka, 1x Iva, 2x Pavel, 1x Martin, 1x Rasťo and other LAB compounds, I would never feel so comfortable and welcome here.

My life in Prague out of lab was highly affected by a number of people. However, the most significant effect on my functioning during the past years had Lukáš Pastorek, and I am very thankful to him for everything he has done for me.

I would like to thank again to Betka for her ENG-CZ translation activity during my "autoreferát" writing and Irina Studenyak for her proofreading activity across my dissertation.

And finally, my biggest thanks belong to my family. Although they absolutely do not know what I am doing, they always supported me in all respects.

Thank you all

Abbreviations

5´UTR, 5´untranslated region

AA, amino acid

ADP, adenosine diphosphate

ATP, adenosine triphosphate

CTD domain, C-terminal domain of RNA Polymerase II

DAG, diacylglycerol

Fib, fibrillarin

GFP, Green fluorescent protein

Glut4, Glucose transporter type 4

$InsP_3$, inositol(1,4,5)-triphosphate

KO, knock-out

Myo1c, myosin 1c

NM1, nuclear myosin 1

Pi, inorganic phosphate

PH domain, plecstrin homology domain

PIP_2, phosphatidylinositol 4,5-bisphosphate

PIPKIα, phosphatidylinositol 4-phosphate 5-kinase

PLCδ1, phospholipase C δ1

Pol I, RNA polymerase I

Pol II, RNA polymerase II

$PtdIns(4,5)P_2$, phosphatidylinositol 4,5-bisphosphate

RT-qPCR, Reverse transcriptase quantitative polymerase chain reaction

TIF-1A, transcription initiation factor I A

WSTF, Williams syndrome transcription factor

WT, wild type

Table of content

1. Abstract

Nuclear myosin 1 (NM1) was the first myosin described in the cell nucleus. From its discovery, it has been found to function in processes of Pol I and Pol II transcription, chromatin remodeling, and chromosomal movements. However, direct mechanisms of how NM1 works in the cell nucleus were still missing. We therefore decided to prepare NM1 knock-out mice to answer questions about phyiological functioning of this protein. Myo1c is an isoform of NM1 protein, previously described in the cytoplasm. The only difference between these isoforms is 16 amino-acids at the N-terminus of NM1, which were thought to be the nuclear localization signal. However, we discovered that the nuclear localization signal is located in the neck domain of myosin, and therefore it is able to direct both isoforms to the nucleus. Moreover, we found that the ratio between both proteins is nearly the same in the nucleus and deletion of NM1 does not cause compensatory overexpression of Myo1c.

NM1 KO mice are fully viable with minor changes in bone mineral density and red blood cells size. We found that the function of NM1 in processes such as Pol I transcription can be fully covered by Myo1c protein, suggesting redundancy and interchangeability of these two isoforms in the cell nucleus.

We also found that PIP_2, a phosphoinositol lipid known to bind to Myo1c in cytoplasm, works in the nucleus where it contributes to crosslinking early and late steps of Pol I transcription via its interaction with UBF, fibrillarin and NM1. Finally, we found that NM1 is predominantly localized to cytoplasm and plasma membrane, and the localization pattern highly overlaps with Myo1c. Moreover, microarray analysis from NMI KO mice revealed several genes with changed expression most of which were cytoplasmic. This suggests similar roles for nuclear myosin 1 in the cytoplasm as was described for Myosin 1c.

In conclusion, we found that two myosin isoforms are translocated to the nucleus by the same mechanism and can contribute to the same functions. We found that NM1, previously described as nuclear protein, is highly localized to the cytoplasm and plasma membrane where it contributes to similar processes as Myo1c. Finally, we showed that PIP_2, phosphoinositol lipid binding to Myo1c in the cytoplasm is able to bind both isoforms also in the nucleus and contribute to rRNA biogenesis via interaction with UBF and fibrillarin proteins.

2. Souhrn

Jaderný myosin 1 je první myosin, který byl nalezený v buněčném jádře. Účastní se procesů jako je transkripce polymerasami I a II, remodelace chromatinu a pohyby chromosomů. Dosud však nebyl popsán přesný mechanismus funkce NM1 v buněčném jádře. Proto jsme připravili myš, která má deleci v genu kódujícím NM1 (NM1 KO).
Myo1c je izoforma NM1, která byla charakterizována jako cytoplasmatická. Jediným rozdílem mezi těmito dvěma izoformami je 16 aminokyselin, které obsahuje NM1 na svém N-konci a které byly dříve považovány za jaderný lokalizační signál. Nám se ale podařilo ukázat, že obě izoformy jsou translokovány do jádra, protože jaderný lokalizační signál se nachází v krku, což je doména, která je společná pro obě izoformy. Navíc jsme ukázali, že poměr mezi oběma izoformami je v jádře i v cytoplasmě stejný a delece NM1 nezpůsobuje kompenzační expresi Myo1c.

NM1 KO myši jsou životaschopné a vykazují minoritní změny v minerální hustotě kostí a velikosti červených krvinek. Dále jsme zjistili, že Myo1c může NM1 zastoupit ve funkcích jako je transkripce polymerasou I, což naznačuje, že tyto dvě izoformy jsou v buněčném jádře zaměnitelné a duplicitní. V cytoplasmě byla popsána interakce mezi Myo1c a PIP2, lipidem ze skupiny fosfoinositolů. Ukázali jsme, že PIP2 se nachází i v jádře, kde přispívá k propojení rané a pozdní fáze transkripce polymerasou I prostřednictvím interakce s UBF, fibrillarinem a NM1. Z našich výsledků vyplývá, že NM1 je preferenčně lokalizován v cytoplasmě a na plasmatické membráně a schéma jeho lokalizace je vysoce podobné s Myo1c. Navíc, z microarray analýzy KO myší vyplývá, že většina genů ovlivněných delecí NM1 je cytoplasmických, což naznačuje, že i NM1 má funkce v cytoplasmě, které jsou podobné funkcím Myo1c.

V souhrnu, obě izoformy myosinu jsou schopny translokovat do jádra stejným mechanismem, mají stejné funkce a myši s knock-outem NM1 proteinu nemají žáden výrazný fenotyp. Dále jsme zjistili, že NM1, v předchozích pracech popsaný jako jaderný protein, se nachází především v cytoplasmě a také na plasmatické membráně, kde se účstní podobných procesů jako Myo1c. PIP2, lipid ze skupiny fosfoinositolů, který se váže na Myo1c v cytoplasmě je schopen vázat obě izoformy také v jádře a navíc přispívá ke vzniku rRNA prostřednictvím interakce s UBF a fibrillarinem.

3. Introduction

3.1 Myosins

3.1.1 Myosin superfamily

Myosins are molecular motors that convert chemical energy into mechanical work. The myosin superfamily is a large and diverse protein family, and its members are grouped to at least 24 classes based on head domain sequence similarity and domain organization (Foth et al. 2006). Myosins were found in all eukaryotes and are localized to different organs or cell types depending on their structural and functional peculiarities.

The first myosin discovered, myosin II, was isolated from muscle extracts in 1864 and belongs to the so-called “conventional” class II myosins which have long coiled-coil domains allowing formation of multimers (Hartman and Spudich 2012).

In comparison, all other myosins are referred as “unconventional”, and do not form filaments, although some can dimerize. The first unconventional myosin was isolated from *Acanthamoeba* and and because in comparison to myosin II it had only a single head domain, it was called myosin I (Pollard and Korn 1973). All other unconventional myosins and myosin classes were then numbered in order of the discovery of the founding member of the class.

Unconventional myosins were thought to be responsible for organelle trafficking on actin filaments, however there are a few myosins (for example myosin-5 in budding yeast) found to work in point-to-point transport along actin filaments(Hoepfner et al. 2001). More than molecular transporters, unconventional myosins act as tension-sensitive tethers in a wide variety of cellular processes, such as anchoring of calcium channels in hair cell stereocilia(Holt et al. 2002), organization of dynamic actin (Sokac et al. 2006), modulation of microtubule-actin interactions (Waterman-Storer et al. 2000), or regulation of transcription (Philimonenko et al. 2004).

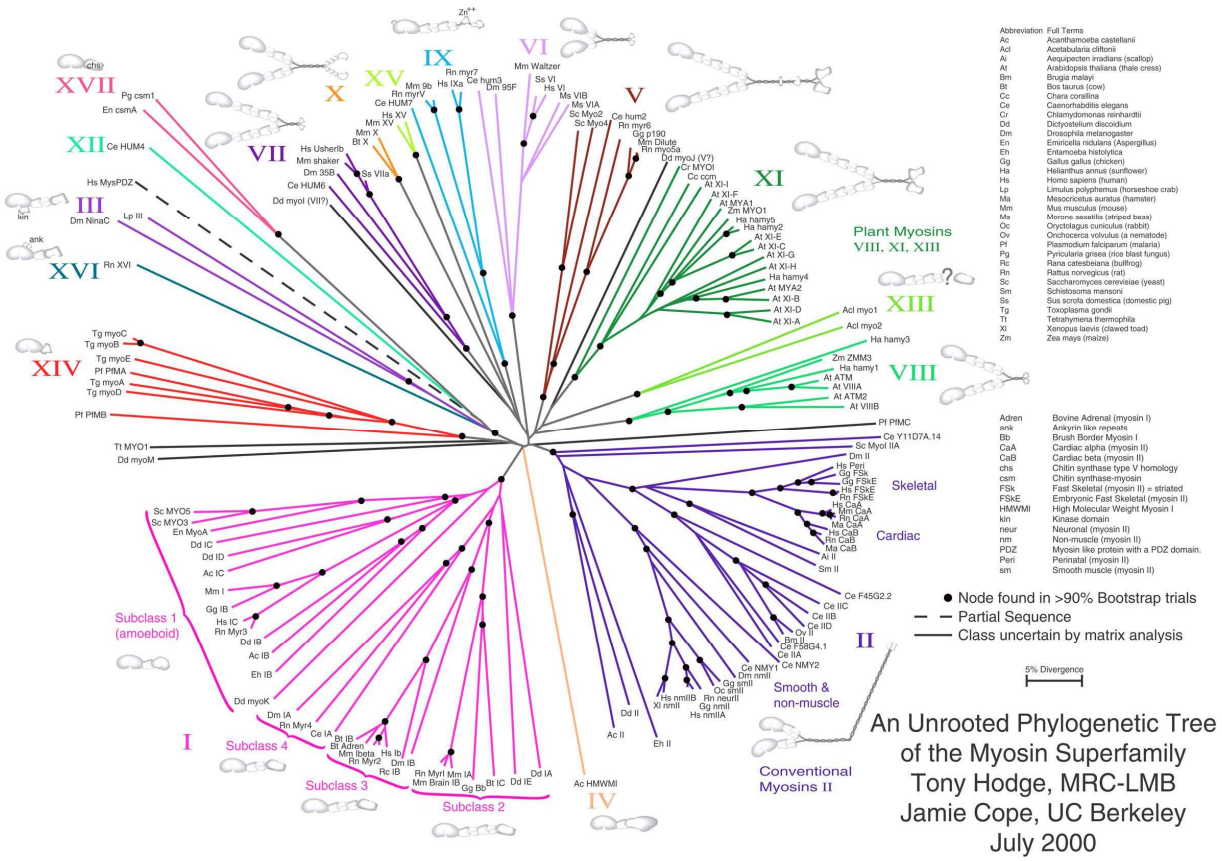

Fig. 1 Myosin superfamily

3.1.2 Myosin structure and working cycle

The typical myosins are 1000-2000 residues long and comprise of three functional subdomains: (1) head domain, which harbors an ATP binding site and actin binding site, (2) neck domain, which binds light chains or calmodulins, and (3) tail domain often containing a cargo binding domain (Syamaladevi et al. 2012), such as SH3 domains, GAP domains, FERM domains, or plecstrin homology PH domains (Sellers 2000). Whereas the catalytic head domain shares a number of highly conserved elements differing only in some surface loops and the N-terminus, the tail domain regions of various myosin classes are highly divergent (Thompson and Langford 2002). The neck domain is relatively stable, consisting of a various number (0 – 6) of helical sequences termed IQ motives with consensus sequence IQXXXRGXXXR (Cheney and Mooseker 1992).

As molecular motors, all myosins described to date are able to interact with actin, hydrolyze ATP and produce movement and/or force. Chemical energy stored in ATP is converted into mechanical movement by conformational changes within the head domain that are amplified by the neck domain, whereby the hydrolysis of ATP is promoted by the binding of filamentous actin. In the ATP-free conformation, the myosin head domain is strongly bound to actin filaments. This state is called rigor state. After binding of ATP to the ATPase site on the head domain, myosin dissociates from actin filaments. Myosin then

hydrolyzes ATP into ADP and Pi, which are still bound to the myosin, and the myosin head domain moves between two actin molecules. With the release of Pi from the ATPase catalytic site, the myosin molecule undergoes conformational change accompanied by the generation of force and movement. The next step of the cycle involves the binding of myosin to actin filaments and the release of ADP from the ATPase (active) site (Holmes and Geeves 2000).

3.1.3 Myosin 1c

Myosin 1c (Myo1c) was the first single-headed myosin isolated from mammals and was therefore called mammalian myosin I (Barylko et al. 2005; Wagner et al. 1992). Based on its similarity to partial myosin sequence from mouse cDNA library, it was later renamed to myosin 1β (Reizes et al. 1994), and finally, after the unification of myosin I nomenclature, to myosin 1c (Gillespie et al. 2001). The human MYOIC gene located on the 17th chromosome encodes three isoforms (Fig 2.). Myosin 1c isoform C is the classic 1063 amino acid "cytoplasmic" form (Wagner et al. 1992). Myosin 1c isoform B, also known as nuclear myosin 1 (NM1), includes 16 extra N-terminal amino acids arising from an upstream exon -1 (Nowak et al. 1997; Pestic-Dragovich et al. 2000). The newest isoform is myosin 1c, isoform A, which includes additional 35 amino acids at the N-terminus from an upstream exon -3 and was shown to function in the cell nucleus (Ihnatovych et al. 2012). In mice there are only two known myosin isoforms – Myo1c and NM1.

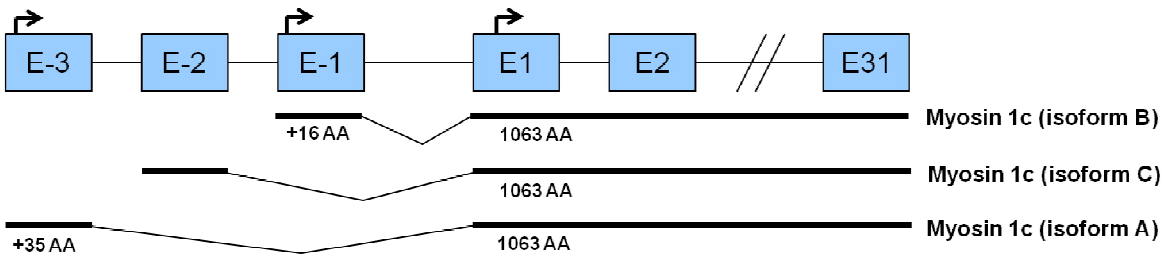

Fig. 2: Structure of human *MYO1C* gene.

3.1.3.1 Myosin 1c isoform C ("cytoplasmic" Myo1c)

Myo1c isoform C belongs to a group of molecular motors that link cellular membranes to actin cytoskeleton, and it is involved in membrane tension generation, membrane dynamics, and mechanosignal transduction. In particular, Myo1c was found to be associated with Neph1 and nephrin proteins at the podocyte cell membrane that forms the structural framework for a functional glomerular filtration barrier. Myo1c mediates localization of both proteins to plasma membrane and its depletion causes defects in tight junctions formation

and cell migration (Arif et al. 2011). In the neuronal growth cone, Myo1c affects lamellipodial motility and is responsible for the retention of lamellipodia (Wang et al. 1996) and retrograde flow (Diefenbach et al. 2002). In *Xenopus laevis*, Myo1c participates in egg activation by coupling dynamic actin to membranes of cortical granules, and this linkage is essential for their compression and retrieval. Myosin 1c is specifically up-regulated by polyadenylation during meiotic maturation and rapidly recruited to exocyting cortical granules. Myo1c depletion in eggs perturbs several events of egg activation, including compensatory endocytosis (Sokac et al. 2006). Insulin stimulates glucose transport in adipocytes by promoting exocytosis of the population of vesicles containing glucose trasporter protein GLUT4. Myo1c was found to participate in this process by facilitating exocytosis of these GLUT4-containing vesicles to the plasma membrane (Bose et al. 2002; Bose et al. 2004). Perhaps the most extensively studied function of Myo1c is in the process of hearing. Sensory cells of the inner ear detect sound and transmit signals from those stimuli to the central nervous system. When a hair bundle receives a sustained excitatory deflection, the transduction current is initially high, and then declines as transduction channels close. Depending on the size and speed of hair-bundle displacement, the adaptation to noise can be fast or slow (Gillespie and Cyr 2004). Myo1c was shown to have a direct function in these processes, since upon its inhibition the adaptation is slow and inefficient (Stauffer et al. 2005). Moreover, clinical studies revealed 6 missense mutations in Myo1c that have been associated with bilateral hearing loss (Zadro et al. 2009). All mentioned functions relate Myo1c to the plasma membrane and actin filaments. This was further demonstrated by Nambiar et al. (2009), who showed that Myo1c together with other Myosin I family members mediate membrane/cytoskeleton adhesion, and thus make major contributions to membrane tension, which is one of the main parameters in endo- and exocytosis, membrane repair, cell motility, and cell spreading (Nambiar et al. 2009).

3.1.3.2 Myosin 1c isoform B (nuclear myosin I, NM1)

Nuclear myosin I (isoform B) was accidentally discovered by testing of affinity-purified polyclonal antibodies to adrenal myosin 1. The antibody was staining a 120-kDa nuclear protein with ATPase activity, and ATP-, actin- and calmodulin- binding sites which are the typical features of unconventional myosins (Nowak et al. 1997). The mass spectrometric analysis of the immunopurified protein showed high homology to the Myo1c protein. Due to the fact that at that time, NM1 was the first myosin found in the cell nucleus, it was called nuclear myosin I (Pestic-Dragovich et al. 2000). In the nucleus, NM1 associates with nuclear actin and is required for RNA polymerase I (Pol I) and RNA polymerase II (Pol II) transcription (Pestic-Dragovich et al. 2000; Philimonenko et al. 2004). Both NM1 and actin co-localize and co-immunoprecipitate with Pol I and Pol II complexes. *In vitro*

immunodepletion of NM1 inhibits transcription by both polymerases and the addition of purified NM1 increases the level of transcription in a dose-dependent manner. While both proteins associate with Pol I, actin associates with Pol I regardless of the transcriptional state. In contrast, NM1 only associates with initiation-competent RNA polymerase I complexes through an interaction with the basal transcription factor TIF1A (Philimonenko et al. 2004). In addition to the transcription initiation, NM1 is needed in further steps during the elongation phase where it interacts with chromatin remodeling complex WSTF-SNF2h and facilitates Pol I transcription on chromatin (Percipalle et al. 2006). It is therefore believed that NM1 bound to TIF-1A is recruited to the pre-initiation complex along with Pol I and associated actin, assembling a functional transcription initiation complex. Recruitment of Pol I to the NM1-TIF-1A complex might facilitate the interaction of NM1 with actin bound to Pol I. Finally, by interacting with NM1, chromatin remodeling complexes join the initiation complex to promote Pol I movement through chromatin (Grummt 2006). This is also supported by the finding that both actin polymerization and the motor function of NM1 are required for the association with the Pol I transcription machinery and transcription activation (Ye et al. 2008). Moreover, NM1 was found to interact with RNA and RNA-protein complexes present in the nucleoplasm and in the nucleoli (Fomproix and Percipalle 2004). It participates in maturation of pre-rRNA, and accompanies rRNA transcripts to nuclear pores where NM1 decorates actin-rich pore-linked filaments (Obrdlik et al. 2010). Aside from its functions in transcription, Chuang et al. (2006) showed that the actin-NM1 complex is needed for long-range directional movement of interphase chromosome sites independently from their engagement in transcription. NM1 binds to DNA directly via its tail domain (Hofmann et al. 2006), and NM1 together with gelsolin were identified as key determinants for assembling and/or stabilization of complexes containing estrogen receptor α (ERα) and actin in the nucleus, early after receptor activation by its ligands (Ambrosino et al. 2010).

3.1.3.3 Myosin 1c isoform A

Recently, a new isoform of human myosin 1c protein - isoform A - was discovered and found to localize to the nucleus. Similar to NM1, this isoform contains a unique N-terminal peptide sequence and co-localizes with RNA polymerase in the nucleoplasm. However, unlike NM1, upon exposure to inhibitors of RNA polymerase II transcription, the newly identified isoform translocates to nuclear speckles. Furthermore, in contrast to NM1, this new isoform is absent from nucleoli and does not co-localize with RNA polymerase I (Ihnatovych et al. 2012). In mouse, Myo1c gene is transcribed to three transcript variants containing distinct 5' UTRs. Variant 1 represents the shortest transcript but encodes the longer isoform, also known as nuclear myosin I. Variants 2 and 3 encode the same isoform,

called “cytoplasmic” Myo1c. Mice therefore do not have a third protein isoform described in humans.

3.2 Lipids

3.2.1 Phosphoinositide lipids and phosphoinositide cycle

Phosphatidylinositol is a negatively charged lipid molecule, which serves as a backbone for the synthesis of other lipid molecules and is the most abundant inositol lipid in mammalian cells under normal conditions. Phosphatidylinositol can be phosphorylated to form phosphatidylinositol phosphate (PIP), phosphatidylinositol bisphosphate (PIP_2) and phosphatidylinositol trisphosphate (PIP_3). PIP, PIP_2 and PIP_3 are collectively called phosphoinositides and play important roles in lipid signaling, cell signaling and membrane trafficking. The inositol ring can be phosphorylated by different kinases on the three, four and five hydroxyl groups and then utilized back by different phosphatases to complete the cycle (Bunce et al. 2006; Martelli et al. 2005).

Phosphorylated products of phosphatidylinositol play a pivotal role in several physiological processes in the cytoplasm, ranging from signalling via the generation of the second messengers inositol (1,4,5)-triphosphate ($InsP_3$) and diacylglycerol (DAG), to the homeostasis of intracellular compartments (Di Paolo and De Camilli 2006; Toker 1998).

Over the past few decades, all components of the “classical” cytoplasmic phosphoinositide cycle have been also found in the cell nucleus, suggesting that not only similar metabolic cycle exists in the nucleus but also that it is independent from the cytoplasmic cycle (Cullen et al. 2001).

3.2.2 Nuclear lipids

The existence of nuclear lipids has been known since the 1970s. However, first direct evidence about nuclear lipid signalling was not shown until 1983, when Smith and Wells showed phosphatidylinositol kinase activity in nuclear membrane enriched fractions (Smith and Wells 1983). Later on, the purification of nuclei from Friend cells using Triton showed that phosphoinositides are made in the nucleus of the cell (Cocco et al. 1987). Moreover, stimulation of Swiss 3T3 cells by Inslulin-like-Growth Factor I resulted in a rapid decrease in the mass of polyphosphoinositol lipids within the nuclei and concomitantly results in an increase in nuclear diacylglycerol and the translocation of protein kinase C to the nuclear region. This was in contrast with the effect of compound bombesin, which has similar effect on inositol lipids in the plasma membrane, but has no impact on nuclear levels of these lipids. This suggested existence of a discrete nuclear polyphosphoinositide signalling system entirely distinct from the well-known plasma membrane located system, which is under regulatory control by cell surface-located receptors (Divecha et al. 1991). Finally Vann et al.

(1997) showed that while DAG and PtdIns are more enriched in the nuclear membrane, PtdIns(4,5)P_2 is highly localized inside of the nucleus, probably bound to nuclear proteins. Moreover, they were able to reconstitute lipid phosphorylation in membrane depleted nuclei, suggesting a predominantly intranuclear location for the respective kinases previously described in the cytoplasm (Vann et al. 1997). This was further proved by specific antibodies against phosphatidylinositol phosphate kinases (PIPKs), type I and type II isoforms, which showed predominant localisation of these PIPKs in nuclear speckles with components of small nuclear ribonucleoprotein particles (snRNPs). Moreover, a small pool of PtdIns(4,5)P_2, the product of these kinases, has also been observed at the same sites by monoclonal antibody staining (Boronenkov et al. 1998).

3.2.3 Nuclear functions of PtdIns(4,5)P_2

In the cytoplasm, despite its function as a second messenger, PtdIns(4,5)P_2 has been shown to bind to the plekstrin homology domain (Harlan et al. 1994) and the phosphotyrosine-binding domain of different proteins (Zhou et al. 1995), as well as to actin-binding proteins. Therefore a lot of attention has been paid to the immunoprecipitation of PIP_2 with nuclear extracts to identify potential interacting partners and functions of this lipid in the cell nucleus.

Some lipids, such as PtdIns, phosphatidic acid or cardiolipin, have been suggested to modify the activity of DNA polymerase and topoisomerase I (Yoshida et al. 1989), and phosphatidylglycerol or cardiolipin have been reported to influence RNA transcription (Hirai et al. 1992). Moreover, PtdIns(4,5)P_2 binds to histones H1 and H3, and the binding to H1 counteracts histone H1-mediated repression of basal transcription by RNA Pol II in *Drosophila* (Yu et al. 1998). Thus, the regulation of nuclear phosphatidylinositol 4-phosphate 5-kinase results in the regulation of the levels of PtdIns(4,5)P_2, which in turn has an effect on the rate of basal transcription (Cheng and Shearn 2004).

During lymphocyte activation, the chromatin structure undergoes visible changes. PtdIns(4,5)P_2 is one of the key players in signal transduction from a membrane receptor to the nucleus, resulting in SWI/SNF-like BAF remodeling complex rapidly binding to chromatin. Purification and sequencing of the BAF complex revealed β-actin and a novel actin-related protein, BAF53, to be required for maximal association of the BAF complex to chromatin (Zhao et al. 1998) and PIP_2 enhances this actin filament binding by the BAF complex (Rando et al. 2002).

Certain pool of nuclear PtdIns(4,5)P_2 is associated with cell-cycle dependent interchromatin granules. Elements of the transcriptional and pre-mRNA processing machinery interact with this pool of PIP_2, and these interactions are essential for pre-mRNA

splicing. It was therefore suggested that PtdIns(4,5)P_2 is a component of pre-mRNA processing machinery (Osborne et al. 2001).

Interestingly, Doughman et al. (2003) showed that phosphatidylinositol 4-phosphate 5-kinase (PIPKIα) regulates cellular functions of PIP_2 through the interaction with PIP_2 protein partners, or effectors, that target PIPKIα to discrete subcellular compartments, resulting in the spatial and temporal generation of PtdIns(4,5)P_2 required for the regulation of specific signaling pathways (Doughman et al. 2003). In this manner, PIPKIα interacts with non-canonical poly(A) polymerase Star-PAP at nuclear speckles. Star-PAP polymerase is specifically regulated by PtdIns(4,5)P_2 produced by PIPKIα, and therefore PIPKIα kinase and Star-PAP polymerase function together in a complex to control the expression of selected mRNAs (Mellman et al. 2008).

3.2.4 PIP2 and myosins

PtdIns(4,5)P_2 is a negatively charged phospholipid which has been shown to modulate the functions of different cytoplasmic proteins as ADP-ribosylation factor 1 (Randazzo and Kahn 1994), protein kinase C (Huang and Huang 1991), and phospholipase D (Liscovitch et al. 1994). Moreover, it also binds to actin-binding proteins such as cofilin (Yonezawa et al. 1991), gelsolin (Janmey and Stossel 1987), α-actinin or vinculin (Fukami et al. 1992).

Myosin 1c, another actin-binding protein, is known to faciliate the translocation of membrane proteins, such as glucose transporters in adipocytes. Moreover Myo1c highly colocalizes with plasma membrane which suggest direct or indirect binding to the membrane. Like other myosin 1 members, the Myo1c tail domain is rich in basic amino-acid residues suggesting that it can bind to negatively charged phospholipids by this part of the molecule (Reizes et al. 1994). This idea was supported by the finding that myosin 1 from *Acanthamoeba* is bound to membrane lipids via its basic tail domain (Adams and Pollard 1989). However, measuring of the effectiveness of Myo1c binding to different lipids revealed that PIP_2 is a dominant and specific lipid isoform tightly bound to Myo1c (Hokanson and Ostap 2006). Finally, the putative plekstrin homology domain found within the Myo1c tail domain was shown to be responsible for direct binding to PIP_2 (Hokanson et al. 2006) as had been shown for other proteins previously (Harlan et al. 1994).

NM1 differing from Myo1c only at N-terminus, but having a conserved tail domain, should bind PIP_2 either in the cytomplasm or the nucleus.However, the binding properties of NM1 to PIP_2 have not been described yet.

4. Motivation and aims

Nuclear myosin I is a nuclear isoform of the well-known “cytoplasmic” Myosin 1c protein, which results from alternative splicing and an alternative start of transcription of the *MYO1C* gene adding an extra 16 amino-acids at the N-terminus. 15 years of intense research revealed NM1 to be involved in RNA Pol I and RNA Pol II transcription, chromatin remodeling, and chromosomal movements. However, no nuclear localisation signal or nuclear export/import mechanisms have been discovered. Naturally, one could predict that these 16 AA are responsible for translocation of NM1 into the nucleus. Moreover, both Myo1c and NM1 proteins were shown to be expressed in a wide variety of tissues and cultured cell lines. Their expression pattern is similar but not completely overlapping, which suggested possible tissue-specific functions for both proteins (Dzijak et al. 2012; Kahle et al. 2007; Wagner et al. 1992). However, solid data supporting these hypotheses were missing. Unfortunately, no NM1 knock-out mouse answering this question has been prepared to date. And least but not last, despite the evidence that NM1 is involved in the control of transcription, the molecular mechanism is unknown. Its structural similarity to the “cytoplasmic” Myo1c suggests its direct binding to acidic phospholipids, but the function of these lipids in the nucleus is not entirely known.

This thesis has therefore following specific aims:

Which NM1 domain is responsible for nuclear localization of the protein, and what is the mechanism?

What is the phenotype of NM1 KO mice? Does NM1 have tissue-specific functions?

What are the binding properties, localization and function of PIP_2 in the cell nucleus during Pol I transcription?

Does NM1 function in some other non-nuclear processes?

5. Research papers

Specific nuclear localizing sequence directs two myosin isoforms to the cell nucleus in calmodulin-sensitive manner.

Dzijak R, Yildirim S, Kahle M, Novák P, Hnilicová J, Venit T, Hozák P.

PLOS ONE. 2012;7(1):e30529. doi: 10.1371/journal.pone.0030529. Epub 2012 Jan 25.

IF: 4,092 (2011)

Involvement of PIP2 in RNA Polymerase I transcription

Yildirim S, Castano E, Sobol M, Philimonenko VV, Dzijak R, Venit T, Hozák P

Journal of Cell Science, 2013, in press
IF: 6,11 (2011)

Mouse nuclear myosin I knock-out shows interchangeability and redundancy of myosin isoforms in the cell nucleus

Venit T, Dzijak R, Kalendová A, Kahle M, Rohožková J, Schmidt V, Rülicke T, Rathkolb B, Hans W, Bohla A, Eickelberg O, Stoeger T, Wolf E, Yildirim AÖ, Gailus-Durner V, Fuchs H, Hrabě de Angelis M, Hozák P

PLOS ONE, 2013, in press
IF: 4,092 (2011)

Cytoplasmic functions for nuclear myosin I

Kalendová A and Venit T, Dzijak R, Rohožková J, Petr M, Hozák P

Manuscript

5.1 Specific nuclear localizing sequence directs two myosin isoforms to the cell nucleus in calmodulin-sensitive manner.

Dzijak R, Yildirim S, Kahle M, Novák P, Hnilicová J, Venit T, Hozák P.

PLOS ONE. 2012;7(1):e30529. doi: 10.1371/journal.pone.0030529. Epub 2012 Jan 25.

IF: 4,092 (2011)

My contribution to this work:

Preparation and handling of mice and mice cell lines, mice necroscopy and excision of mice organs

OPEN ACCESS Freely available online

PLoS one

Specific Nuclear Localizing Sequence Directs Two Myosin Isoforms to the Cell Nucleus in Calmodulin-Sensitive Manner

Rastislav Dzijak[1], Sukriye Yildirim[1], Michal Kahle[1], Petr Novák[2], Jarmila Hnilicová[1], Tomáš Venit[1], Pavel Hozák[1]*

1 Department of Biology of the Cell Nucleus, Institute of Molecular Genetics of the ASCR, v.v.i., Prague, Czech Republic, **2** Laboratory of Molecular Structure Characterization, Institute of Microbiology of the ASCR, v.v.i., Prague, Czech Republic

Abstract

Background: Nuclear myosin I (NM1) was the first molecular motor identified in the cell nucleus. Together with nuclear actin, they participate in crucial nuclear events such as transcription, chromatin movements, and chromatin remodeling. NM1 is an isoform of myosin 1c (Myo1c) that was identified earlier and is known to act in the cytoplasm. NM1 differs from the ''cytoplasmic'' myosin 1c only by additional 16 amino acids at the N-terminus of the molecule. This amino acid stretch was therefore suggested to direct NM1 into the nucleus.

Methodology/Principal Findings: We investigated the mechanism of nuclear import of NM1 in detail. Using over-expressed GFP chimeras encoding for truncated NM1 mutants, we identified a specific sequence that is necessary for its import to the nucleus. This novel nuclear localization sequence is placed within calmodulin-binding motif of NM1, thus it is present also in the Myo1c. We confirmed the presence of both isoforms in the nucleus by transfection of tagged NM1 and Myo1c constructs into cultured cells, and also by showing the presence of the endogenous Myo1c in purified nuclei of cells derived from knock-out mice lacking NM1. Using pull-down and co-immunoprecipitation assays we identified importin beta, importin 5 and importin 7 as nuclear transport receptors that bind NM1. Since the NLS sequence of NM1 lies within the region that also binds calmodulin we tested the influence of calmodulin on the localization of NM1. The presence of elevated levels of calmodulin interfered with nuclear localization of tagged NM1.

Conclusions/Significance: We have shown that the novel specific NLS brings to the cell nucleus not only the ''nuclear'' isoform of myosin I (NM1 protein) but also its ''cytoplasmic'' isoform (Myo1c protein). This opens a new field for exploring functions of this molecular motor in nuclear processes, and for exploring the signals between cytoplasm and the nucleus.

Citation: Dzijak R, Yildirim S, Kahle M, Novák P, Hnilicová J, et al. (2012) Specific Nuclear Localizing Sequence Directs Two Myosin Isoforms to the Cell Nucleus in Calmodulin-Sensitive Manner. PLoS ONE 7(1): e30529. doi:10.1371/journal.pone.0030529

Editor: Joanna Mary Bridger, Brunel University, United Kingdom

Received May 20, 2011; **Accepted** December 23, 2011; **Published** January 25, 2012

Funding: This study was supported by Grant Agency of the Czech Republic (http://www.gacr.cz Reg. Nos. 204/07/1592, 204/09/H084 and P305/11/2232), Ministry of Education, Youth and Sports of the Czech Republic (http://www.msmt.cz/index.php?lang=2 Reg. Nos. LC 545 and LC06063). Institutional research plan Reg. No. AV0Z50520514, was funded by Academy of Sciences of the Czech Republic (http://www.isvav.cz/researchPlanDetail.do?rowId=AV0Z50520514). Dr. Dzijak was supported by the Boehringer Ingelheim Fonds travel grant (http://www.bifonds.de). The funders had no role in study design, data collection and analysis, decision to publish, or preparation of the manuscript.

Competing Interests: The authors have declared that no competing interests exist.

* E-mail: hozak@img.cas.cz

Introduction

Nuclear myosin I (NM1) was the first unconventional myosin motor detected in the cell nucleus [1]. NM1 is an isoform of earlier identified cytoplasmic myosin Ic (Myo1c) containing additional 16 amino acids at the N-terminus. The mRNA of NM1 is differently spliced yielding 5′ introduction of exon containing alternative start of translation [2]. Importantly, the ubiquitous expression and nuclear localization of NM1 in mouse organs along with high degree of conservation of the N-terminal sequence across species has been confirmed [3,4].

This corresponds to its important functions. In the nucleus, there is ample evidence for functional involvement of NM1 in transcription by RNA polymerase I and II (Pol I and Pol II). NM1 co-localizes with both polymerases at the sites of transcription [2,5] and physically associates with both Pol I and Pol II complexes [6,7]. In-vivo rate of transcription is negatively affected by NM1 overexpression, and inhibited by NM1 knock-down and nuclear microinjections of anti-NM1 antibodies [7]. In an in-vitro transcription system, anti-NM1 antibodies inhibit transcription by both polymerases in a dose-dependent manner, whereas adding purified NM1 increases transcription [2,6,8]. Transcription initiation assays have revealed that NM1 exerts its function in early steps of Pol I and II transcription after the formation of pre-initiation complexes [6,7]. Indeed, NM1 interacts with Pol I transcription factor TIF-IA, which is present only in initiation-competent fraction of Pol I complexes [9], and actin that is associated with RNA polymerase I independently of active transcription [7]. According to Grummt [10], the binding of NM1 to Pol I via actin may help to initiate transcription by

recruiting TIF-IA to pre-initiation complex. This model is further supported by the fact that functional motor domain is needed for interaction of NM1 and Pol I [11]. In addition to transcription initiation, NM1 is also involved in Pol I transcription elongation since it associates with the chromatin remodeling complex WSTF-SNF2h and might therefore recruit this complex to the actively transcribing genes [12].

Interestingly, nascent ribosomal particles seem to be accompanied by NM1 during transport from nucleolus toward nuclear pores [13] and blocking of NM1 or actin by antibodies results in nuclear retention of small ribosomal subunits [14,15].

A role of acto-myosin motor in repositioning of chromosomes is emerging [16,17]. In pioneering work, Chuang and co-workers [18] showed that labeled artificial gene loci move, upon activation, toward the center of nucleus and that overexpression of mutated NM1 that lacks motor activity inhibits this effect. However, the exact mechanism behind these translocation phenomena is not clear.

Using specific antibodies generated against its N-terminal epitope, NM1 can be detected predominantly in the nucleus, nucleolus and at the plasma membrane of interphase cells [1,5,19]. NM1 is a short-tailed class I myosin that binds directly to actin via its head domain and the headgroups of acidic phospholipids via putative PH domain within positively charged tail [20]. Neck domain, located between head and tail, contains three IQ motifs that bind calmodulin [1]. To date, there are no data about biochemical characteristics of this protein. Because NM1 is almost identical to Myo1c, one can expect that its basic function is to maintain tensions as proposed for Myo1c [21] however, the exact function of the N-terminal extension in NM1 molecule that makes the only known difference form Myo1c is uncertain. The observation that NM1 is localized mainly in the nucleus and Myo1c at the plasma membrane has led to the opinion that the N-terminus could function as a nuclear targeting or nuclear sequestering sequence [2].

In this paper we identify the domains that direct the nuclear translocation of NM1 and decipher the mechanism of intracellular trafficking of NM1. We demonstrate that the N-terminal extension of NM1does not act as a nuclear localization sequence (NLS); instead, we identified a novel NLS within the the neck region of NM1 as crucial for nuclear import. In search for the possible import receptors of NM1 we found importin 5, importin-β1, importin 7 and Heat shock protein 90 (HSP90) to associate with truncated constructs as well as with the endogenous NM1. Since the identified NLS sequence is also present in the Myo1c protein we also investigated the localization of Myo1c. Using various experiments including the NM1 knockout mice derived cells we discovered the "cytoplasmic" Myo1c was also present in nuclei. This adds the traditional "cytoplasmic" Myo1c to the few molecular motors of the nucleus with potentially important functions in nuclear metabolism.

Results

NM1 is transported to the nucleus after mitosis

To study the dynamics of NM1 compartmentalization during cell cycle we followed the localization pattern of the endogenous NM1 during and after mitosis. Immunofluorescent labeling of NM1 in unsynchronized U2OS (Fig. 1A) and in NIH 3T3 (Fig. 1B) cells synchronized by mitotic shake off has shown that NM1 did not stay bound to chromatin during the mitosis and that its majority was released into the cytoplasm after the nuclear envelope breakdown in prophase (Fig. 1B). Soon after the reconstitution of nuclear envelope in early G1, most of NM1 was in the cytoplasm as shown in Fig. 1A and 1B (Early G1). In unsynchronized population of cells, this pattern was very rarely observed, and the vast majority of cells had clearly nuclear staining of NM1 (Fig. 1A, Interphase). This demonstrates that nuclear import of endogenous NM1 is accomplished in G1 phase.

To begin identifying import signals in NM1, we first tested the localization of full length NM1 constructs fused to different tags. Untagged overexpressed mouse and human NM1 localized predominantly in the nucleus in 80% of cells, and V5/His-tagged NM1 was predominantly nuclear in 50%, whereas EGFP-tagged or FLAG-tagged NM1 was predominantly nuclear in less than 20% of cells (data not shown). Further studies used the V5/His-tag because it interfered with nuclear import the least.

To visualize the timing of V5/His-tagged NM1 (NM1-V5/His) transport into the nucleus after mitosis, we transfected U2OS cells and the next day added either nocodazole (depolymerizes microtubules) or aphidicolin (DNA polymerase inhibitor) for 16 hours to accumulate cells in M-phase or S-phase respectively, then washed out the inhibitor and used indirect immunofluorescence to localize NM1-V5/His at different times after release from the block (Fig. 1C,D). Nocodazole-treated (metaphase-enriched) cells continued with mitosis after washout. The lowest nuclear levels of tagged NM1 were seen at 2 and 4 hours after release, but increased gradually at 6–10 hours after release (Fig. 1C). After release from aphidicolin, cells maintained high nuclear levels of NM1-V5/His for ~11 hours, consistent with the expected time needed to complete S-phase and enter G2 (Fig. 1D). The lowest levels of nuclear NM1-V5/His were detected 17 hours after release from aphidicolin (Fig. 1D), when many cells were in mitosis or early G1. Together these results suggested both endogenous and tagged NM1 are released from the nucleus during mitosis. Endogenous NM1 is transported into renewed nuclei shortly after the nuclear envelope reconstitution in the early G1, while nuclear import of the ectopically expressed NM1 with a tag is slower.

First two IQ domains are needed for nuclear transport of NM1

Because the N-terminal part of NM1 was suggested to be crucial for nuclear localization [2], we prepared various deletion and truncation mutants of the NM1 in fusion with V5/His at its C-terminus. We compared their localization in U2OS cells with the full length NM1-V5 which was detected in the cytoplasm and faintly in the nucleus (Fig. 2A, anti-V5). Surprisingly, the deletion of the neck and the tail domain led to the cytoplasmic retention of the mutant (Fig. 2B). This suggested that the NLS sequence is located within the neck or in the tail domains. After deletion of the head domain, we observed enhanced nuclear signal with short C-terminal V5/His (not shown) as well as with the bulky N-terminal EGFP tag (Fig. 2C). This suggested that the EGFP-fused myosin neck-tail fragment is imported efficiently. Further deletion of half of the tail disrupted the plasma membrane association of the protein but not its nuclear translocation (Fig. 2D). The tail together with the third IQ domain of the neck stayed out of the nucleus and associated with plasma membrane (Fig. 2E) while the construct with first two IQ domains was located exclusively to the nucleus and nucleoli (Fig. 2F). This localized a putative nuclear localizing sequence within the first two IQ domains of NM1 neck residues 712–770.

The second IQ domain contains a novel NLS sequence

To pinpoint the exact part of the neck needed for nuclear translocation, we prepared a set of fusion constructs containing GFP and the cytosolic pyruvate kinase (PK) enzyme [22]. We used PK to enlarge the proteins so that they would not diffuse passively

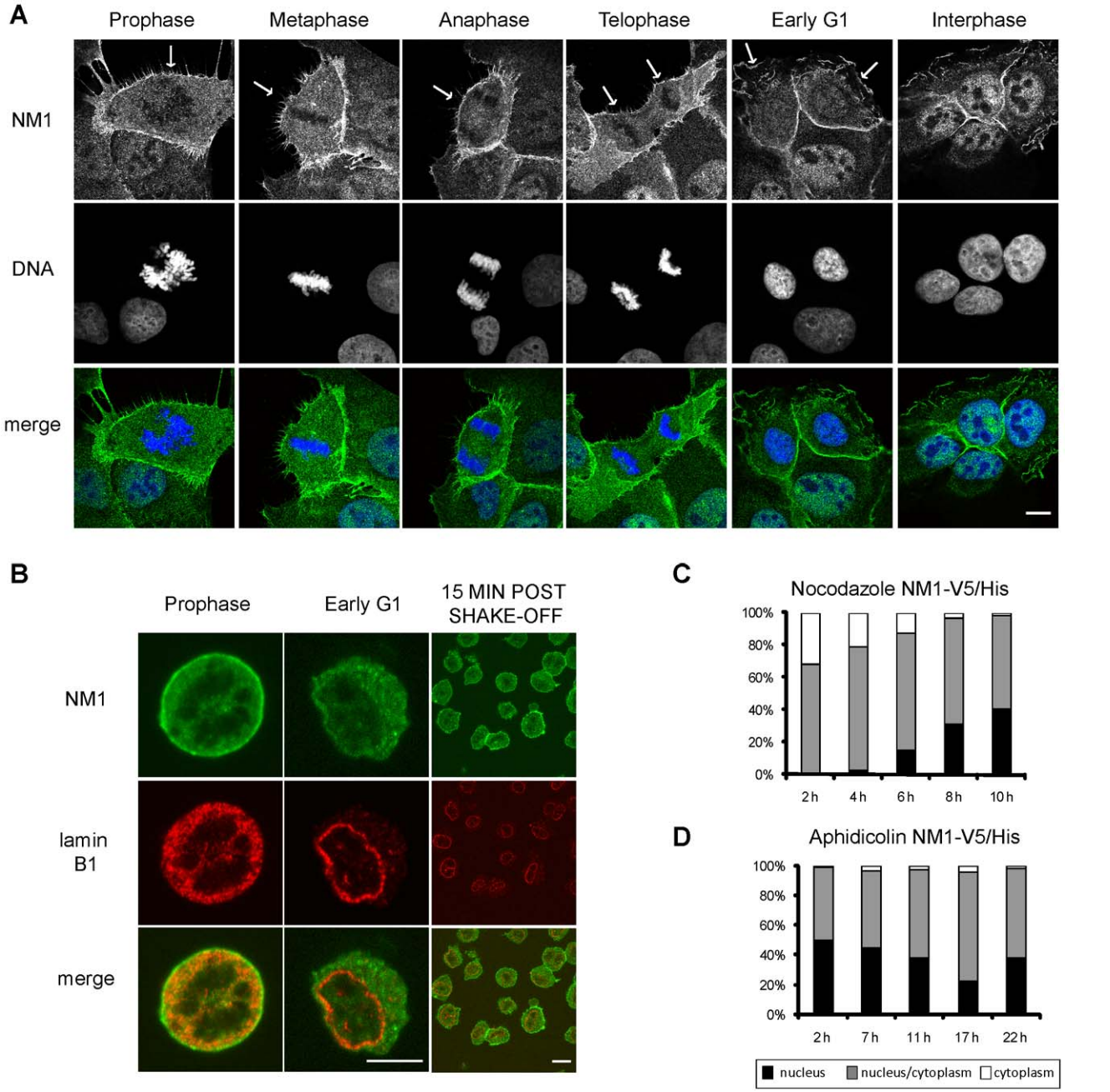

Figure 1. Localization NM1 during mitosis. (**A**) Unsynchronized U2OS cells were fixed and labeled with antibody to NM1. Localization of NM1 is shown at various stages of mitosis. DNA was visualized by DAPI. (**B**) Mitotic NIH 3T3 cell were seeded onto the poly-L-lysine coated coverslips, fixed and labeled with antibodies to NM1 and Lamin B1. Cells fixed immediately after seeding (**Prophase**) and 15 min after seeding (**Early G1, 15 min post shake-off**). Nuclear lamina was reconstituted in Early G1 as visualized by Lamin B1 labeling. All immunofluorescence pictures were obtained using confocal microscope, single confocal sections are shown. Scale bar: 10 μm. U2OS cells were transiently transfected with NM1-V5/His. 24 hours after transfection cells were treated with nocodazole (**C**) or aphidicolin (**D**), to stall the cells either in G2/M or in G1/S phase of cell cycle. After the release from the block cells were cultivated for another 24 hours. Samples were taken in indicated time points. Cells were labeled with antibody to V5 tag, patterns counted and divided into three groups according to the localization of fluorescent proteins. More than 100 cells were counted in each time point, experiment was repeated twice with similar result.
doi:10.1371/journal.pone.0030529.g001

to the nucleus as GFP alone would [23]. The 87 kDa GFP-PK fusion construct was located solely to the cytoplasm (Fig. 2G). When the sequence of the first two IQ domains was added to GFP-PK strong nuclear and nucleolar signal was observed (Fig. 2H). Next, we examined the capability of each IQ domain to drive the nuclear transport (Fig. 2I, J). Nuclear accumulation was specifically driven by the second IQ motif (Fig. 2J), not the first IQ motif (Fig. 2I). The IQ2 motif and its c-terminal flanking sequence contains two clusters of basic amino acids. Next, we preserved only the basic amino acid clusters with the intermitting non-polar amino acids, resulting in 13 amino acid peptide, ^{754}GRRKAAKRKWAAQ^{766}. This sequence was sufficient for

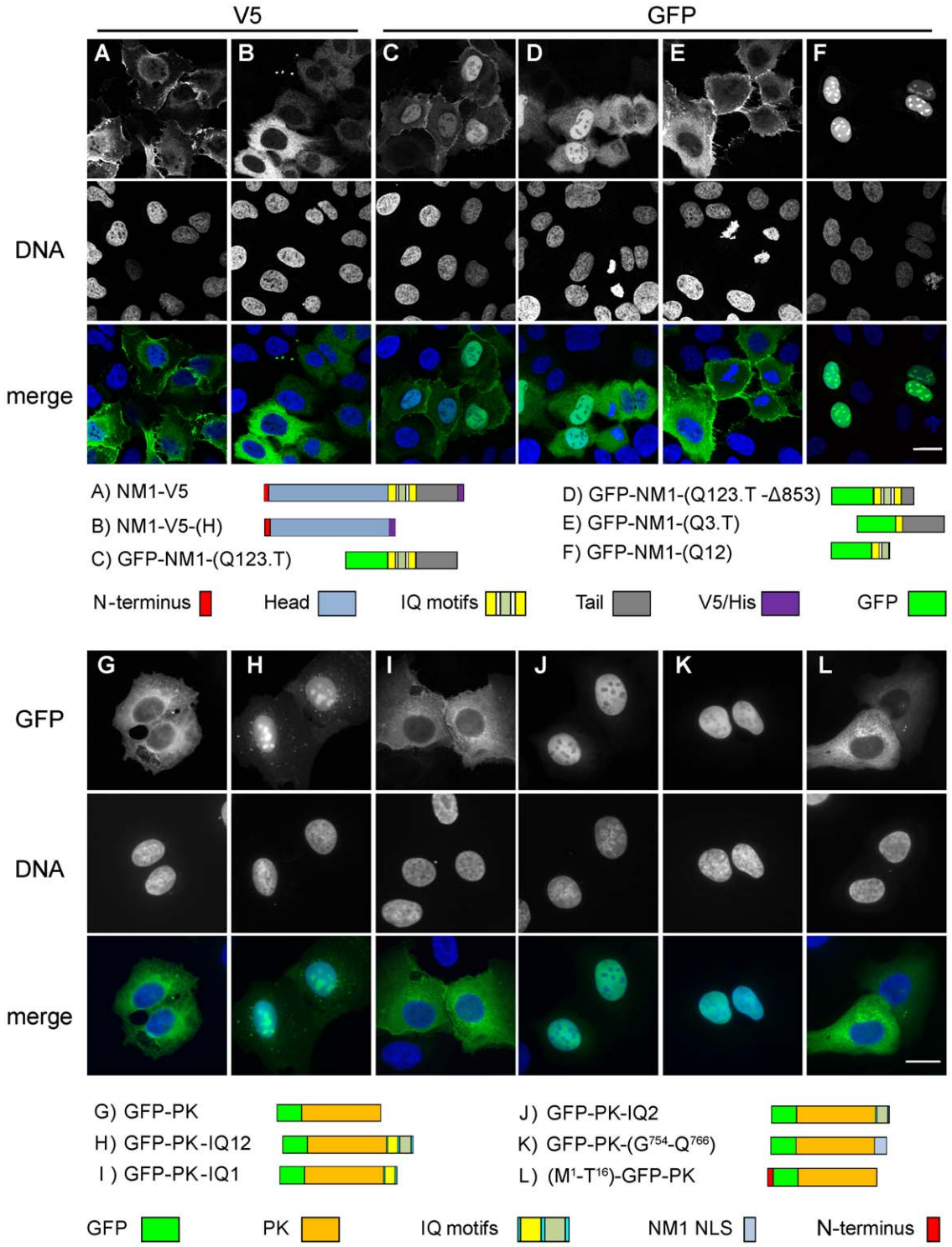

Figure 2. Neck domain of NM1 contains the NLS. U2OS cell transfected with a panel of truncation constructs of full length NM1 (**A–F**) and IQ domains fused to GFP-PK (**G–L**). Cells were fixed 48 hours post transfection. Below the pictures are schematic representations of the truncations affecting various NM1 domains as well as the GFP-PK phusions. Pictures (**A–F**) were acquired using confocal microscope, single confocal planes are shown. Pictures (**G–L**) were photographed using wide-field fluorescent microscope. Scale bar: 10 μm.
doi:10.1371/journal.pone.0030529.g002

nuclear translocation (Fig. 2K). On the other hand, the N-terminal 16 amino acids from NM1, fused to the N-terminus of the GFP-PK construct, did not localize to the nucleus at all (Fig. 2L). To rule out the possibility that it serves as a nuclear retention signal, we fused the N-terminal sequence to EGFP that diffuses freely into nucleus. We did not observe nuclear enrichment of the signal that would be caused by an interaction of the protein inside the nucleus (not shown). In contrast to the full length NM1 (Fig. 3A), a C-

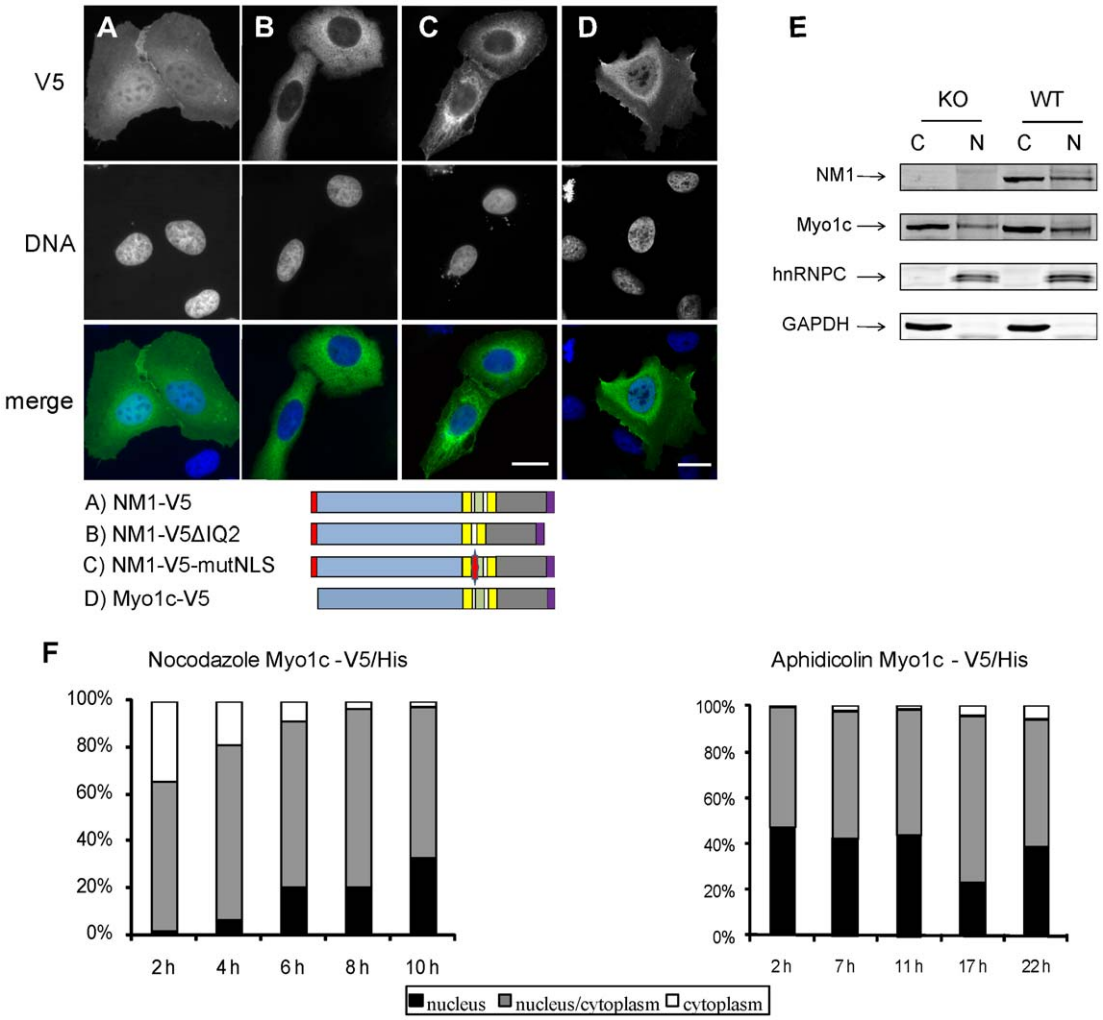

Figure 3. Mutation of basic residues in the neck of NM1/Myo1c abolishes its nuclear import. U2OS cells were transfected with full length NM1-V5/His (**A**), NM1-V5/His lacking the second IQ motif (**B**), and NM1-V5/His with point mutation of basic amino acids within the NLS into alanines (**C**). Below the pictures are schematic representations of constructs used. Color coding is the same as in **Fig. 2**. Cells were fixed 48 hours post transfection and labeled with anti-V5 antibody, pictures were obtained using wide-field microscope, scale bar: 10 μm (**D**) U2OS cells transiently transfected with Myo1c-V5/His show nuclear localization of the protein Picture is a single confocal plane, obtained by confocal microscope. Scale bar: 10 μm. (**E**) Nuclear and cytosolic extracts were prepared from liver of either wild type (WT) or NM1 knock-out (KO) mice. Equal amount of protein was resolved using SDS-PAGE and electro-transferred to nitrocellulose. Membrane was probed with anti-NM1, anti-Myo1c, anti hnRNP C1/C2 and GAPDH antibody. Signal was detected using LI-COR Odyssey infrared imaging system. (**F**) U2OS cells were transiently transfected with Myo1c-V5/His. 24 hours after transfection cells were treated with nocodazole or aphidicolin to stall the cells either in G2/M or in G1/S phase of cell cycle. After the release from the block cells were cultivated for another 24 hours. Samples were taken in indicated timepoints. Cells were labeled with antibody to V5 tag, patterns counted and divided into three groups according to the localization of fluorescent proteins. More than 100 cells were counted in each timepoint, expreriment was repeated twice with similar result.
doi:10.1371/journal.pone.0030529.g003

terminally fused NM1 construct lacking the residues 739–762 accumulated in the cytoplasm of U2OS cells (Fig. 3B), supporting an important role for the second IQ. No single K/R-to-A substitution in residues 754–766 was able to disrupt the NLS activity (data not shown). However mutating all 6 basic residues to Ala completely abolished nuclear import (Fig. 3C; NM1-V5-mutNLS). NLS Database [24] and literature searches revealed no known NLS homologous to that of NM1. We therefore conclude that NM1 and cytoplasmic Myo1c share a novel type of NLS.

Myo1c is able to translocate into the nucleus

N-terminus of NM1 alone did not possess a nuclear localization potential and the NLS was located in region shared by both the NM1 and Myo1c. We therefore inspected the localization of Myo1c under overexpressed condition. V5/His tagged Myo1c was localized to the nuclei of transfected U2OS cells (Fig. 3D). The nuclear localization of Myo1c-V5/His in nocodazole- or aphidicolin-treated cells was also cell cycle dependent, with profiles (Fig. 3F) similar to that of cells that overexpressed NM1 (Fig. 1F).

To test the influence of the N-terminal 16 amino acids on NM1 functions we prepared knock-out mice lacking the exon-1 that contains the NM1 start codon (Venit et al, in preparation). Resulting mRNA contains only the downstream start of translation which gives rise to Myo1c protein. We used purified liver nuclei from NM1 knock-out mice to confirm that the N-terminus is not required for nuclear transport of endogenous NM1. Fig. 3E shows the presence of Myo1c in the purified liver nuclei from NM1 knock-out mice visualized by antibody to the C-terminus of NM1/

Myo1c. Weak signal of GAPDH indicates negligible contamination of nuclei with cytosol, while signal of hnRNP C1/C2 shows marked enrichment of nuclear proteins compared to cytosolic liver extract. This shows that both NM1 and Myo1c have the ability to enter the nucleus. Further, we have observed the co-localization of NM1 and myo1c in a single cell. However, we were not able to co-localize NM1 and myo1c in nuclei of untransfected cells using the polyclonal antibody directed to the tail region of NM1/Myo1c (R2652) [25] since it failed to label endogenous epitopes within nuclear environment. Therefore, U2OS cells were cotransfected with FLAG tagged NM1 and V5/His tagged Myo1c. Fig. 4A shows a cell expressing both proteins. Myo1c and NM1 co-localized at the plasma membrane (arrows) and in the nucleus. Interestingly, R2652 antibody revealed the signal in nucleus and nucleolus when myo1c was overexpressed Fig. 4B.

Importins bind the NM1 neck region

The transport of nuclear proteins through nuclear pores is often facilitated by importins that recognize their NLS in cytoplasm [24]. To discriminate between cytoplasmic and nucleus/plasma membrane-associated myosin, cells were extracted with buffers containing digitonin that is known to extract cytosolic myosin 1c [26]. We sought to identify the transport receptors that bind NM1/Myo1c NLS. Using pull down assay with recombinant IQ12 as the bait we identified importin 5 (IPO5) and Heat shock protein 90 beta (HSP90) as the proteins that associate with IQ12 in the cytoplasm of HeLa cells (Fig. 5A). To verify the obtained result by another method, we looked for interacting partners of GFP-NM1-(Q123.T) in HEK-293T cells. Mass spectrometry analysis of bands that co-purify specifically with GFP-NM1-(Q123.T) but not with the control Str-GFP contruct, revealed importin 5, importin 7 (IPO7), importin-β1 (KPNB1) and HSP90 beta (Fig. 5B). Additional bands that were present on the gel were not identified. To verify that the importin 5, importin 7 and importin-β1, which were found to bind the truncated constructs, recognize also the endogenous protein, we performed co-immunoprecipitation with a polyclonal antibody directed to N-terminus of NM1. Since most of endogenous NM1 molecules potentially accessible to importins are located in cytosol of the G1 cells (Fig. 1A), we synchronized the HeLa cells with nocodazole and harvested them 3 hours after nocodazole wash-out. As shown by western blot (Fig. 5C), endogenous NM1 specifically binds to importin 5 (IPO5), importin 7 (IPO7), and importin-β1 (KPNB1) in digitonin extracts of the G1 cells.

Next, to confirm that importin 5 binds specifically to NM1 NLS via the interaction with positively charged amino acids, we compared the proteins that co-purify with headless NM1 with wild type NLS (GFP-NM1-(Q123.T) ^{NLSwt}) and headless NM1 with all basic residues in the NLS mutated to alanines (GFP-NM1-(Q123.T) ^{NLSmut}) from electroporated HEK293T cells. Fig. 5D shows that importin 5 interacts only with GFP-NM1-(Q123.T) ^{NLSwt} and that this interaction occurs in digitonin extract in contrast to triton X-100 that liberates the plasma membrane bound myosin [26]. Taken together, the aforementioned data show that the importin 5, importin 7 and importin-β1 bind the newly identified NLS.

NM1 nuclear import does not follow the canonical nuclear import pathway

The direction of canonical nuclear import pathway is controlled by the small GTPase Ran. High levels of GTP-loaded Ran in the nucleoplasm cause the dissociation of importin-cargo complex upon translocation through the nuclear pore complex [27]. We probed the stability of the NM1-importin complexes in the presence of RanGTP in order to test whether the nuclear import of NM1 follows the canonical nuclear import pathway.

Complexes containing Str-GFP-NM1-(Q123.T) and associated importins were purified from electroporated HEK293T cells using streptactin affinity column and incubated with recombinant Q69L mutant of Ran, preloaded with GTP. This mutant is not able to hydrolyze GTP [28] and should cause elution of importins from the Str-GFP-NM1-(Q123.T) column The activity of Q69L mutant of Ran was confirmed by its ability to dissociate importin β1 from its well known cargo, SV40 NLS (Fig. 5E). In contrast to SV40 NLS, the GFP-NM1-(Q123.T) remained associated with importin 5 even in the presence of RanGTP Q69L. As shown by western blot (Fig. 5E), the complex of GFP-NM1-(Q123.T) and importin 5 co-eluted from the column by the addition of biotin that disrupts the binding of Str-GFP-NM1-(Q123.T) to the streptactin resin. Taken together, these data suggested that the NM1 nuclear import does not follow the canonical nuclear import pathway regulated by GTPase Ran.

Overexpression of calmodulin negatively influences NM1 nuclear import

Neck region of NM1 is characterized by the presence of IQ motifs that bind calmodulin in Ca^{2+}-dependent manner [29]. As NLS sequence of NM1 is present within one of these IQ motifs, we tested the influence of increased calmodulin levels on the NM1 localization. When GFP-PK-IQ12 was co-expressed with calmodulin in U2OS cells, elevated levels of calmodulin blocked the nuclear import of the IQ12 construct (Fig. 6B). Calmodulin, on the other hand, did not block the import of GFP-PK-IQ2 (Fig. 6C). Importantly, calmodulin did not inhibit the nuclear import of the GFP-PK-SV40 NLS construct, suggesting that the observed effect is not a general inhibition of nuclear import pathways (Fig. 6A). To compare the amount of calmodulin associated with GFP-PK-IQ2 and GFP-PK-IQ12 we immunoprecipitated the proteins from extracts of electroporated HEK293T cells using GFP-trap magnetic beads. As shown in Fig. 6D calmodulin associated with GFP-PK construct only when both IQ domains were present (GFP-PK-IQ12). In conclusion calmodulin binding to IQ12 appears to regulate nuclear import of NM1.

Discussion

Nuclear myosin 1 is ubiquitously expressed protein that localizes to the nuclei of all cell types tested so far with the exception of cells in germinal stage of spermiogenesis [3]. Our previous work described the dynamics of intranuclear relocalization of NM1 [8,19] and involvement of NM1 in important nuclear processes – namely gene transcription. In this paper, we further contribute to the knowledge of NM1 cellular trafficking by describing the dynamics of its nuclear import and identification of the sequence that is necessary for the nuclear entry of NM1.

NM1 contains NLS within the IQ domain

We used tagged constructs in search for the NLS of NM1. By deletions and truncations of the full length protein, we narrowed down the region of NM1 required for its nuclear import to a short sequence within the second IQ motif of the neck domain. The sequence contains clusters of basic amino acids intermingled with non-polar amino acids and mutation of the basic residues into alanines blocked the nuclear import of NM1. The NLS does not resemble to any of the NLSs already described in the literature and, thus, it might be expected to have some unique properties. Similarly to NM1, also the neck of other unconventional myosin, myosin Vb, contains IQ sequence, that was shown to be

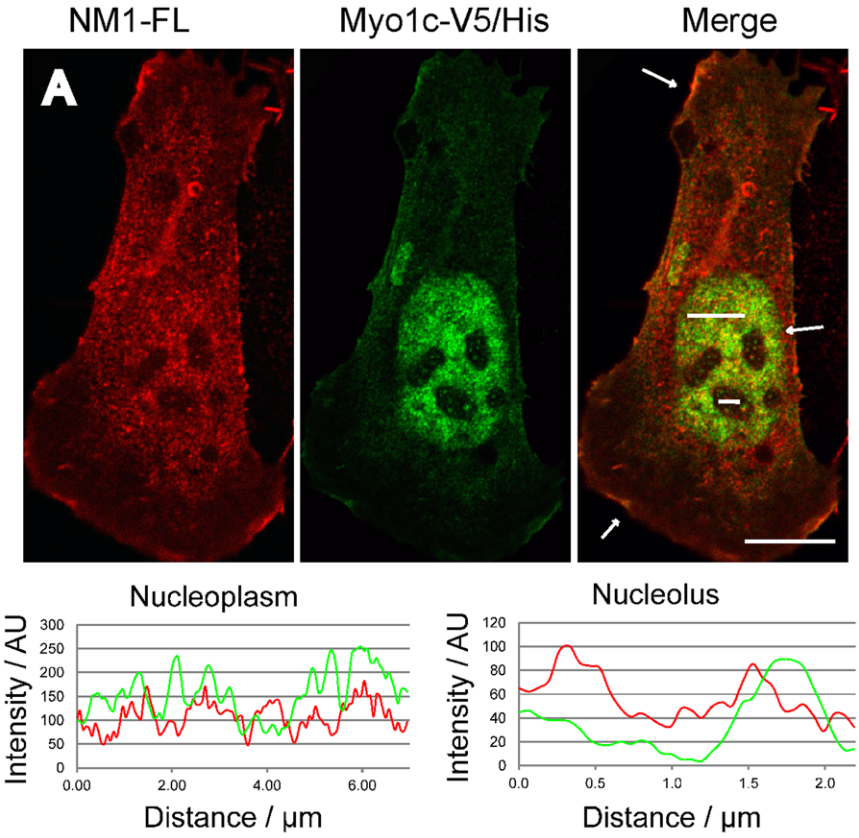
NM1-FL
Myo1c-V5/His
Merge
A
Nucleoplasm
Intensity / AU
300
250
200
150
100
50
0
0.00
2.00
4.00
6.00
Distance / µm
Nucleolus
Intensity / AU
120
100
80
60
40
20
0
0.0
0.5
1.0
1.5
2.0
Distance / µm

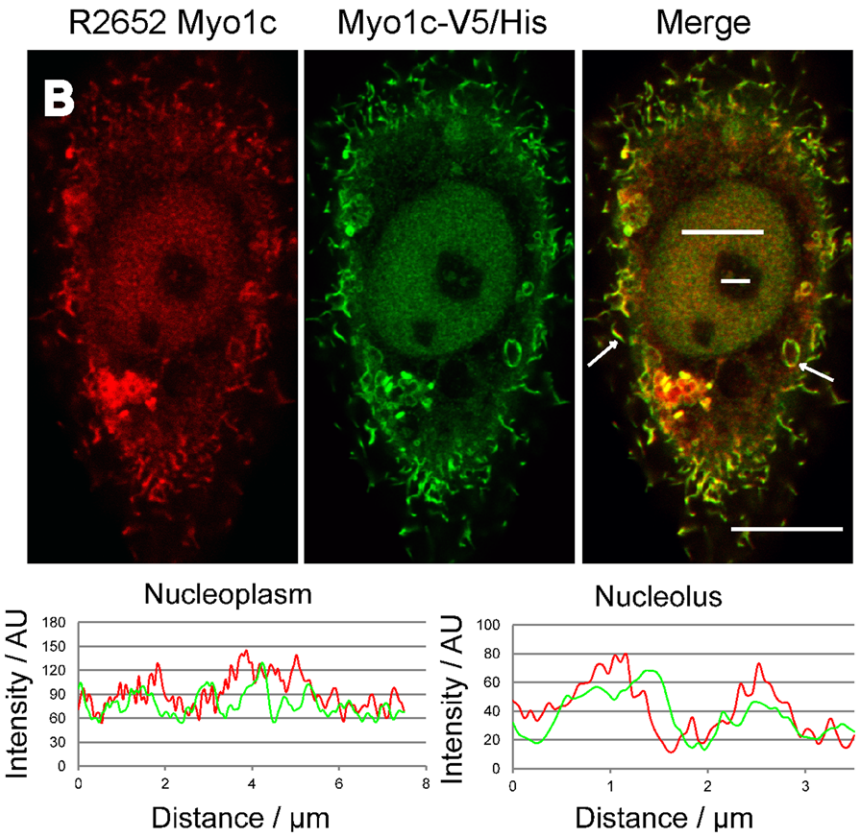
R2652 Myo1c
Myo1c-V5/His
Merge
B
Nucleoplasm
Intensity / AU
180
150
120
90
60
30
0
0
2
4
6
8
Distance / µm
Nucleolus
Intensity / AU
100
80
60
40
20
0
0
1
2
3
Distance / µm

Figure 4. Co-localization of overexpressed NM1 and Myo1c. U2OS cells were co-transfected with FLAG-tagged NM1 (**NM1-FL**) and V5/His tagged Myo1c (**Myo1c-V5/His**). Cell showing nuclear localization of NM1 and Myo1c was photographed using confocal microscope (**A**). U2OS were transfected with Myo1c-V5/His. 48 h post transfection cells were fixed, and labeled with polyclonal antibody (R2652) directed toward the tail region of NM1/Myo1c and with monoclonal antibody against V5 (**B**). Intensity profiles along the regions of interest in the nucleus and nucleolus are shown under the pictures. White arrows are pointing to regions at the plasma membrane where both proteins are enriched. Scale Bar: 10 μm.
doi:10.1371/journal.pone.0030529.g004

responsible for nuclear and nucleolar localization of this myosin. Furthermore, it also mediates interaction with RNA pol I [30]. An IQ motif of another actin and PIP2 binding protein, the neural Wiskot-Aldrich syndrome protein (N-WASP), serves as an NLS [31]. In conclusion, the ability to drive nuclear import appears to be common to various IQ motifs.

Role of IQ2 in plasma membrane localization of NM1/Myo1c

NM1/Myo1c neck-tail domain (NM1-(Q123.T)), was shown previously to associate with the plasma membrane through interaction with PIP2. This interaction was assigned to the putative PIP2-specific PH domain in the tail region of myo1c [20]

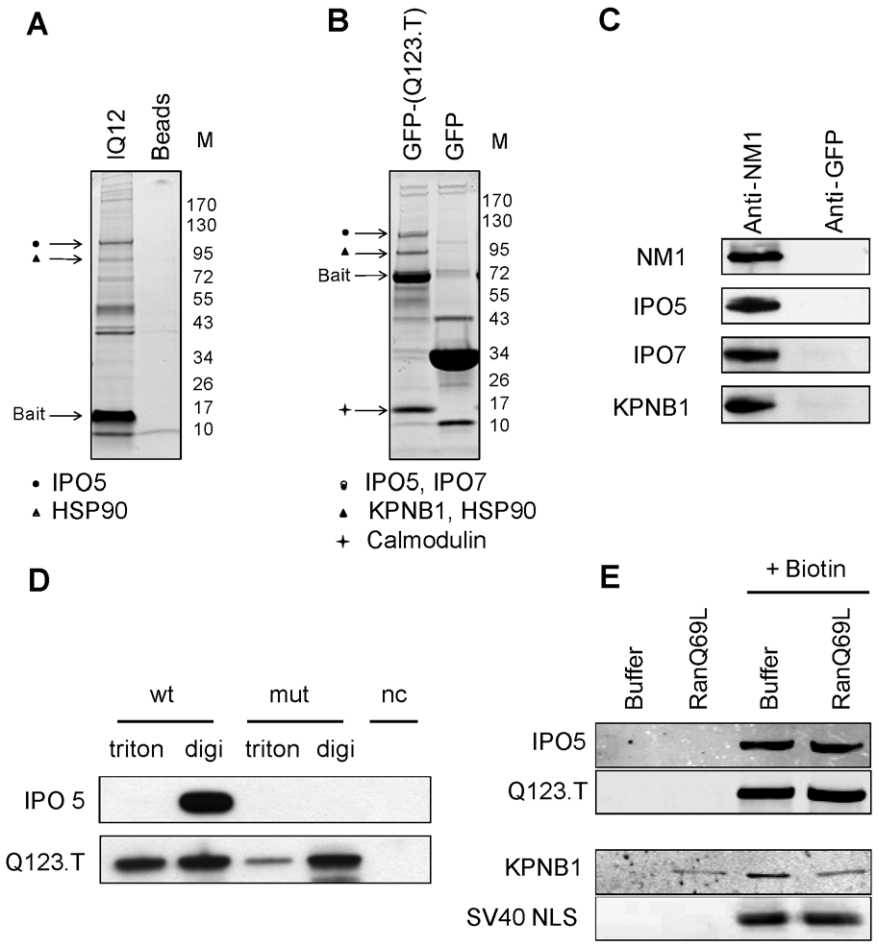

Figure 5. Identification of NM1 interacting proteins in the cytosol. Digitonin extract from suspension HeLa cells was incubated with recombinant Str-IQ12-His peptide containing N-terminal OneStrep tag (IQ12) and Streptactin beads as a control for background binding. Bound proteins were resolved on 4–20% SDS-PAGE gel and stained with SimplyBlue. Mass spectrometric analysis of the protein bands that co-purified with bait (arrows) identified importin 5 and heat shock protein 90 beta (HSP90) (**A**). SimplyBlue stained 4–20% SDS-PAGE gel with proteins that interacted with Str-GFP-NM1-(Q123.T) and Str-GFP as a control in digitonin extract of HEK293T cells. The arrows show positions of bands that contained proteins identified using mass spectrometry as importin 5, importin 7, importin-β1, HSP90 beta and calmodulin (**B**). Proteins that co-immunoprecipitate with antibody to endogenous NM1 from HeLa extracts were resolved using SDS-PAGE and tranferred onto nitrocelulose membrane. Membrane was probed with with anti-NM1, anti-importin 5 (IPO5), anti-importin 7 (IPO7), anti-importin-β1 (KPNB1). Rabbit polyclonal antibody against GFP was used as a control for backgroung binding (**C**). N-terminally Strep tagged GFP-NM1-(Q123.T) ^{NLSwt} (wt), GFP-NM1-(Q123.T) ^{NLSmut} (mut) and GFP as negative control (nc) were expressed in HEK293T cells. Cells were extracted with buffer containing digitonin (digi) to obtain soluble cytosol; pellet was re-extracted with the same buffer containing 1% Triton X-100 (triton). Bound proteins were resolved on SDS-PAGE, transferred to nitrocelulose. Membrane was incubated with antibody to importin 5 ans GFP (**D**). Beads containing Str-GFP-NM1-(Q123.T) and Str-GFP-SV40 NLS and associated proteins were eluted first with buffer containing GTP-loaded RanQ69L or buffer alone and then with biotin containig buffer that liberated Strep-tagged bait proteins from the column. Proteins eluted from the beads were resolved on SDS-PAGE and transferred to nitrocelulose membrane. GFP, importin 5 and importin-β1 signals were detected using specific antibodies (**E**). Signal from secondary antibodies was detected using LI-COR Odyssey infrared imaging system.
doi:10.1371/journal.pone.0030529.g005

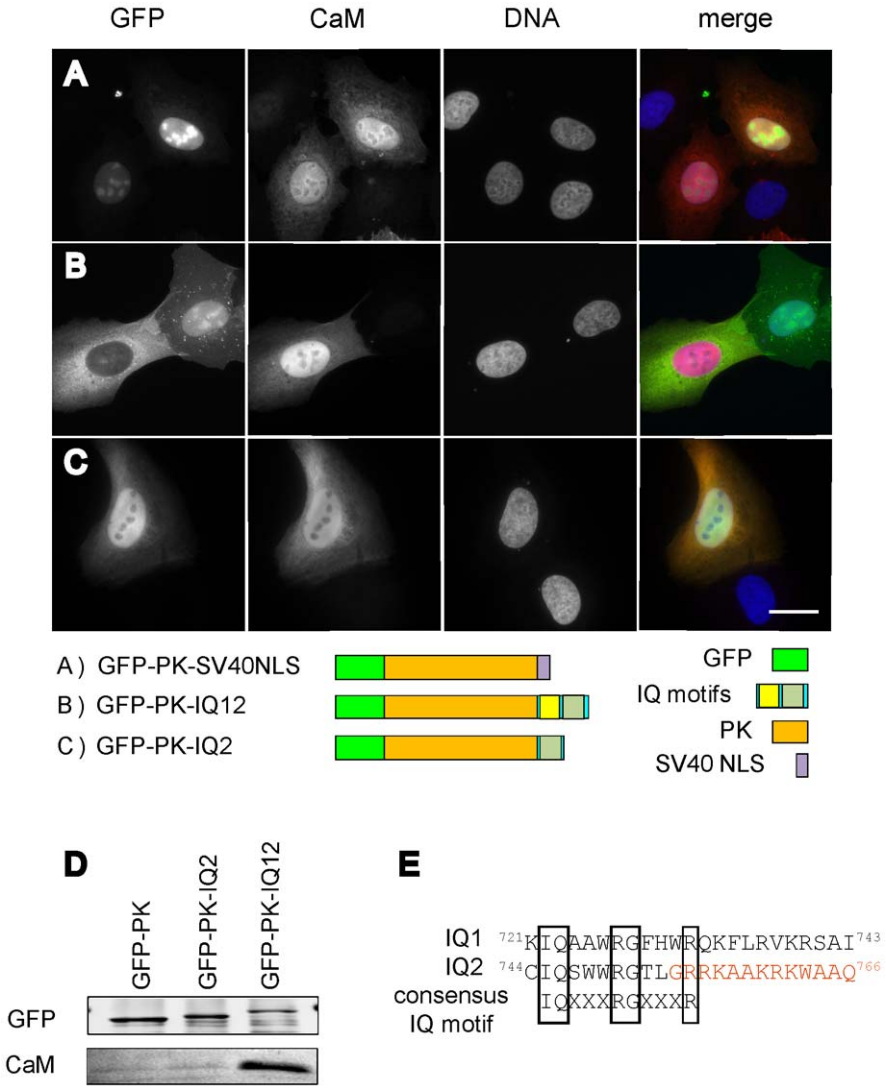

Figure 6. Overexpression of calmodulin influences the nuclear import of NM1. U2OS cells were co-transfected with GFP-PK constructs containing IQ domains, and calmodulin. Calmodulin was visualized using specific antibody (**A**,**B**,**C**). Scale bar 10 μm. HEK293T cells electroporated with the same constructs as in (**A**,**B**,**C**). Whole cell extracts were subjected to immunoprecipitation with anti-GFP nanobody. Bound proteins were resolved on SDS-PAGE and transferred to nitrocelulose. GFP and CaM were visualized using specific antibodies (**D**). (**E**) Comparison of IQ1 and IQ2 sequences. The consensus IQ motif is shown below. The NM1 NLS sequence is highlighted in red.
doi:10.1371/journal.pone.0030529.g006

and/or another less specific to the neck region [32]. Interestingly, NM1 mutants which either lacked the second IQ motif or the basic residues within the second IQ sequence were misslocalized from the plasma membrane to the cytosol (Fig. 3B and 3C). These data are in agreement with previously published work that identified the IQ2 as additional plasma membrane binding site [32].

Mechanism of NM1 nuclear import

The basic mechanism of NM1 nuclear import appears to involve karyopherins, because importin 5, importin 7 and importin-β1 were found to be associated with both overexpressed and endogenous NM1. The interaction of importin 5 with NM1 NLS seems to be specific since NM1 mutant lacking the basic amino acids in NLS did not bind this karyopherin.

Canonical importin-mediated nuclear entry is controlled by the nuclear RanGTP which, upon binding to importins, releases their cargos. Surprisingly, the complex of NM1 with importin 5 is stable in the presence of RanGTP (Fig. 5E) and its nuclear import is rather dependent on the levels of calmodulin (Fig. 6B). This suggests that nuclear import of NM1 is mediated by a non-canonical pathway. Indeed, such a calmodulin-dependent and Ran-independent nuclear import pathway has been shown to regulate the nucleocytoplasmic localization of several transcription factors (SOX9, SRY, c-Rel). The N-terminal domain of SRY and SOX9 contains a calmodulin-binding domain followed by an NLS [33]. It was shown that calmodulin binding stimulates the nuclear entry of SRY and SOX9 [34,35]. On the other hand the NF-κB/Rel family protein c-Rel binds Ca^{2+}-calmodulin via sequence near the NLS and this binding blocks its nuclear accumulation [36]. The NLS of NM1 resides in close vicinity of the second IQ motif. We showed that IQ2 alone is able to drive the translocation of heterologous construct GFP-PK to the nucleus (Fig. 2J). Interestingly, IQ1 seems to play a key role in regulation of NM1 nuclear

import (Fig. 6B). In presence of elevated levels of calmodulin, IQ1 mediated the inhibition of nuclear import (Fig. 6B) and it also substantially increased the binding of CaM the IQ2 (Fig. 6D).

On the other hand, the crystallographic [37] and biochemical studies have shown that calmodulin binds the IQ motifs of unconventional myosins in Ca^{2+}-free state and that elevated Ca^{2+} dissociates calmodulin from the neck of Myo1c [29]. More recent study showed that in the absence of calcium, Ca^{2+}-free calmodulin (apo-CaM) was bound to the IQ1 with highest affinity whereas in the presence of calcium IQ1 dissociated Ca^{2+}-CaM most rapidly. Ca^{2+} - induced dissociation of calmodulin molecules from the neck increases ATPase rate and inhibits the motility of Myo1c [38]. We propose a scenario in which the calmodulin occupies the IQ12 at low Ca^{2+} cellular levels preventing the importin from binding to NM1. The Ca^{2+} oscilations which occur during G1 phase of cell cycle [39] or which follow the signal transduction events [40] might cause the calmodulins to dissociate from the NM1 neck. As a result, the CaM-free IQ2 will subsequently bind to the import receptor that transports the NM1 to the nucleus. Taken together, at the cellular level, both the motor function of NM1/Myo1c and its localization appear to be dynamically regulated by transient transient changes in Ca^{2+} concentration. Obviously, further experiments are needed to reveal the details of the mechanism.

Nuclear localization of NM1/Myo1c

The fact that both Myo1c and NM1 contain the same NLS sequence points to the question whether also Myo1c would be present in the nucleus along with NM1. NM1 was first detected in the nucleus in 1997 [1] using the antibody specific to N-terminus of NM1. Myo1c has never been reported in the nucleus since the antibody directed to the C-terminus [41] does not label the nuclei of cells. Intriguingly, upon transfection with either NM1 or Myo1c, the nuclear signal could be readily detected also by this antibody (Fig. 4B). One plausible explanation of this discrepancy would be that the epitope is probably masked by nuclear binding partners, posttranslational modifications or adopts a different conformation. However, the steady-steate cytosol to nucleus distribution of endogenous NM1 and Myo1c in mouse liver is approximately 70% (cytosol) to 30% (nucleus) Fig. 3E. Therefore another possible intepretation is that the level of endogenous nuclear myosins at steady state is is below the detection limit of the antibody directed to the C-terminus.

In conclusion, our work revealed a novel NLS sequence responsible for nuclear translocation of NM1. This sequence acts as an efficient NLS when fused to different otherwise cytosolic proteins, while the AA 1–16 lacks this capacity. This means that NM1 does not need N-terminal sequence for nuclear import, and that both NM1 and Myo1c can function in the cell nucleus which is supported by detection of both isoforms in the cell nucleus. Finally, our work suggests a complex regulation of myosin 1c nuclear import, mediated by both CaM and importins. This data opens additional interesting questions: Do the two myosins serve the same functions in the nucleus and in the cytoplasm? Do these two myosins have the same molecular properties (e.g. binding to actin, nucleotide, mechanism of strain-dependent release of ADP) or do they somehow differ? Are they tuned to serve the same function at the level of cell, tissue and organism? Obviously, further investigation is needed to answer these questions.

Materials and Methods

Antibodies

In immunofluorescence and co-immunoprecipitation experiments we used affinity purified antibody directed to the NM1 N-terminus M3567 (Sigma), antibodies to lamin B (M-20, Santa Cruz Biotechnology), V5-tag (Serotec), V5-tag (V8137-Sigma), FLAG-tag (Stratagene) and to calmodulin (Upstate, cat. No. 05-173). Anti-importin 5 (sc-17802), importin beta (sc-1919) and importin 7 (sc-55235) were purchased from Santa Cruz Biotechnology. R2652 rabbit polyclonal antibody against the tail domain of Myo1c was kindly provided by Peter G. Gillespie, Oregon Hearing Research Center and Vollum Institute [41]; rabbit polyclonal anti-NM1 for western blots was kindly provided by Piergiorgio Percipalle [5], and EGFP antibody was purchased from Invitrogen (cat. No. A11122).

Cells and transfections

Cell lines cells were obtained from American Type Culture Collection. NIH/3T3 (ATCC No. CRL-1658), U2OS (ATCC No. HTB-96), HeLa (ATCC No. CCL-2) and HEK 293T/17 (ATCC No CRL-11268) were kept in DMEM supplemented with 10% fetal bovine serum (FBS) in 5% CO2/air, 37°C, in humidified atmosphere. HeLa S3 (ATCC No. CCL-2.2) were kept in S-MEM supplemented with 5% FBS and grown in spinner flasks. The U2OS cells were transfected with FUGENE 6 (Roche) according to the manufacturer's protocol, fixed after 48 h and either observed directly under the microscope or labeled with antibodies. HEK293T cells were electroporated using GenePulser (Biorad) electroporator as described [42]. The efficiency of electroporation was about 90%.

Immunofluorescence microscopy

Cells grown on coverslips were fixed with freshly prepared 3% formaldehyde for 10 minutes, permeabilized with 0.1% Triton X-100 in PBS for 10 minutes, incubated with primary antibodies for 1 hour at room temperature. Primary antibodies were diluted in PBS containing 0.05% Tween-20 (PBST) to 16 μg/ml (NM1), 5 μg/ml (lamin B1), 5 μg/ml (calmodulin), 1 μg/ml (V5-tag), 5 μg/ml (Flag-tag). After washing in PBST, coverslips were incubated with FITC or Cy5-conjugated goat anti-rabbit or goat anti-mouse secondary antibodies (Jackson ImmunoResearch). Coverslips were mounted with Mowiol (Sigma) containing DABCO (Sigma) as an anti-fading agent and 0.1 μg/ml DAPI (Sigma), and observed under fluorescent or confocal microcopes (LEICA DM 6000, LEICA DMI 6000, LEICA TCS SP5 AOBS TANDEM). Brightness and contrast of captured digital images was adjusted with Photoshop software (Adobe).

Cell synchronization

U2OS cells were treated with nocodazole (80 ng/ml or 400 ng/ml) for 16 h. Mitotic cells were washed off the dish with medium, spun down and resuspended in fresh medium, and seeded on coverslips. Cells on coverslips were cultivated further in fresh medium and fixed 2,4,6,8, and 10 hours after the nocodazole block. Aphidicolin (1 μg/ml) was applied for 16 hours, cells were washed, cultivated in fresh medium, and then fixed 2, 7, 11, 17, and 22 hours post aphidicolin block. NIH 3T3 cells were synchronized by mitotic shake-off. Harvested cells were seeded on poly-lysine coated coverslips, and allowed to attach for 15 min. HeLa cells, used for co-immunoprecipitation of endogenous NM1, were incubated for 16 hours with nocodazole (400 ng/ml), washed in PBS, and then cultivated in complete medium for additional 3 h prior to the harvest.

Plasmid DNA preparation

NM1-GFP, GFP-NM1, Myo1c-GFP, NM1-V5, Myo1c-V5 were obtained by ligation of full length mouse NM1 (amino acids

1–1024) and Myo1c (aa 1–1028) [2] cDNA into pEGFP-C3, pEGFP-N3 (Clontech) and pcDNA3.1/V5-His (Invitrogen) vectors. Truncations containing head (H) neck with IQ domains (Q123) and tail (T) domains were generated using inverse PCR. NM1-V5-(H) (aa 1 to 716) was generated from NM1-V5.GFP-NM1-(Q123.T) (aa 712 to 1044),GFP-NM1-(Q3.T) (aa 763 to 1044), GFP-NM1-(Q123.T -Δ853) (aa 712 to 853), GFP-NM1-(Q12) (aa 712 to 770) were constructed from GFP-NM1 using standard cloning methods. For inspection of NLS-peptide localization, we produced a testing construct GFP-PK that contains in-frame fusion of EGFP and cytosolic enzyme pyruvate kinase (PK) [22], GFP-PK-IQ-12 was produced by ligation NM1-(Q12) sequence into GFP-PK vector. GFP-PK-IQ1 (aa 712 to 740), GFP-PK-IQ2 (aa 739 to 766) GFP-PK-NLS $^{(NM1)}$ (aa 754 to 766) were generated by PCR deletions from GFP-PK-IQ1,2. Nt-GFP-PK was produced by ligation of NM1 N-terminal sequence (aa 1–16) in front of EGFP in GFP-PK vector. Ligation of the OneStrep tag sequence (IBA) in front of EGFP in the pEGFP-C3 vector generated Str-GFP. Str-GFP-NM1-(Q123.T) was produced by ligating the Q123.T (aa 712 to 1044) sequence into Str-GFP vector. Calmodulin cDNA was prepared from HeLa total cell RNA using RT-PCR and cloned into pcDNA3.1 vector (Invitrogen). Bacterial expression vector pET-Str-His was generated by ligation of OneStrep sequence into the pET28b vector (Novagen). Str-IQ12-His was produced by an in-frame ligation of the PCR-amplified fragment of NM1-(Q12) (aa 712 to 770) between the OneStrep- and His-tag. Point mutations in the NLS sequence of NM1 were generated by the site directed mutagenesis protocol (Stratagene). Bacterial expression plasmid pQE-RanQ69L was kindly provided by Prof. Dirk Görlich. Detailed description of all cloning procedures is available upon request. Recombinant proteins were expressed in bacteria and purified using Ni-NTA agarose column as described [28,38].

Pull-down assays and immunoprecipitation

Digitonin extract from suspension HeLa cells, prepared as described [43], was diluted to 2 mg/ml of total protein in lysis buffer (50 mM HEPES pH 7.4, 150 mM NaCl, 75 mM potassium acetate, 5 mM magnesium acetate, 1 mM DTT, protease inhibitors). After dilution, purified bacterially expressed Str-IQ12-His was added to the lysate. After 3 hours of incubation, the extract was centrifuged to remove precipitated proteins and supernatant was further incubated for 1 hour with StrepTactin Beads (IBA) to capture the bait and associated proteins. Beads were briefly washed 3 times with 1 ml of the lysis buffer followed by brief wash with IBA wash buffer (100 mM Tris pH 7.5, 100 mM NaCl, 1 mM EDTA) and captured proteins were eluted from beads with the wash buffer supplemented with 2 mM biotin. HEK 293T cells electroporated with Str-GFP-NM1-(Q123.T) or Str-GFP were collected by trypsinization into serum-containing medium. After centrifugation 300 g/3 minutes, the cells were washed twice with ice-cold PBS and extracted twice with lysis buffer containing 50 mM HEPES pH 7.4, 150 mM potassium acetate, 5 mM magnesium acetate, 1 mM DTT, 1 mg/ml digitonin (Fluka), EDTA-free COMPLETE inhibitors (Roche). After 4 hours of incubation with StrepTactin resin, the captured protein complexes were washed briefly 3 times with 1 ml of the lysis buffer followed by wash with 1 ml of IBA wash buffer. Proteins were eluted from beads with 2 mM biotin added into the wash buffer. The experiments with RanQ69L mutant were performed as described above, with the exception that after the 3rd wash a half of the beads was incubated for 10 min with buffer containing recombinant RanQ69L and the other half was incubated only in buffer. Elution with Ran mutant was repeated twice and remaining proteins were eluted from beads with IBA elution buffer containing 2 mM biotin. Eluates were concentrated ultrafiltration (Ultracel 10K, Milipore) and resolved on 6–20% gradient polyacrylamide gel.

Endogenous NM1 was immunoprecipitated from adherent HeLa cells synchronized with nocodazole. Cells were extracted twice in lysis buffer (50 mM HEPES pH 7.4, 150 mM NaCl, 75 mM potassium acetate, 5 mM magnesium acetate, 1 mM DTT, 1 mg/ml of digitonin and protease inhibitors), lysates were clarified by centrifugation (10 min, 16 000 g, 4°C), and incubated with beads containing either covalently bound antibody antibody to NM1 (Sigma, cat no M3567) or to EGFP (Exbio, Czech Republic, cat no 11-473-C100). After 3 washes in 1 ml of lysis buffer beads were washed in 1 ml of 50 mM amonium bicarbonate pH 7.5 to remove salts and detergent. Bound proteins were eluted twice with 500 µl of 500 mM amonium hydroxide. Eluates were evaporated using SpeedVac concentrator (Savant, Holbrook, NY, USA), dry pellets were resuspended in 20 ul of 1× SDS loading buffer, boiled and resolved on 6–20% gradient SDS PAGE. After transfer to nitrocelulose proteins were visualized using specific antibodies.

GFP-PK constructs in Fig. 6D were immnuoprecipitated from lysates of electroporated HEK23T cells as follows. Cells were harvested by trypsinization, washed in PBS and lysed in lysis buffer (150 mM NaCl, 50 mM Tris-HCL pH-7.5, 10 mM EGTA, 2 mM EDTA, 1% Triton X-100, protease inhibitors ROCHE). After clarification by centrifugation (10 min, 16 000 g, 4°C), supernatans were incubated with 20 µl of GFP-trap magnetic particles (ChromoTek GmbH, Germany). After 5 washes in 1 ml of lysis buffer particles were washed in 1 ml of 50 mM amonium bicarbonate pH 7.5 to remove salts and detergent. Bound proteins were eluted twice with 500 µl of 500 mM amonium hydroxide. Eluates were evaporated using SpeedVac concentrator (Savant, Holbrook, NY, USA), dry pellets were resuspended in 20 ul of 1× SDS loading buffer, boiled and resolved on 6–20% gradient SDS PAGE. After transfer to nitrocelulose proteins were visualized using specific antibodies.

Proteolytic digestion and sample preparation

Protein bands were cut from the gel, sliced into the small pieces, and decolorized in sonic bath at 60°C several times with 0.1 M 4-ethylmorpholine acetate (pH 8.1) in 50% acetonitrile (ACN). After complete destaining, proteins were reduced by 50 mM TCEP in 0.1 M 4-ethylmorpholine acetate (pH 8.1) for 5 min at 80°C and alkylated using 50 mM iodoacetamide in 0.1 M 4-ethylmorpholine acetate (pH 8.1) for 30 min in dark at room temperature. Then, the gel was washed with water, shrunk by dehydration with ACN and reswollen in water. The rehydratation and dehydration of the gel was repeated twice. Next, the gel was reswollen in 0.05 M 4-ethylmorpholine acetate (pH 8.1) in 50% acetonitrile (ACN) and then the gel was partly dried using a SpeedVac concentrator (Savant, Holbrook, NY, USA). Finally, the gel was reconstituted with cleavage buffer containing 0.01% 2-mercaptoethanol, 0.05 M 4-ethylmorpholine acetate (pH 8.1), 10% ACN, and sequencing grade trypsin (Promega, 10 ng/µl). Digestion was carried out overnight at 37°C; the resulting peptides were extracted with 30% ACN/0.1% TFA and subjected to mass spectrometric analysis.

Mass spectrometric analysis

Mass spectra were acquired in the positive ion mode on a MALDI-FTMS APEX-Ultra (Bruker Daltonics, Bremen, Germany) equipped with 9.4 T superconducting magnet and SmartBeam laser. The acquisition mass range was 700–3500 m/

z and 512k data points were collected. A 280 V potential was applied on the MALDI plate. The cell was opened for 2500 ms, 4 experiments were collected for one spectrum where one experiment corresponds to 300 laser shots. The instrument was externally calibrated using PepMix II peptide standard (Bruker Daltonics, Bremen, Germany). It results in typical mass accuracy below 2 ppm. A saturated solution of α-cyano-4-hydroxy-cinnamic acid in 50% ACN/0.2% TFA was used as a MALDI matrix. A 1 µl of matrix solution was mixed with a 1 µl of the sample on the target and the droplet was allowed to dry at ambient temperature. After the analysis the spectra were apodized using square sin apodization with one zero fill. The interpretation of mass spectra was done using DataAnalysis version 3.4 and BioTools 3.2 software packages (Bruker Daltonics, Billerica, MA). Proteins were identified by peptide mass fingerprinting (PMF) using a search algorithm MASCOT (Matrix Science).

Generation of the NM1 knock-out mice

To generate NM1-KO mice, loxP-recombination sites were introduced into NM1 gene by homologous recombination in R1 embryonic stem cell line [44]. Cre-mediated recombination in germline cells, achieved by cross breeding with the meu-cre expressing mice [45] resulted in removal of the loxP-flanked exon-1 from the mouse NM1 genomic sequence (sequence from −165 to +116 base pairs from NM1 translation initiation site). In the mutant NM1 allele, only the start codon initiating the translation of Myo1c is present. As a result, only Myo1c protein is expressed in all tissues. Mice were genotyped using genomic PCR, and the absence of NM1 protein was confirmed by Western blotting (Venit et al., in preparation).

Isolation of nuclei from mouse liver

Nuclei from mouse liver were isolated as described [46]. Briefly, mice were killed by CO_2 and liver was homogenized in ice-cold buffer A (250 mM sucrose, 5 mM $MgCl_2$, 10 mM HEPES pH 8) in glass Dounce homogenizer. The homogenate was spun down (600 g/10 min), the supernatant was taken as the cytosolic fraction and the pellet was washed once in buffer A. The crude nuclear pellet was resuspended in buffer B (2.0 M sucrose, 1.5 mM $MgCl_2$, 10 mM HEPES pH 8) and centrifuged 30 minutes/16000 g. Purified nuclei were resuspended in buffer Z (62.5 mM Tris pH 6.8, 10% glycerol, 2% SDS), heated to 90°C for 10 minutes, sonicated, and centrifuged again (16000 g/10 min). The amount of protein in the supernatant was measured using BCA (Pierce).

Acknowledgments

We thank Prof. Thomas Ruelicke and Dr. Volker Schmidt (Research Center Biomodels Austria, Veterinary University, Vienna) for their great contribution on producing knock-out mice, Pavel Kríž and Iva Jelínková for excellent technical assistance, Lenka Rossmeislová and Jindřiška Fišerová for critical reading of the manuscript. We are very grateful to Prof. Peter Gillespie and Prof. Piergiorgio Percipalle for providing the antibodies.

Author Contributions

Conceived and designed the experiments: RD MK PH. Performed the experiments: RD SY MK PN JH TV. Analyzed the data: RD SY MK PN JH TV PH. Wrote the paper: RD PH.

References

1. Nowak G, Pestic-Dragovich L, Hozak P, Philimonenko A, Simerly C, et al. (1997) Evidence for the presence of myosin I in the nucleus. J Biol Chem 272: 17176–17181.
2. Pestic-Dragovich L, Stojiljkovic L, Philimonenko AA, Nowak G, Ke Y, et al. (2000) A myosin I isoform in the nucleus. Science 290: 337–341.
3. Kahle M, Pridalova J, Spacek M, Dzijak R, Hozak P (2007) Nuclear myosin is ubiquitously expressed and evolutionary conserved in vertebrates. Histochem Cell Biol 127: 139–148.
4. Hofmann WA, Richards TA, de Lanerolle P (2009) Ancient animal ancestry for nuclear myosin. J Cell Sci 122: 636–643.
5. Fomproix N, Percipalle P (2004) An actin-myosin complex on actively transcribing genes. Exp Cell Res 294: 140–148.
6. Hofmann WA, Stojiljkovic L, Fuchsova B, Vargas GM, Mavrommatis E, et al. (2004) Actin is part of pre-initiation complexes and is necessary for transcription by RNA polymerase II. Nat Cell Biol 6: 1094–1101.
7. Philimonenko VV, Zhao J, Iben S, Dingova H, Kysela K, et al. (2004) Nuclear actin and myosin I are required for RNA polymerase I transcription. Nat Cell Biol 6: 1165–1172.
8. Philimonenko VV, Janacek J, Harata M, Hozak P (2010) Transcription-dependent rearrangements of actin and nuclear myosin I in the nucleolus. Histochem Cell Biol 134: 243–249.
9. Grummt I (2003) Life on a planet of its own: regulation of RNA polymerase I transcription in the nucleolus. Genes Dev 17: 1691–1702.
10. Grummt I (2006) Actin and myosin as transcription factors. Curr Opin Genet Dev 16: 191–196.
11. Ye J, Zhao J, Hoffmann-Rohrer U, Grummt I (2008) Nuclear myosin I acts in concert with polymeric actin to drive RNA polymerase I transcription. Genes Dev 22: 322–330.
12. Percipalle P, Farrants AK (2006) Chromatin remodelling and transcription: be-WICHed by nuclear myosin 1. Curr Opin Cell Biol 18: 267–274.
13. Obrdlik A, Louvet E, Kukalev A, Naschekin D, Kiseleva E, et al. (2010) Nuclear myosin 1 is in complex with mature rRNA transcripts and associates with the nuclear pore basket. FASEB J 24: 146–157.
14. Cisterna B, Necchi D, Prosperi E, Biggiogera M (2006) Small ribosomal subunits associate with nuclear myosin and actin in transit to the nuclear pores. FASEB J 20: 1901–1903.
15. Cisterna B, Malatesta M, Dieker J, Muller S, Prosperi E, et al. (2009) An active mechanism flanks and modulates the export of the small ribosomal subunits. Histochem Cell Biol 131: 743–753.
16. Mehta IS, Amira M, Harvey AJ, Bridger JM (2010) Rapid chromosome territory relocation by nuclear motor activity in response to serum removal in primary human fibroblasts. Genome Biol 11: R5.
17. Hu X, Li X, Valverde K, Fu X, Noguchi C, et al. (2009) LSD1-mediated epigenetic modification is required for TAL1 function and hematopoiesis. Proc Natl Acad Sci U S A 106: 10141–10146.
18. Chuang CH, Carpenter AE, Fuchsova B, Johnson T, de Lanerolle P, et al. (2006) Long-range directional movement of an interphase chromosome site. Curr Biol 16: 825–831.
19. Kysela K, Philimonenko AA, Philimonenko VV, Janacek J, Kahle M, et al. (2005) Nuclear distribution of actin and myosin I depends on transcriptional activity of the cell. Histochem Cell Biol 124: 347–358.
20. Hokanson DE, Laakso JM, Lin T, Sept D, Ostap EM (2006) Myo1c binds phosphoinositides through a putative pleckstrin homology domain. Mol Biol Cell 17: 4856–4865.
21. Laakso JM, Lewis JH, Shuman H, Ostap EM (2008) Myosin I can act as a molecular force sensor. Science 321: 133–136.
22. Frangioni JV, Neel BG (1993) Use of a general purpose mammalian expression vector for studying intracellular protein targeting: identification of critical residues in the nuclear lamin A/C nuclear localization signal. J Cell Sci 105(Pt 2): 481–488.
23. Mohr D, Frey S, Fischer T, Guttler T, Gorlich D (2009) Characterisation of the passive permeability barrier of nuclear pore complexes. EMBO J 28: 2541–2553.
24. Cokol M, Nair R, Rost B (2000) Finding nuclear localization signals. EMBO Rep 1: 411–415.
25. Dumont RA, Zhao YD, Holt JR, Bahler M, Gillespie PG (2002) Myosin-I isozymes in neonatal rodent auditory and vestibular epithelia. Journal of the Association for Research in Otolaryngology: JARO 3: 375–389.
26. Chen J, Wagner MC (2001) Altered membrane-cytoskeleton linkage and membrane blebbing in energy-depleted renal proximal tubular cells. American journal of physiology Renal physiology 280: F619–627.
27. Pemberton LF, Paschal BM (2005) Mechanisms of receptor-mediated nuclear import and nuclear export. Traffic 6: 187–198.
28. Kutay U, Bischoff FR, Kostka S, Kraft R, Gorlich D (1997) Export of importin alpha from the nucleus is mediated by a specific nuclear transport factor. Cell 90: 1061–1071.
29. Gillespie PG, Cyr JL (2002) Calmodulin binding to recombinant myosin-1c and myosin-1c IQ peptides. BMC Biochem 3: 31.

30. Lindsay AJ, McCaffrey MW (2009) Myosin Vb localises to nucleoli and associates with the RNA polymerase I transcription complex. Cell Motil Cytoskeleton 66: 1057–1072.
31. Suetsugu S, Takenawa T (2003) Translocation of N-WASP by nuclear localization and export signals into the nucleus modulates expression of HSP90. J Biol Chem 278: 42515–42523.
32. Hirono M, Denis CS, Richardson GP, Gillespie PG (2004) Hair cells require phosphatidylinositol 4,5-bisphosphate for mechanical transduction and adaptation. Neuron 44: 309–320.
33. Harley VR, Lovell-Badge R, Goodfellow PN, Hextall PJ (1996) The HMG box of SRY is a calmodulin binding domain. FEBS letters 391: 24–28.
34. Sim H, Rimmer K, Kelly S, Ludbrook LM, Clayton AH, et al. (2005) Defective calmodulin-mediated nuclear transport of the sex-determining region of the Y chromosome (SRY) in XY sex reversal. Molecular endocrinology 19: 1884–1892.
35. Argentaro A, Sim H, Kelly S, Preiss S, Clayton A, et al. (2003) A SOX9 defect of calmodulin-dependent nuclear import in campomelic dysplasia/autosomal sex reversal. The Journal of biological chemistry 278: 33839–33847.
36. Antonsson A, Hughes K, Edin S, Grundstrom T (2003) Regulation of c-Rel nuclear localization by binding of Ca2+/calmodulin. Molecular and cellular biology 23: 1418–1427.
37. Houdusse A, Gaucher JF, Krementsova E, Mui S, Trybus KM, et al. (2006) Crystal structure of apo-calmodulin bound to the first two IQ motifs of myosin V reveals essential recognition features. Proceedings of the National Academy of Sciences of the United States of America 103: 19326–19331.
38. Manceva S, Lin T, Pham H, Lewis JH, Goldman YE, et al. (2007) Calcium regulation of calmodulin binding to and dissociation from the myo1c regulatory domain. Biochemistry 46: 11718–11726.
39. Kahl CR, Means AR (2003) Regulation of cell cycle progression by calcium/calmodulin-dependent pathways. Endocrine reviews 24: 719–736.
40. Yip MF, Ramm G, Larance M, Hoehn KL, Wagner MC, et al. (2008) CaMKII-mediated phosphorylation of the myosin motor Myo1c is required for insulin-stimulated GLUT4 translocation in adipocytes. Cell metabolism 8: 384–398.
41. Dumont RA, Zhao YD, Holt JR, Bahler M, Gillespie PG (2002) Myosin-I isozymes in neonatal rodent auditory and vestibular epithelia. J Assoc Res Otolaryngol 3: 375–389.
42. Galvez T, Duthey B, Kniazeff J, Blahos J, Rovelli G, et al. (2001) Allosteric interactions between GB1 and GB2 subunits are required for optimal GABA(B) receptor function. EMBO J 20: 2152–2159.
43. Kutay U, Lipowsky G, Izaurralde E, Bischoff FR, Schwarzmaier P, et al. (1998) Identification of a tRNA-specific nuclear export receptor. Mol Cell 1: 359–369.
44. Nagy A, Rossant J, Nagy R, Abramow-Newerly W, Roder JC (1993) Derivation of completely cell culture-derived mice from early-passage embryonic stem cells. Proceedings of the National Academy of Sciences of the United States of America 90: 8424–8428.
45. Leneuve P, Colnot S, Hamard G, Francis F, Niwa-Kawakita M, et al. (2003) Cre-mediated germline mosaicism: a new transgenic mouse for the selective removal of residual markers from tri-lox conditional alleles. Nucleic Acids Res 31: e21.
46. Nagata T, Redman RS, Lakshman R (2010) Isolation of intact nuclei of high purity from mouse liver. Anal Biochem 398: 178–184.

5.2 Involvement of PIP2 in RNA Polymerase I transcription

Yildirim S, Castano E, Sobol M, Philimonenko VV, Dzijak R, Venit T, Hozák P

Journal of Cell Science, 2013, in press
IF: 6,11 (2011)

My contribution to this work:
I generated Fl-tagged fibrillarin and UBF constructs and PLδ1 construct for purification and further use of these proteins.

Involvement of PIP2 in RNA Polymerase I transcription

Sukriye Yildirim[1*], Enrique Castano[1,2*], Margarita Sobol[1], Vlada V. Philimonenko[1], Rastislav Dzijak[1], Tomáš Venit[1] and Pavel Hozák[1+]

[1] Institute of Molecular Genetics ASCR v.v.i. Department of Biology of the Cell Nucleus, Vídenská 1083, 142 20, Prague 4, Czech Republic.

[2] Biochemistry and Molecular Plant Biology Department, CICY. Calle 43, No.130, Colonia Chuburná de Hidalgo C.P. 97200, Mérida, Yucatán, México.

*These authors contributed equally to this work

[+]Corresponding Author: Pavel Hozák, hozak@img.cas.cz

Tel: +420 241 062 219

Fax: +420 241 062 289

Running title: PIP2 in RNA Pol I transcription

Keywords: Nucleolus, transcription, PIP2, UBF, fibrillarin

Word count: 8199

Summary

RNA polymerase I (Pol I) transcription is essential for the cell cycle, growth, and overall protein synthesis in eukaryotes. We found that phosphatidylinositol 4,5-bisphosphate (PIP2) is a part of the protein complex on the active ribosomal promoter during the transcription. PIP2 makes a complex with Pol I and Pol I transcription factor UBF in the nucleolus. PIP2 depletion reduces Pol I transcription which can be rescued by the addition of exogenous PIP2. In addition, PIP2 also binds directly to the pre-rRNA processing factor, fibrillarin (Fib), and co-localizes with nascent transcripts in the nucleolus. PIP2 binding to UBF and Fib modulates their binding to DNA and RNA, respectively. In conclusion, PIP2 interacts with a subset of Pol I transcription machinery, and promotes Pol I transcription.

Introduction

The eukaryotic nucleus is a highly structured organelle composed mainly of proteins and nucleic acids. However, in addition to these abundant molecules, the nuclear interior was also shown to contain minor components such as lipids (Rose and Frenster, 1965). Several biochemical studies (Boronenkov et al., 1998; Cocco et al., 1987; Divecha et al., 1991; Vann et al., 1997) have shown that purified nuclei contain enzymes involved in the production and degradation of phosphoininositides (PI). These studies also suggested that PIs could be divided into physically separate pools within the nucleus. Initial experiments with the antibody against PIP2 and the pleckstrin homology domain of phospholipase C δ1 (PLCδ1PH) as probes (Osborne et al., 2001; Watt et al., 2002) revealed the presence of their cognate lipid in distinct nuclear compartments such as the interchromatin granule clusters and the nucleolus. While there have been no reports on the function of nucleolar PIP2, a number of studies have shown PIP2 function in nuclear speckles (Boronenkov et al., 1998; Mellman et al., 2008; Osborne et al., 2001). Phosphatidylinositol-4-phosphate 5-kinase, type 1 alpha and a non-canonical poly (A) polymerase, called Star-PAP, were detected in the nuclear speckles where 3'-end processing of select mRNAs by Star-PAP was stimulated by PIP2 (Mellman et al., 2008). PIP2 immunodepletion from HeLa nuclear extracts caused inhibition of precursor mRNA splicing due to the loss of PIP2 and its binding partners (Osborne et al., 2001). Moreover, apart from mRNA processing, mRNA export was also shown to be regulated by PIP2 in speckles. PIP2 binding to mRNA export protein Aly directed the protein to nuclear speckles, while the disruption of PIP2 binding caused a reduction in its mRNA export activity (Okada et al., 2008). A few studies showed the involvement of PIP2 in RNA polymerase II (Pol II) transcription. In *Drosophila*, PIP2 binding to histone H1 reversed the inhibitory effect of histone H1 on transcription (Yu et al., 1998). Similarly, a Drosophila trithorax group protein, ASH2, binding to nuclear phosphatidylinositol 4-phosphate 5-kinase, called SKTL, was shown to be involved in maintaining transcriptionally active chromatin via reducing histone H1 hyperphosphorylation (Cheng and Shearn, 2004). In mammalian cells, PIP2 was found to bind only the hyperphosphorylated active form of Pol II (Pol IIO), implying its role in Pol II transcription (Osborne et al., 2001). PIP2 was required for activation of SWI-SNF like BAF complex binding to nuclear matrix/chromatin in actin-dependent manner (Zhao et al., 1998). PIP2 also facilitated

the synthesis of filamentous actin in the nucleus by interfering with BRG1-actin binding at the C-terminus of BRG1 (Rando et al., 2002). Even though PIP2 presence was shown in the nucleolus (Mortier et al., 2005; Osborne et al., 2001), nucleolar PIP2 function has not been yet investigated. The nucleolus is composed of well-defined subdomains such as fibrillar centers (FCs), a dense fibrillar component (DFC), and a granular component (GC). Transcription of pre-ribosomal genes takes place at the FC/DFC border while ribosomal subunits assemble in the GC (Nemeth and Langst, 2011). Nucleoli are formed around nucleolar organizer regions (NORs), which contain tandem rRNA gene repeats. Each ribosomal gene unit usually consists of a transcribed sequence and an external non-transcribed spacer (Liau and Perry, 1969). Even though 400 copies of rDNA exist in diploid somatic cells, only a small fraction is transcribed and the transcription is driven by Pol I upon binding to UBF together with the SL1 complex at the enhancer region of rDNA. UBF binds to rDNA not only at the promoter, but also in the transcribed region, and it is involved in the formation of open chromatin structures at actively transcribed genes (Denissov et al., 2011). Since UBF recruitment to UBF-binding site arrays outside the nucleolus forms pseudo-NORs (Mais et al., 2005), it is suggested that UBF is involved in structural organization of rDNA for the assembly of FC and DFC regions.

Upon transcription initiation, rRNA transcripts proceed through several maturation stages before ribosomal subunit assembly (Mayer and Grummt, 2006). In the early stages of rRNA processing, Fib, being a component of ribonucleoprotein complex called box C/D small nucleolar RNP, binds to precursor rRNA in the DFC region and functions in site-specific 2'-*O*-methylation of rRNA (Hernandez-Verdun, 1991). Mutations affecting Pol I elongation also have an effect on precursor rRNA cleavage by the Spt4-Spt5 complex in yeast linking both machineries (Anderson et al., 2011; Schneider et al., 2006; Schneider et al., 2007). Fib is recruited to nucleoli upon transcription initiation in telophase, and its presence at this point of the cell cycle was shown to be essential for cell survival (Dundr et al., 1997; Kopp et al., 2007).

Here we document that PIP2 interacts directly or indirectly with Pol I in the nucleolus. We also show that direct binding of PIP2 to UBF and Fib may change their respective conformation and thus the ability to bind nucleic acids. Moreover, nascent rRNAs co-localize with PIP2 in vivo, and in vitro ribosomal gene transcription is compromised when PIP2 is depleted. Addition of exogenous PIP2 can rescue the transcription inhibition while exogenous IP3 [Ins (1,4,5)P3] and

DAG have no effect. Pre-incubation with anti-PIP2 antibodies and PIP2 depletion by addition of PLC before transcription initiation abolishes nucleolar transcription. These results indicate that PIP2 might be involved in Pol I transcription by interacting with pre-rRNA production and processing machineries.

Results

PIP2 is required for optimal Pol I transcription in vitro

Based on existing evidence suggesting involvement of PIP2 in Pol II transcription (Yu et al., 1998), we investigated PIP2 influence on Pol I transcription using several strategies for in vitro transcription assays. When anti-PIP2 antibody was added to in vitro transcription assay, the level of Pol I transcription was reduced by more than 80% (Fig. 1A, lane 2). On the other hand, anti-histone H3 antibody, which was used as a control antibody at similar concentration, had a minor inhibitory effect on transcription (Fig. 1A, lane 3). It was possible to neutralize the inhibitory effect of anti-PIP2 antibody in transcription by pre-blocking the antibody with PIP2 before its addition to the transcription reaction in a dose-dependent manner (Fig. S1). We then tested if degradation of existing nuclear PIP2 by phospholipase C (PLC) enzyme has an effect on transcription. Indeed, the addition of purified PLC to the nuclear extract prior to transcription initiation (before the addition of nucleotides) caused almost 60% inhibition in transcription, while the addition of the PLC at the time of transcription initiation (after the addition of nucleotides) showed no significant effect as seen in Fig. 1B. To further test the effect of PIP2 on transcription we compared Pol I transcription levels using nuclear extracts in which PIP2 was depleted using GST-tagged PLCδ1PH domain. The PLCδ1PH domain binds to the PIP2 head group with a high affinity and a single basic amino acid replacement in the N-terminal part of the domain (R40A) results in the abolishment of PIP2 binding (Yagisawa et al., 1998). When PLCδ1PH domain was added to the nuclear extract, Pol I transcription was reduced significantly as compared to nuclear extract where PIP2-binding mutant PLCδ1PH domain was added (Fig. 1C). PIP2 cleavage by nuclear PLCs results in the production of second messengers (IP3 and DAG) in the nucleus (for review see Irvine, 2003). In order to confirm that PIP2 or products of PIP2 cleavage are the executive molecules in Pol I transcription modulation, PIP2, IP3 or DAG were added into PIP2

depleted extract and used for in vitro transcription assays. While IP3 and DAG addition showed no effect on transcription, PIP2 addition significantly restored (~50%) Pol I transcription in PIP2-depleted extracts However, PI3P or PI4P addition resulted in only 15% increase in transcription (Fig. 1D). These results clearly show that PIP2 acts in Pol I transcription directly, but not as a source for second messengers. The PIP2 presence on the promoter along with the transcription machinery was checked at different stages of transcription using the rDNA promoter bound to magnetic beads. Addition of GST-tagged PLCδ1PH domain to the transcription reaction showed the presence of PIP2 at the transcription machinery on the promoter when successful transcription was achieved by the addition of all four rNTPs (N) as shown in Fig. 1E, lane 9. Alternatively, when only ATP (A) was added to the transcription mixtures during transcription preinitiation to promote the phosphorylation required before the transcription, there was no detectable PIP2 level on the promoter as seen in Fig. 1E, lane 6. When PIP2-binding mutant PLCδ1PH domain was added to the transcription reaction, there was no staining with anti-GST antibody, indicating the inability of mutant domain to bind to PIP2 (Fig. 1E, lanes 7 and 10). The amounts of Fib, BRG1, and TBP on the promoter were approximately 2x higher during transcription compared to preinitiation reactions. The presence of PIP2 in transcription complexes on the promoter region was also directly shown in TLC after lipid extraction (Fig. 1F). In summary, this is the first report showing that PIP2 is a part of Pol I transcription machinery on the promoter and promotes Pol I transcription in vitro.

PIP2 participates in the formation of Pol I transcription foci

PIP2 presence in the nucleolus has been previously shown by Osborne et al. (2001) and Mortier et al. (2005), however, there has been no report on the interacting partners and functions of nucleolar PIP2. Since PIP2 was found to be a part of the transcription machinery on the promoter during rDNA transcription, we continued to identify the components of Pol I transcription machinery that interact with PIP2. For this purpose, GST-tagged PLCδ1PH domain and its PIP2-binding mutant were added to the nuclear extract and pulled down by glutathione beads. Since wild type PLCδ1PH domain can bind to PIP2, but not the mutant form, proteins pulled down by only wild type PLCδ1PH domain were considered as interacting partners of PIP2. As a second approach, PIP2-coupled agarose beads and control agarose beads were used for pull-down experiments. For microscopy studies, anti-PIP2 antibody or GST-tagged PLCδ1PH domain and

anti-GST antibody were used. The use of recombinant PLCδ1PH domain as a PIP2 probe provided a reliable and consistent staining of PIP2 on the plasma membrane (Fig. 2A) and in the nucleus and nucleolus (Fig. 2B), while the mutant PLCδ1PH domain which does not bind to PIP2 did not provide a signal with immunofluorescent staining (Fig. 2B), thus proving the specificity of PLCδ1PH domain binding.

Pull-downs with PLCδ1PH domain showed that PIP2 and the largest subunit of Pol I (RPA116) are present in the same complex (Fig. 2C and Fig. S2). In agreement, the immunofluorescence detection in U2OS cells showed PIP2 in concrete foci in the nucleolus together with Pol I (Fig. 2D). The co-localization of PIP2 and Pol I is documented by the intensity profile showing that fluorescence maxima of both proteins along the line crossing nucleolus clearly coincide (Fig. 2D). On the other hand, TBP and TAF 95/110 which are also members of transcription initiation machinery were not detected in the protein complex along with PIP2 (Fig. 2E and Fig. S3), indicating that PIP2 interacts with a subset of proteins of Pol I transcription machinery. This selective composition of PIP2-bound protein complex is also reflected in PIP2 localization in the nucleolus. Fib is localized to DFC where transcription takes place while B23 is localized in GC where ribosomal subunits assemble (Nemeth and Langst, 2011). Since Fib is present in PIP2-protein complex and B23 is absent (Fig. 2E), we suggest that the restricted PIP2 localization to the transcriptionally active sites of the nucleolus might be dictated by the binding partners of PIP2.

UBF and Fib are both essential components of rRNA biogenesis during Pol I transcription initiation and early steps of rRNA maturation, respectively. We pulled both of them down from nucleolar extracts via PIP2-coupled agarose beads (Fig. 3A and Fig. S4). After cheking the specificity of the antibodies (Fig. S5), co-localization studies of PIP2 with UBF and Fib were performed. PLCδ1PH domain showed a prominent co-localization of PIP2 with UBF and Fib in the nucleoli of interphase cells as documented by the corresponding intensity profiles (Fig. 3B). In addition, superresolution structured illumination microscopy (SIM) allowed us to demonstrate PIP2 co-localization with UBF and Fib in subnucleolar, due to its higher resolution as compared to confocal microscopy (Fig. 3C). In order to improve the resolution even further, immunoelectron microscopy (IEM) revealed PIP2 co-localization with UBF in the inner space of FCs where proteins involved in rDNA transcription reside, and on the border between FC and

DFC where rDNA transcription takes place. PIP2-Fib co-localization was detected in the DFC region (Fig. 3D). To reveal the fine details of nucleolar compartmentalization in terms of PIP2 localization, 3D electron tomography was used, which demonstrated that PIP2-containing structures are found between individual FCs through the DFC and stretch out to the nucleoplasm as seen in Fig. 3E and in Movie 1 in supplementary material. These results support the data showing PIP2 involvement in rRNA biogenesis. In accordance with our previous observation showing the absence of B23 in PIP2 pull-down (Fig. 2E), PIP2 was not detected in GC, suggesting that PIP2 is not involved in the late maturation of pre-ribosome particles.

Even though proteins involved in ribosomal gene transcription and rRNA processing were shown to be interacting with PIP2, it was not clear if these interactions were direct. We therefore probed for direct interactions of PIP2 with recombinant UBF and Fib (Fig. 4A) on nitrocellulose membranes where PIP2 and PI4P were spotted. The results clearly showed direct binding of UBF and Fib to PIP2, but not to PI4P (Fig. 4B). As a control, we used recombinant OSH1PH domain (Fig. 4A), which binds to PI4P with high affinity (Roy and Levine, 2004), and importin 5 (Imp 5, Fig. 4A). OSH1PH was found to bind to PI4P with greater affinity than to PIP2, while Imp 5 did not show any binding to either PI4P or PIP2 (Fig. 4B). To clearly show direct protein-lipid interaction, we performed pull-down experiments with the recombinant proteins (UBF, Fib and Imp 5) using PIP2-coupled agarose beads and control agarose beads. Recombinant UBF and Fib were pulled down by PIP2, while Imp 5 failed to bind to PIP2 (Fig. 4C, Fig. S6-1, Fig. S6-2 and Fig. S6-3). In addition, trypsin digestion of UBF and Fib showed that PIP2 binding blocked a particular region of UBF for trypsin accessibility (Fig. 4D), while PIP2 binding to Fib resulted in higher accessibility for trypsin (Fig. 4E). These changes in digestion patterns point to the alteration of conformation or protection at certain sites of UBF and Fib due to binding to PIP2.

In order to understand the effect of PIP2 binding on UBF-rDNA interaction, footprinting experiment was carried out by incubating purified recombinant UBF with PIP2, IP3 or DAG. Upon PIP2 binding, the overall binding of UBF to rDNA was reduced and a more selective footprint to the UBF binding sequence was observed (Fig. 4F, lane 4) compared to DAG (Fig. 4F, lane 2) or IP3 (Fig. 4F, lane 3). Normalized densitometric profiles of the footprint (left panel) show tighter binding of UBF with PIP2 at the UBF footprint sequence as compared to all the other conditions (Fig. 4F).

The influence of PIP2 on the binding of Fib to U6 small nuclear RNAs (snRNAs) was further investigated in gel shift mobility assays (Fig. 4G and Fig. S7). The mobility of the Fib/U6 snRNA complex was altered in the gel during electrophoresis upon addition of PIP2, thus suggesting changes in RNA topology or other alterations resulting from PIP2 binding to Fib (Fig. 4G). Densitometric profile of the gel shift assay (below) clearly shows the increase in mobility of U6 snRNA/Fib complex upon binding to PIP2 as shown by the arrows at the peaks in the density profile (Fig. 4G).

PIP2 co-localizes with rRNA nascent transcripts in nucleoli

To assess the presence of PIP2 during early steps of rDNA transcription, we visualized nascent rRNA transcripts by short pulse incorporation of BrUTP in permeabilized cells. A clear co-localization between PIP2 and Br-rRNA was observed by immunofluorescence (Fig. 5A) and IEM (Fig. 5B). The labeling of nascent rRNA and PIP2 showed that both localize at the border between FC and DFC and in the DFC. PIP2 and Br-rRNA clusters were intermingled; most of the transcription signals were associated with PIP2 signal. However, there were also zones in DFC where only PIP2 labeling was present (Fig. 5B). These results demonstrate the presence of PIP2 at the sites of nucleolar transcription in situ and, in parallel with the in vitro data, show the importance of PIP2 for rDNA transcription and possibly nucleolar compartmentalization.

Discussion

PIP2 is the source of the second messengers IP3 for intracellular Ca^{2+} mobilization and DAG for protein kinase C activation. In addition to the role of PIP2 in cytoplasmic signal transduction, the presence of its biosynthetic machinery inside the nucleus indicates a distinct nuclear signaling pathway (Irvine, 2003). The presence of phospholipids in the nucleus was shown more than 70 years ago (Stoneburg, 1939), however, little is known about their physico-chemical properties and functions in the nucleus. Since there are no membranous structures inside of the nucleus, it is suggested that proteins with hydrophobic pockets bind to PIPs to protect them from the hydrophilic environment (for review see Irvine, 2003). Here we demonstrate that PIP2 binds to some of the principal components of the Pol I transcription machinery and is anchored via these interactions in the fibrillar regions of the nucleolus where rDNA transcription occurs.

Over the years, only few studies reported the involvement of PIP2 in Pol II transcription. PIP2 addition was shown to promote Pol II transcription (Yu et al., 1998) and the binding of chromatin remodeling complex to DNA (Zhao et al., 1998). However, there have been no reports on the modulation of Pol I transcription by PIP2. Therefore, we first tested if PIP2 is required for Pol I transcription. Pol I transcription inhibition by the addition of either anti-PIP2 antibody or PLC enzyme indicated the involvement of PIP2 in Pol I transcription. We also observed a reduction in Pol I transcription upon depletion of PIP2, which was reversed by the addition of exogenous PIP2 to the depleted extract, but not by the addition of IP3 and DAG. Taken together, our data suggest that PIP2 acts as itself in Pol I transcription rather than as a substrate of nuclear PI-PLC, since neither IP3 nor DAG rescue the inhibitory effect of PIP2 depletion in Pol I transcription.

The presence of PIP2 on the Pol II promoter was recently shown by Toska et al. (2012). BASP1 binding to PIP2 was shown to be required for the interaction with HDAC1 which resulted in the recruitment of HDAC1 to the promoter of WT1-targeted genes to repress transcription of Pol II (Toska et al. 2012). Here we report for the first time the presence of PIP2 in the transcription complex on the promoter during Pol I transcription. Pol I, UBF and Fib were detected in PIP2-bound protein complex while TBP and TAF 95/110 were not. This result indicates that instead of binding to the whole transcription machinery, PIP2 selectively binds to a subset of proteins involved in transcription. We found that PIP2 binds directly to UBF and they co-localize in FC region. UBF is a scaffold protein that binds to rDNA promoter and bends it to establish proper DNA-protein structure (Stefanovsky et al. 2001). According to the model proposed by Denissov et al. (2011), together with other components of SL1 complex, UBF creates a core-helix DNA structure where the transcribed regions are cylindrically wrapped around. Pol I initiates the transcription in the core and elongates along the cylindrical helix (Denissov et al., 2011). In addition, UBF is required for the formation of secondary constrictions of NORs (Mais et al., 2005). Since PIP2 binding to UBF results in a somewhat tighter binding to rDNA promoter, it is plausible that the interaction between PIP2 and UBF has a regulatory role in the formation of transcription initiation complex at the rDNA promoter.

Fib is known to have a role in nucleolar assembly by gathering prenuclear bodies together (Fomproix et al., 1998). Direct binding of PIP2 to Fib caused an increase in the mobility of U6 snRNA/Fib complex, but did not significantly affect the amount of bound complex under the

assay conditions. The change in mobility may arise from the altered physico-chemical properties of the complex due to PIP2 addition, or from conformational changes in Fib as suggested by the trypsin digestion in Fig. 4E. Similarly, it was reported that conformational opening of ezrin upon binding to PIP2 results in more extensive contacts with F-actin (Jayasundar et al., 2012). Since PIP2 localization is restricted to the transcriptionally active regions in the nucleolus, we suggest that a particular hydrophobic protein-lipid-RNA enviroment might exist in that particular region and contribute to the detergent-resistant nuclear PIP2 pools, which were shown to make up to 40% of the total PIP2 mass (Vann et al., 1997). The morphology of nuclear speckles was shown to be dependent on PIP2 binding to PDZ domain of syntenin-1 (Mortier et al., 2005). Therefore, it is likely that PIP2 also contributes to the formation of transcriptionally active sites of the nucleolus and acts as a structural interface between the nucleolar skeletal elements (like FC) and the macromolecular complexes involved in rDNA transcription and in early rRNA processing (FC/DFC interphase and DFC).

Our observation that nascent rRNA co-localizes with PIP2 contributes to a conclusion that PIP2 is associated with transcription machinery on active rDNA and has a role in Pol I transcription as well as in early stages of rRNA maturation. RNA was shown to be required for the localization of PIP2 to nuclear speckles (Osborne et al., 2001), and therefore it was suggested that the interaction with RNA/protein complex might stabilize PIP2 in the absence of intranuclear membranous structures. Similarly, PIP2 might be tethered within the nucleolus by the interaction with nascent rRNA transcripts and Fib, bridging the processes of nascent transcript production and early processing. To our knowledge, this is the first report on PIP2 involvement in Pol I transcription and rRNA processing.

All these findings led us to suggest a model in which PIP2 modulates UBF binding to rDNA, and Fib binding to rRNA. Upon active transcription Fib binds to PIP2 and associates with nascent rRNA in a Fib complex to enforce methylation for further rRNA processing. PIP2 may act as a bridge between Pol I, UBF and Fib to connect transcription initiation and early maturation steps. After the initial methylation, the Fib complex may release the rRNA to be further processed in the GC region (Fig. 6). The link between RNA synthesis and maturation may dictate nucleolar structures in the FC and DFC regions, where PIP2 may form a framework which allows gathering of proteins to work in concert for efficient transcription of ribosomal RNA genes.

Materials and methods

Cell culture

Human osteosarcoma (U2OS) cells and cervical carcinoma (HeLa) cells were kept in DMEM with 10% fetal calf serum in 5% CO_2/air, 37°C, humidified atmosphere.

Plasmids

GST-tagged PLCδ1PH (1-140) (pGST3) and PLCδ1PH-Mut (R40A), which lacks binding to PIP2, were provided by Dr. Hitoshi Yagisawa (Yagisawa et al., 1998). pECHU plasmid was constructed by PCR of the human rDNA promoter (-514 to +20) from prHU3 with EcoRI-XhoI site into pEC111/80 (Castano et al., 2000) after the HIV LTR promoter removal. prHU3 was a kind gift from Dr. Lucio Comai. UBF1 (gift from Dr. Sui Huang) and Fib were cloned into pET15b vector for protein purification studies. In order to produce recombinant protein, OSH1PH domain (gift from Dr. Tamas Balla) was cloned into pET42a(+) vector. Imp 5 in pQE30 vector was received from Dr. Dirk Görlich (Jäkel and Görlich, 1998).

Expression and purification of recombinant proteins

Recombinant Fib, UBF, PLCδ1PH and PLCδ1PH-Mut were expressed in *Escherichia coli (E. coli)* BL21 (DE3)-pLysS (Stratagene, La Jolla, CA, USA). Both UBF and Fib had histidine tags and were purified over Ni-agarose in a buffer (20mM Tris pH 8, 0.1 mM EDTA, 20% glycerol, 500 mM NaCl, 0.1% NP40, 1 mM DTT). UBF was further purified by passing through Q sepharose fast flow column (17-0510-10, GE Healthcare, Uppsala, Sweden) followed by SP sepharose fast flow column (17-0729-10, GE Healthcare, Uppsala, Sweden). For GST-tagged PLCδ1PH and PLCδ1PH-Mut, the purification was carried on glutathione-agarose column (G4510, Sigma Aldrich, St. Louis, MO, USA), which had been equilibrated with BC100 (20 mM Tris pH 8, 0.1 mM EDTA, 20% glycerol, 100 mM NaCl). Proteins were eluted with 50 mM Tris-HCL, pH 8 having 0.1g reduced L-Glutathione (G4251, Sigma Aldrich, St. Louis, MO, USA).

11 mg of partially purified PLC from *Clostridium perfrigens* (*C. welchii*) (P7633-125 UN, Sigma Aldrich, St. Louis, MO, USA) was further purified by passing through SP sepharose fast flow column followed by Q sepharose fast flow column. Proteins were eluted in a KCl gradient at 500 mM.

Recombinant OSH1PH domain was expressed in Rosetta™(DE3)pLysS competent cells (70956, Millipore EMD, Billerica, MA, USA) and purified over glutathione-agarose column followed by Ni-agarose column. Elution from Ni-agarose column was performed in a buffer consisted of 25 mM HEPES, pH 8, 100 mM NaCl and 250 mM imidazole.

Recombinant Imp 5 was expressed in Qiagen Rep4 strain of *E. coli* and purified over Ni-agarose column as described previously (Kutay et al., 1997).

Confocal microscopy

Primary antibodies: Anti-GST antibody (gift from Dr. Igor Shevelev; 5 µg/ml), anti-PIP2 antibody (2C11, Abcam, Cambridge, UK; 16 µg/ml), anti-Fib antibody (38F3, Abcam, Cambridge, UK; dilution 1:100), anti-UBF antibody (sc13125, Santa Cruz Biotechnology, Inc, CA, USA; 2 µg/ml), anti-RPA116 antibody (gift from Dr. Ingrid Grummt; 2µg/ml). Secondary antibodies: Donkey anti-mouse IgG conjugated with Alexa 488 (Invitrogen, CA, USA), goat anti-rabbit IgG conjugated with Alexa 647 (Invitrogen, CA, USA) and donkey anti-mouse IgM conjugated with Cy3 (Jackson ImmunoResearch Laboratories Inc., West Grove, PA, USA). Images were taken using a confocal microscope (Leica TCS SP5 AOBS TANDEM, Germany) with 100x (NA 1.4) oil immersion objective lense. In order to test the specificity of the primary antibodies, anti-UBF, anti-Fib and anti-PIP2 antibodies were preblocked with an excess amount of purified UBF, Fib and PIP2, respectively. Preblocking incubations were performed in PBS with 1% BSA. After 30 min incubation, immunostaining was performed with these preblocked primary antibodies.

IEM

Primary antibodies used in IEM were already described in confocal microscopy section. Secondary antibodies: Goat anti-mouse IgG (H+L chains) antibody coupled with 6 nm colloidal gold particles, goat anti-mouse IgM (µ-chain specific) antibody coupled with 12 nm colloidal gold particles, goat anti-rabbit IgG (H+L chains) antibody coupled with either 6 nm or 12 nm colloidal gold particles (Jackson ImmunoResearch Laboratories Inc., West Grove, PA, USA). The thin sections (70-90 nm) were examined by a FEI Morgagni 268 transmission electron microscope at 80 kV. The images were captured with Mega View III CCD camera. Multiple sections of at least three independent immunogold labeling experiments were analyzed.

Detection of transcription sites by confocal microscopy and IEM

Bromouridine triphosphate (BrUTP; Sigma Aldrich, St. Louis, MO, USA) incorporation was performed as described previously (Pombo et al., 1999). For Br-RNA labeling anti-bromodeoxyuridine antibody IgG1 (BMC9318, Roche Diagnostics GmbH, Mannheim, Germany; 20 µg/ml) was used.

SIM

Images were taken with a superresolution structured illumination microscope (ELYRA PS.1, Carl Zeiss, Munich, Germany) with Plan-Apochromat 63x/1.4 Oil DIC M27 oil immersion objective lens using the parameters as follows: number of SIM rotations - 5; SIM grating periods varied according to the excitation wavelength from 34.0 µm to 42.0 µm

PIP strips

Purified UBF, Fib, OSH1PH domain and Imp 5 were tested on PIP Strips (Echelon Biosciences Inc, CA, USA). The membranes were blocked with 5 ml of blocking buffer (PBST, 3% BSA) for 1 h at RT. UBF and Fib were added in 5 ml blocking buffer over night at 4°C. After binding, membranes were washed 3 times with PBST and followed the same protocol as Western blots.

Limited protease digestion assay

Purified UBF (100 ng) and Fib (200 ng) were incubated for 30 min at RT with or without PIP2 (1 µg) in BC100 buffer. After the incubation, trypsin (0.5 ng) was added and the mixtures were incubated for 1 min at 4°C, as indicated. The digestion reactions were stopped by adding 10 µl Laemmli buffer (0.25 M Tris, pH 6.8, 20% glycerol, 5% mercaptoethanol, 2% SDS, 0.025% bromophenol blue) and the samples were denatured at 95 °C for 5 min, electrophoresed through a 15% SDS-PAGE. Western blot was carried out as described previously.

Footprint

10 ng of radioactively end labeled PCR reactions from rDNA -514 to 100 from prHU3 were used as template for binding to purified UBF (100 ng) in the presence or absence of added compounds with the amounts mentioned in the legends for 30 min at 4°C in a buffer containing 20 mM Tris pH 7.4, 1 µg pUC 18, 5% glycerol, protease inhibitors. After binding, the reactions were digested with 1 unit of DNAse I (Fermentas, MA, USA) for 1 min at 4°C, followed by phenol/chloroform

extraction and ethanol precipitation. Purified DNA was run on a 6% PAGE with 6M urea. Footprint image was analyzed as previously published (Hofmann et al. 2011). For quantitative analysis of the footprint, ImageJ 1.42q software was used. We normalized the plot using the measurements from the non-UBF binding region of the footprint for each lane.

Gel shift

Radioactively labeled U6 snRNA (40 Kcpm, gift from Dr. Gary R. Kunkel) was used as a template for binding to purified Fib (200 ng). The reactions were incubated on ice for 30 min then loaded onto a 1% agarose gel and ran in cold room for 2 h at 40 V. Bands were visualized by autoradiography. For quantitative analysis of the gel shift, ImageJ 1.42q software was used. Photoshop was used to assign a particular color for each plot profile and compiled into one plot for easier comparison.

In vitro pull-down of PIP2

Nuclear and nucleolar lysates were prepared from HeLa cells as previously described (Andersen et al., 2002). Nuclear lysates were incubated with glutathione agarose beads (G4510, Sigma Aldrich, St. Louis, MO, USA) in the presence of GST-tagged PLCδ1PH and PLCδ1PH-Mut for 2 h or overnight at 4^{o}C and washed thoroughly with 10 mM HEPES pH 7.9, 1 mM $MgCl_2$, 0.5 mM DTT. Nuclear and nucleolar lysates were incubated with control agarose beads or agarose beads coupled with PIP2 (Echelon Biosciences Inc, CA, USA) for 2 h at 4^{o}C and thoroughly washed with RIPA buffer (50 mM Tris, pH 7.5, 150 mM NaCl, 1% NP-40, 0.5% DTT and protease inhibitors). Beads were boiled in Laemmli buffer for 5 min and resolved by SDS-PAGE for immunoblotting detection. In order to check direct interactions between proteins and PIP2, recombinant proteins (approximately 2 µg of recombinant protein used in each incubation) were incubated with control agarose beads or PIP2-coupled agarose beads which were previously blocked with 1% BSA in PBS. The beads were then thoroughly washed with BC100 buffer and were boiled in Laemmli buffer for 5 min and resolved by SDS-PAGE for immunoblotting detection.

In vitro transcription assays

Run-off transcription assays were performed using HeLa nuclear extracts or HeLa nuclear extracts depleted for PIP2 using PLCδ1PH coated beads and as a control PLCδ1PH-Mut coated

beads used for depletion. The reactions contained 15 mM HEPES pH 7.9, 100 mM KCl, 5 mM $MgCl_2$, 10% glycerol, 1 mM DTT, 0.1 mM EDTA, 100 μg/ml of α-amanitin, 100 mg/ml β-cyclodextrin, in the presence or absence of added compounds with the amounts mentioned in the legends. Extracts were incubated at 25°C for 20 min before initiating the transcription reaction by adding 500 μM ATP, GTP, CTP, 50 μM UTP, [α-32P] UTP (8 Ci/mmol) and 100 ng of prHU3 plasmid digested with SalI endonuclease. PLC was added before or after nucleotides as stated in the figure legend. The reactions were incubated for 1 h at 30°C and transcripts were purified by phenol extraction and ethanol precipitation. The RNA was electrophoretically resolved on a 6% acrylamide sequencing gel with 6M urea and visualized and quantified with a PhosphorImager. For quantitative measurement of each band, background was subtracted and each lane was normalized to a labeled primer, which was added as an internal loading control. The data were compared in two independent experiments. Having set the initial control condition at 100%, the plots represent the mean of each measurement and standard error of the mean for each condition.

In order to assay if PIP2 was bound to the transcription machinery on the promoter during the in vitro transcription, rDNA promoter region was produced by using biotinylated F-primer 5`CCAACGCGTTGGATGCATAGCTT 3´ and R-primer 5`ATCCTTTTTGATAATCTCATGACC3, bound to streptavidin coupled magnetic beads (Dynabeads MyOne Streptavidin C1, 650.01, Invitrogen, CA, USA) and blocked with 5% BSA. The beads were then incubated with HeLa nuclear extract in a transcription buffer without nucleotides. For PIP2 detection purified PLCδ1PH or PLCδ1PH-Mut domains were also added to the nuclear extracts. The beads were incubated with nuclear extracts for 1 h. After incubation of the beads, half of the reactions were allowed to transcribe in the presence of only ATP or all the rNTPs to distinguish between transcription initiation and elongation, respectively. Afterwards, the beads were washed six times with wash buffer and loaded onto a SDS-PAGE for Western blot analysis.

Thin layer chromatography for PIP2 in cell free system

In vitro transcription reactions were carried out using rDNA promoter region or control DNA which is a part of the vector pGEM7z+ bound to magnetic beads and blocked with 5% BSA. The beads were then incubated with nuclear extract in a transcription buffer with only ATP or all the rNTPs. After transcription, the beads were washed and lipid extractions were processed. We used

an earlier published protocol (Yu et al., 1998) to extract PIP2 from bound protein followed by loading on TLC plates that were gently soaked in 1% (w/v) potassium oxalate and dried. The solution for separation was 90:90:7:22 (CHCl3:MeOH:NH3OH:H20; v/v/v/v). TLC was then stained with acidic phosphomolibdate solution.

3D electron tomography of PIP2 in nucleolus

For 3D electron tomography, HeLa cells were grown on coverslips and fixed with 4% PFA for 15 min, permeabilized in 0.5% Triton-X-100 for 5 min, washed in PBS and blocked in the mixture of 5% BSA, 5% NGS, and 0.1% fish gelatin for 10 min. Then, cells were washed with the incubation buffer (0.1% BSA, pH 7.4) and incubated with a primary antibody overnight at +4^{o}C. After thorough washes, cells were incubated with a secondary antibody conjugated to ultra-small (0.8 nm) gold particles (Aurion, Wageningen, The Netherlands). Then, cells were washed in the incubation buffer, additionally fixed in 2% glutaraldehyde, washed in distilled water and silver-enhanced using the Aurion kit for 45 min. After washing in distilled water, cells were dehydrated in ethanol series and embedded in epon resin by standard procedure. 400-nm sections were cut with ultra microtome for single-axis electron tomography. The tilt series were acquired using TECNAI G2 20 LaB6 electron microscope (FEI, Eindhoven, The Netherlands) operated at 200 kV. The tilt series were aligned using the Inspect 3D software (FEI). Visualization was done using the Amira software (Visage Imaging GmbH, Berlin, Germany).

Acknowledgements

We thank Pavel Kříž, Iva Jelínková and Ivana Nováková for excellent technical assistance. We thank Anatolij A. Philimonenko and Karel Janoušek for their help with 3D tomography. We thank Dr. Sui Huang, Dr. D. Hernandez-Verdun, Dr. Hitoshi Yagisawa, Dr. Tamas Balla, Dr. Lucio Comai, Dr. Igor Shevelev, Dr. Ingrid Grummt, Dr. Gary R. Kunkel for sharing plasmids and antibodies with us. We also thank Dr. Jacques Paysan for his help with SIM. This work was supported by the Grant Agency of the Czech Republic (P305/11/2232, 204/09/H084), Ministry of Education, Youth and Sports of the Czech Republic (LC545, LC06063), CONACYT (176598) and IMG institutional grant (RVO68378050).

References

Andersen, J. S., Lyon, C. E., Fox, A. H., Leung, A. K., Lam, Y. W., Steen, H., Mann, M. and Lamond, A. I. (2002). Directed proteomic analysis of the human nucleolus. *Curr. Biol.* **12**, 1-11.

Anderson, S. J., Sikes, M. L., Zhang, Y., French, S. L., Salgia, S., Beyer, A. L., Nomura, M. and Schneider, D.A. (2011). The transcription elongation factor Spt5 influences transcription by RNA polymerase I positively and negatively. *J. Biol. Chem.* **286**, 18816-18824.

Boronenkov, I. V., Loijens, J. C., Umeda, M. and Anderson, R. A. (1998). Phosphoinositide signaling pathways in nuclei are associated with nuclear speckles containing pre-mRNA processing factors. *Mol. Biol. Cell* **9**, 3547-3560.

Castano, E., Gross, P., Wang, Z., Roeder, R. G. and Oelgeschlager, T. (2000). The C-terminal domain-phosphorylated IIO form of RNA polymerase II is associated with the transcription repressor NC2 (Dr1/DRAP1) and is required for transcription activation in human nuclear extracts. *Proc. Natl. Acad. Sci. USA* **97**, 7184-7189.

Cheng, M. K. and Shearn, A. (2004). The direct interaction between ASH2, a Drosophila trithorax group protein, and SKTL, a nuclear phosphatidylinositol 4-phosphate 5-kinase, implies a role for phosphatidylinositol 4,5-bisphosphate in maintaining transcriptionally active chromatin. *Genetics* **167**, 1213-1223.

Cocco, L., Gilmour, R. S., Ognibene, A., Letcher, A. J., Manzoli, F. A. and Irvine, R.F. (1987). Synthesis of polyphosphoinositides in nuclei of Friend cells. Evidence for polyphosphoinositide metabolism inside the nucleus which changes with cell differentiation. *Biochem. J.* **248**, 765-770.

Denissov, S., Lessard, F., Mayer, C., Stefanovsky, V., van Driel, M., Grummt, I., Moss, T. and Stunnenberg, H.G. (2011). A model for the topology of active ribosomal RNA genes. *EMBO Rep.* **12**, 231-237.

Divecha, N., Banfic, H. and Irvine, R. F. (1991). The polyphosphoinositide cycle exists in the nuclei of Swiss 3T3 cells under the control of a receptor (for IGF-I) in the plasma membrane, and stimulation of the cycle increases nuclear diacylglycerol and apparently induces translocation of protein kinase C to the nucleus. *EMBO J.* **10**, 3207-3214.

Dundr, M., Meier, U. T., Lewis, N., Rekosh, D., Hammarskjold, M. L. and Olson, M. O. (1997). A class of nonribosomal nucleolar components is located in chromosome periphery and in nucleolus-derived foci during anaphase and telophase. *Chromosoma* **105**, 407-417.

Fomproix, N., Gebrane-Younes, J. and Hernandez-Verdun, D. (1998). Effects of anti-Fib antibodies on building of functional nucleoli at the end of mitosis. *J. Cell Sci.* **111**, 359-372.

Hernandez-Verdun, D. (1991). The nucleolus today. *J. Cell Sci.* **99**, 465-471.

Hofmann, N., Wurm, R. and Wagner, R. (2011). The E. coli anti-sigma factor Rsd: studies on the specificity and regulation of its expression. *PLOS One* **6**(5):e19235.doi:10.1371/journal.pone.0019235

Irvine, R. F. (2003). Nuclear lipid signalling. *Nat. Rev. Mol. Cell Biol.* **4**, 349-360.

Jayasundar, J. J., Ju, J. H., He, L., Liu, D., Meilleur, F., Zhao, J., Callaway, D. J. and Bu, Z. (2012). Open conformation of ezrin bound to phosphatidylinositol 4,5-bisphosphate and to F-actin revealed by neutron scattering. *J. Biol. Chem*. **287**, 37119-37133**.**

Jäkel, S. and Görlich, D. (1998). Importin beta, transportin, RanBP5 and RanBP7 mediate nuclear import of ribosomal proteins in mammalian cells. *EMBO J.* **17**, 4491-4502.

Kopp, K., Gasiorowski, J. Z., Chen, D., Gilmore, R., Norton, J. T., Wang, C., Leary, D. J., Chan, E. K., Dean, D. A. and Huang, S. (2007). Pol I transcription and pre-rRNA processing are coordinated in a transcription-dependent manner in mammalian cells. *Mol. Biol. Cell* **18**, 394-403.

Kutay, U., Izaurralde, E., Bischoff, F.R., Mattaj, I.W. and Görlich, D. (1997). Dominant-negative mutants of importin-beta block multiple pathways of import and export through the nuclear pore complex. *EMBO J.* **16**, 1153-1163.

Liau, M. C. and Perry, R. P. (1969). Ribosome precursor particles in nucleoli. *J. Cell Biol.* **42**, 272-283.

Mais, C., Wright, J. E., Prieto, J-L., Raggett, S. L. and McStay, B. (2005). UBF-binding site arrays form pseudo-NORs and sequester the RNA polymerase I transcription machinery. *Genes. Dev*. **19**, 50-64.

Mayer, C. and Grummt, I. (2006). Ribosome biogenesis and cell growth: mTOR coordinates transcription by all three classes of nuclear RNA polymerases. *Oncogene* **25**, 6384-6391.

Mellman, D. L., Gonzales, M. L., Song, C., Barlow, C. A., Wang, P., Kendziorski, C. and Anderson, R. A. (2008). A PtdIns4,5P2-regulated nuclear poly(A) polymerase controls expression of select mRNAs. *Nature* **451**, 1013-1017.

Mortier, E., Wuytens, G., Leenaerts, I., Hannes, F., Heung, M. Y., Degeest, G., David, G. and Zimmermann, P. (2005). Nuclear speckles and nucleoli targeting by PIP2-PDZ domain interactions. *EMBO J.* **24**, 2556-2565.

Nemeth, A. and Langst, G. (2011). Genome organization in and around the nucleolus. *Trends. Genet.* **27**, 149-156.

Okada, M., Jang, S. W. and Ye, K. (2008). Akt phosphorylation and nuclear phosphoinositide association mediate mRNA export and cell proliferation activities by ALY. *Proc. Natl. Acad. Sci. USA* **105**, 8649-8654.

Osborne, S. L., Thomas, C. L., Gschmeissner, S. and Schiavo, G. (2001). Nuclear PtdIns(4,5)P2 assembles in a mitotically regulated particle involved in pre-mRNA splicing. *J. Cell Sci.* **114**, 2501-2511.

Pombo, A., Jackson, D. A., Hollinshead, M., Wang, Z., Roeder, R. G. and Cook, P. R. (1999). Regional specialization in human nuclei: visualization of discrete sites of transcription by RNA polymerase III. *EMBO J.* **18,** 2241-2253.

Rando, O. J., Zhao, K., Janmey, P. and Crabtree, G. R. (2002). Phosphatidylinositol-dependent actin filament binding by the SWI/SNF-like BAF chromatin remodeling complex. *Proc. Natl. Acad. Sci. USA* **99**, 2824-2829.

Rose, H. G. and Frenster, J. H. (1965). Composition and metabolism of lipids within repressed and active chromatin of interphase lymphocytes. *Biochim. Biophys. Acta.* **106**, 577-591.

Roy, A. and Levine, T.P. (2004). Multiple pools of phosphatidylinositol 4-phosphate detected using the pleckstrin homology domain of Osh2p. *J. Biol. Chem*. **279,** 44683-44689.

Schneider, D. A., French, S. L., Osheim, Y. N., Bailey, A. O., Vu, L., Dodd, J., Yates, J. R., Beyer, A. L. and Nomura, M. (2006). RNA polymerase II elongation factors Spt4p and Spt5p play roles in transcription elongation by RNA polymerase I and rRNA processing. *Proc. Natl. Acad. Sci. USA* **103**, 12707-12712.

Schneider, D. A., Michel, A., Sikes, M. L., Vu, L., Dodd, J. A., Salgia, S., Osheim, Y. N., Beyer, A. L. and Nomura, M. (2007). Transcription elongation by RNA polymerase I is linked to efficient rRNA processing and ribosome assembly. *Mol. Cell* **26**, 217-229.

Stefanovsky, V. Y., Pelletier, G., Bazett-Jones, D. P., Crane-Robinson, C. and Moss, T. (2001). DNA looping in the RNA polymerase I enhancesome is the result of non-cooperative in-phase bending by two UBF molecules. *Nucleic Acids Res*. **15**, 3241-3247.

Stoneburg, C. A. (1939). The lipids of the cell nuclei. *J. Biol. Chem.* **129**, 189-196.

Toska, E., Campbell, H. A., Shandilya, J., Goodfellow, S. J., Shore, P., Medler, K. F. and Roberts, S. G. (2012). Repression of Transcription by WT1-BASP1 Requires the Myristoylation of BASP1 and the PIP2-Dependent Recruitment of Histone Deacetylase. *Cell Rep.* **2**, 462-469.

Vann, L. R., Wooding, F. B., Irvine, R. F. and Divecha, N. (1997). Metabolism and possible compartmentalization of inositol lipids in isolated rat-liver nuclei. *Biochem. J.* **327**, 569-576.

Watt, S. A., Kular, G., Fleming, I. N., Downes, C. P. and Lucocq, J. M. (2002). Subcellular localization of phosphatidylinositol 4,5-bisphosphate using the pleckstrin homology domain of phospholipase C delta1. *Biochem. J.* **363,** 657-666.

Yagisawa, H., Sakuma, K., Paterson, H. F., Cheung, R., Allen, V., Hirata, H., Watanabe, Y., Hirata, M., Williams, R. L. and Katan, M. (1998). Replacements of single basic amino acids in the pleckstrin homology domain of phospholipase C-delta1 alter the ligand binding, phospholipase activity, and interaction with the plasma membrane. *J. Biol. Chem.* **273,** 417-424.

Yu, H., Fukami, K., Watanabe, Y., Ozaki, C. and Takenawa, T. (1998). Phosphatidylinositol 4,5-bisphosphate reverses the inhibition of RNA transcription caused by histone H1. *Eur. J. Biochem.* **251,** 281-287.

Zhao, K., Wang, W., Rando, O. J., Xue, Y., Swiderek, K., Kuo, A. and Crabtree, G. R. (1998). Rapid and phosphoinositol-dependent binding of the SWI/SNF-like BAF complex to chromatin after T lymphocyte receptor signaling. *Cell* **95,** 625-636.

Figure Legends

Fig. 1. PIP2 promotes Pol I transcription in vitro. (A) Run-off transcription reaction showed that addition of anti-PIP2 antibody (clone 2C11, Abcam, Cambridge, UK; 0.8 µg) decreases transcription levels by more than 80%. On the other hand, anti-histone H3 antibody (H0164, Sigma Aldrich, St. Louis, MO, USA; 0.5 µl) had a minor effect on Pol I transcription. (Lane 1: control transcription reaction; lane 2: transcription reaction in the presence of anti-PIP2 antibody; lane 3: transcription reaction in the presence of anti-histone H3 antibody). The charts show relative activities (mean ± SEM) normalized to an internal DNA control from two independent experiments. (B) The effect of PLC enzyme on in vitro transcription is shown. PLC (100 ng) addition before the addition of nucleotides (PLC B) inhibited Pol I transcription, while PLC addition after the addition of nucleotides (PLC A) did not inhibit transcription. (Lane 1: control transcription reaction; lane 2: transcription reaction in the presence of PLC added after nucleotides; lane 3: transcription reaction in the presence of PLC added before nucleotides). The charts show relative activities (mean ± SEM) normalized to an internal DNA control from two independent experiments (C) Nuclear extracts were depleted for PIP2 using PLCδ1PH coated beads. As a control, PLCδ1PH-Mut coated beads were used for depletion, since PLCδ1PH-Mut fails in binding to PIP2 (Yagisawa et al. 1998). Transcription intensities were normalized by 700 bp PCR product labeled with [α-^{32}P]. PIP2 depletion by PLCδ1PH domain caused 90% inhibition in transcription while mutant domain did not show such a pronounced inhibitory effect (~40% inhibition). (Lane 1: Non-depleted nuclear extract; lane 2: nuclear extract depleted with PLCδ1PH; lane 3: nuclear extract depleted with PLCδ1PH-Mut domain). The charts show relative activities (mean ± SEM) normalized to an internal DNA control from two independent experiments (D) PIP2-depleted nuclear extracts supplemented with DAG, IP3, PIP2, PI3P and PI4P were tested for Pol I transcription. PIP2 supplementation resulted in the most dramatic rescue of transcription compared to other compounds tested. (Lane 1: PIP2-depleted nuclear extract; lane 2: PIP2-depleted nuclear extract supplemented with DAG (100 ng); lane 3: PIP2-depleted nuclear extract supplemented with IP3 (100 ng); lane 4: PIP2-depleted nuclear extract supplemented with PIP2 (100 ng); lane 5: PIP2-depleted nuclear extract supplemented with PI3P (100 ng); lane 6: PIP2-depleted nuclear extract supplemented with PI4P (100 ng); lane 7: non-depleted control nuclear extract). The charts show relative activities (mean ± SEM) normalized to

an internal DNA control from two independent experiments. (E) In order to visualize PIP2 during transcription; we used rDNA promoter bound to Dynabeads. GST-tagged Wt or Mut PLCδ1PH domains were purified from bacteria, added to in vitro transcription mixtures and probed with anti-GST antibody. There was no detectable binding of Wt PLCδ1PH domain to the promoter in the presence of ATP solely, and only after the addition of all four rNTPs binding was detected; indicating that PIP2 binds to the promoter region only when transcription is active, in vitro. (Lane1: PLCδ1PH domain; lane 2: PLCδ1PH-Mut domain; lane 3 and 4: nuclear extract; lane 5: transcription reaction in the presence of ATP; lane 6: transcription reaction with ATP and PLCδ1PH domain; lane 7: transcription reaction with ATP and PLCδ1PH-Mut domain; lane 8: transcription reaction in the presence of all four rNTPs; lane 9: transcription reaction with rNTPs and PLCδ1PH domain; lane 10: transcription reaction with rNTPs and PLCδ1PH-Mut domain). (F) In order to prove the presence of PIP2 at the transcription machinery on the promoter during transcription, we used rDNA promoter bound to Dynabeads. PIP2 was found on the rDNA promoter upon the addition of all four rNTPs [N] but not on the control DNA after extracting the lipids with chloroform/methanol/HCl and analyzing them by TLC. (Lane 1: purified PIP2; lane 2 and 4: lipids from transcription reactions with all four rNTPs; lane 3 and 5: lipids from in vitro transcription reactions with only ATP added). Lipids were stained with acidic phosphomolibdate solution.

Fig. 2. PIP2 binds to the largest subunit of Pol I. In order to test the suitability of PLCδ1PH domain for PIP2 detection, we performed ultrastructural immunolabelling and immunofluorescence. (A) Immunogold electron microscopy was carried out using PLCδ1PH domain as a PIP2 sensor. PIP2 was localized at the plasma membrane of HeLa cells as expected. Scale bar represents 500 nm. (B) There is no staining in the nucleus when U2OS cells are incubated with PLCδ1PH-Mut domain as a control. Scale bar represents 5 μm. (C) PLCδ1PH domain pulled down RPA116 in vitro but Mut form of PLCδ1PH domain failed in pulling down RPA116. (Lane 1: input; lane 2: protein pulled-down with Wt PLCδ1PH domain; lane 3: protein pulled-down with Mut PLCδ1PH domain). (D) In vivo, anti-PIP2 antibody showed co-localization with Pol I subunit RPA 116 in nucleoli of U2OS cells. Scale bar represents 5μm. (E) Nuclear extract was incubated with agarose beads coupled to PIP2 in order to pull-down proteins interacting with PIP2. Pol I transcription machinery and nucleolar proteins were checked in the

pull-down and fibrillarin was found to be present, while B23, TAF 95/110 and TBP were absent in the PIP2-protein complex. (Lane 1: input; lane 2: pull-down with PIP2-coupled agarose beads; lane 3: pull-down with control agarose beads). In, input; Ctrl, control.

Fig. 3. PIP2 co-localizes with Pol I transcription factor UBF and rRNA early processing factor Fib in intact cells. (A) When nucleolar extract was incubated with PIP2-coupled agarose beads, UBF and Fib were found to be present in the PIP2-bound protein complex. (Lane 1: input; lane 2: protein unbound to PIP2-coupled agarose beads (flow-through); lane 3: protein pulled-down with PIP2-coupled agarose beads; lane 4: protein unbound to control agarose beads (flow-through); lane 5: protein pulled-down with control agarose beads). In, input; FT, flow-through; Ctrl, control. (B) PLCδ1PH domain, used as a PIP2 marker, co-localized with UBF and Fib in U2OS cells. Scale bars represent 5μm. (C) SIM revealed PIP2 co-localization with UBF and Fib in the subnucleolar components, which can be identified as FC and DFC, respectively. Scale bars represent 0.5μm. (D) IEM precisely distinguished PIP2 co-localization with UBF inside and at the periphery of FC, and with Fib in the DFC of HeLa cells. N, nucleus; NL, nucleolus. Scale bars represent 200 nm. (E) Ultrastructural architecture of PIP2 clusters in nucleolar subcompartments by TECNAI G2 20 LaB6 tomography. PIP2 is localized in HeLa cells using pre-embedding procedure with 0.8 nm immunogold particles pseudocoloured in green. Fibrillar center is pseudocoloured in yellow, dense fibrillar component in orange.

Fig. 4. UBF and Fib bind to PIP2 in vitro. (A) Western blot of purified UBF, Fib, OSH1PH and Imp 5 used in binding assays. (B) PIP2 and PI4P strips were incubated with recombinant UBF, Fib, OSH1PH and Imp 5 proteins for direct binding analysis. (C) Control agarose beads or PIP2-coupled agarose beads were incubated with purified UBF, Fib and Imp 5 proteins to study the direct binding to PIP2. (Lane 1: input; lane 2: protein unbound to PIP2-coupled agarose beads (flow-through); lane 3: protein pulled-down with PIP2-coupled agarose beads; lane 4: protein unbound to control agarose beads (flow-through); lane 5: protein pulled-down with control agarose beads). In, input; FT, flow-through; Ctrl, control. (D) Limited protease digestion assays show a difference in the digestion pattern (arrow) of UBF due to a conformational change or specific binding of PIP2. (Lane 1: UBF as an input; lane 2: UBF treated with trypsin; lane 3: UBF treated with trypsin in the presence of PIP2). (E) Limited protease digestion assays show difference in digestion pattern of Fib (arrow) due to the conformational change or specific

736 binding of PIP2. (Lane 1: Fib as an input; lane 2: Fib treated with trypsin; lane 3: Fib treated with
737 trypsin in the presence of PIP2). (F) Footprinting experiment was done using purified
738 recombinant UBF incubated with 100 ng DAG, IP3 and PIP2. (Lane 1: template incubated with
739 UBF; lane 2: template incubated with UBF in the presence of DAG; lane 3: template incubated
740 with UBF in the presence of IP3; lane 4: template incubated with UBF in the presence of PIP2;
741 lane 5: template only). UBF binding sites are indicated in the figure. Normalized densitometry
742 plot analysis of the footprint is shown on the left. (G) PIP2 binding to Fib was tested on mobility
743 assays with U6 snRNA where PIP2 association with Fib altered the mobility of RNA, suggesting
744 an additional conformational bend or loop on RNA. (Lane 1: template; lane 2: template incubated
745 with Fib; lane 3, 4, 5 and 6: template incubated with Fib in the presence of decreasing amounts of
746 PIP2 (0.1 µg, 0.05 µg, 0.025 µg, 0.0166 µg). Lane 7, 8, 9 and 10 are the duplicates of lane 3, 4, 5
747 and 6, respectively. See Fig. S7 for the entire gel pattern. Different conformations of RNA-Fib
748 complexes are reflected in the altered mobility of U6 snRNA shown by arrows. Normalized
749 densitometry plot analysis of the gel shift shows Fib complex with U6 snRNA in blue, the Fib
750 and PIP2 complex with U6 snRNA in black at different concentrations of PIP2 and U6 snRNA
751 only as an orange plot. The peak marked as N.S. shows a nonspecific radioactive signal.

752 **Fig. 5. PIP2 positive foci co-localize with rRNA nascent transcripts in nucleoli.** (A) α-
753 amanitin treated U2OS cells showed very high co-localization of PIP2 and anti-BrdU positive
754 nascent transcripts. Scale bar represents 5µm. (B) Immunogold detection revealed intermingled
755 clusters and strings of PIP2 and rRNA transcripts in the DFC of HeLa cells. Major portion of Br-
756 rRNA transcripts co-localized with PIP2 molecules, while some DFC-zones contained only PIP2.
757 NL, nucleolus. Scale bar represents 200 nm.

758 **Fig. 6. Model for Pol I transcription**. UBF and Pol I interacts with PIP2 during the transcription
759 where PIP2 directs UBF to bind to a more specific site on the promoter compared to its
760 promiscuous binding to the rDNA (Transcription assembly). This specific promoter binding
761 occurs in FC/DFC region. Fib interacts with PIP2 only when RNA is newly synthesized and this
762 interaction takes place in DFC region close to UBF (Transcription initiation/elongation). PIP2 is
763 not involved in further processing of RNA and riboproteins since it is not localized in the GC
764 region where maturation of rRNA takes place. Differences in the hydrophobicity of the
765 complexes may have a role in the formation of subnucleolar structures (Processive transcription).

Supplementary Data Legends

Supplementary Movie 1. **PIP2 localization in nucleolus by 3D electron tomography.** Ultrastructural architecture of PIP2-clusters in nucleolar subcompartments by TECNAI G2 20 LaB6 tomography. PIP2 is localized using pre-embedding procedure with 0.8 nm immunogold particles pseudocoloured in green. Fibrillar center is pseudocoloured in yellow, dense fibrillar component is pseudocoloured in orange.

Supplementary Figures: Fig. S1. Preincubation of PIP2 with anti-PIP2 antibody neutralizes the inhibitory effect of antibody in Pol I transcription. Run-off transcription reaction showed that PIP2 blocked the inhibitory effect of anti-PIP2 antibody (clone 2C11, Abcam, Cambridge, UK; 0.8 µg) in transcription in a dose-dependent manner. (Lane 1: control transcription reaction; lane 2: transcription reaction in the presence of anti-PIP2 antibody; lane 3 and 4: transcription reaction in the presence of anti-PIP2 antibody with the addition of 50 ng and 100 ng PIP2, respectively).

Fig. S2. Ponceau staining of blotted proteins from in vitro pull-down wherein recombinant Wt and Mut PLCδ1PH domains were incubated with nuclear lysates.

Fig. S3. Ponceau staining of blotted proteins from in vitro pull-down performed by incubation of nuclear lysate with control agarose beads or PIP2-coupled agarose beads.

Fig. S4. Ponceau staining of blotted proteins from in vitro pull-down performed by incubation of nucleolar lysate with control agarose beads or PIP2-coupled agarose beads.

Fig. S5. Control experiment showing the specificity of the antibodies used. Specific signals were diminished after blocking the primary antibodies with excess amount of relevant proteins or lipids. When primary antibodies were omitted, secondary antibodies did not produce any visible signal. Scale bar represents 5 µm.

Fig. S6-1,2,3. Ponceau staining of blotted proteins from in vitro pull-down experiments performed by incubation of control agarose beads or PIP2-coupled agarose beads with purified UBF, Fib and Imp 5 proteins, respectively.

Fig. S7. Gel shift assay in which aggregates formed after fibrillarin addition can be seen in the wells. This aggregation leads to an apparent loss of radioactivity in the corresponding gel lanes.

Fig.1

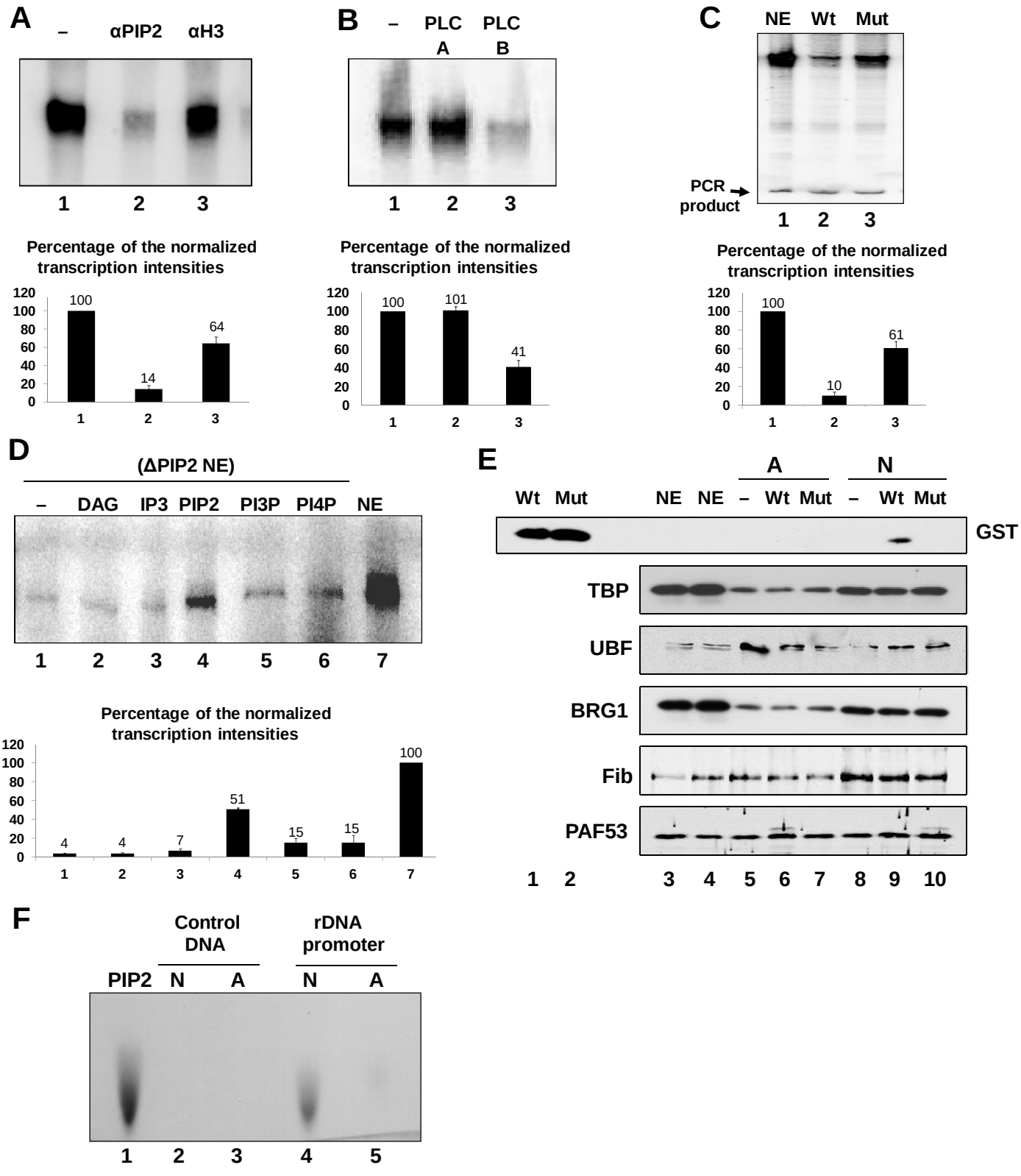
A
–
αPIP2
αH3
1 2 3
Percentage of the normalized transcription intensities
100
14
64
B
–
PLC A
PLC B
1 2 3
Percentage of the normalized transcription intensities
100
101
41
C
NE
Wt
Mut
PCR product
1 2 3
Percentage of the normalized transcription intensities
100
10
61
D
(ΔPIP2 NE)
– DAG IP3 PIP2 PI3P PI4P NE
1 2 3 4 5 6 7
Percentage of the normalized transcription intensities
4
4
7
51
15
15
100
E
A
N
Wt Mut NE NE – Wt Mut – Wt Mut
GST
TBP
UBF
BRG1
Fib
PAF53
1 2 3 4 5 6 7 8 9 10
F
Control DNA
rDNA promoter
PIP2 N A N A
1 2 3 4 5

Fig. 2

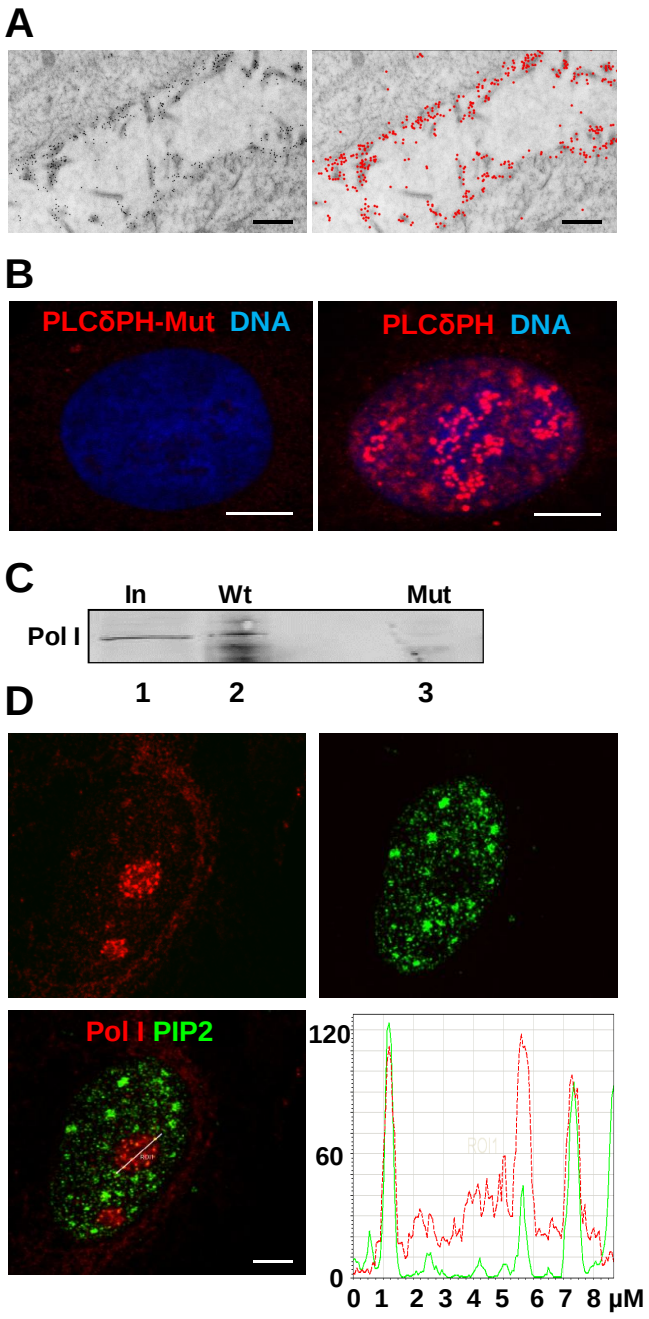
A
B
PLCδPH-Mut DNA
PLCδPH DNA
C
In
Wt
Mut
Pol I
1
2
3
D
Pol I PIP2
120
60
0
0 1 2 3 4 5 6 7 8 µM
E
In
PIP2 beads
Ctrl beads
B23
TAF 95/110
TBP
Fib
1
2
3

Fig. 3

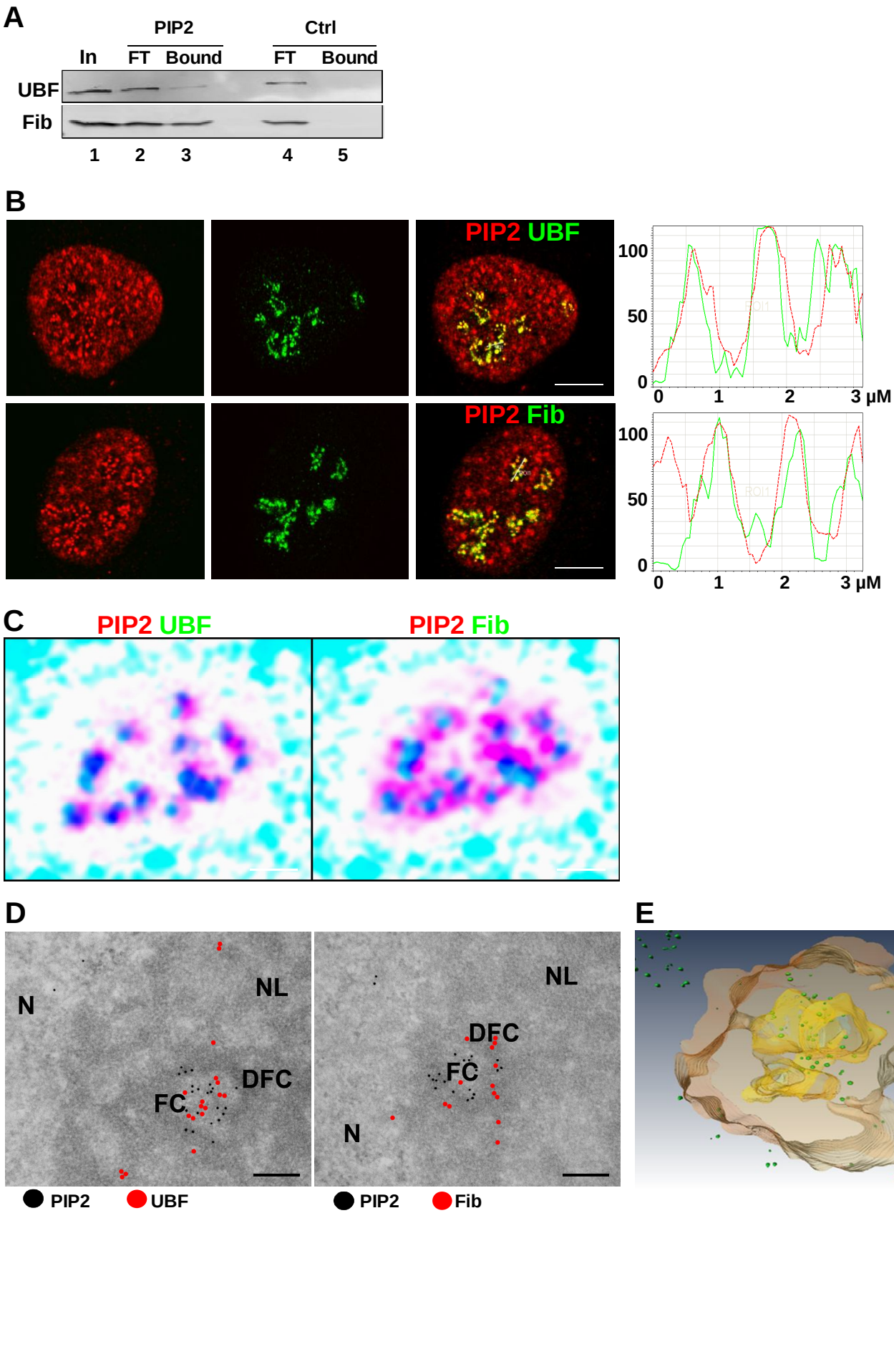
A
PIP2
Ctrl
In
FT
Bound
FT
Bound
UBF
Fib
1
2
3
4
5
B
PIP2 UBF
PIP2 Fib
100
50
0
0
1
2
3 μM
C
PIP2 UBF
PIP2 Fib
D
N
NL
DFC
FC
PIP2
UBF
NL
DFC
FC
N
PIP2
Fib
E

Fig. 4

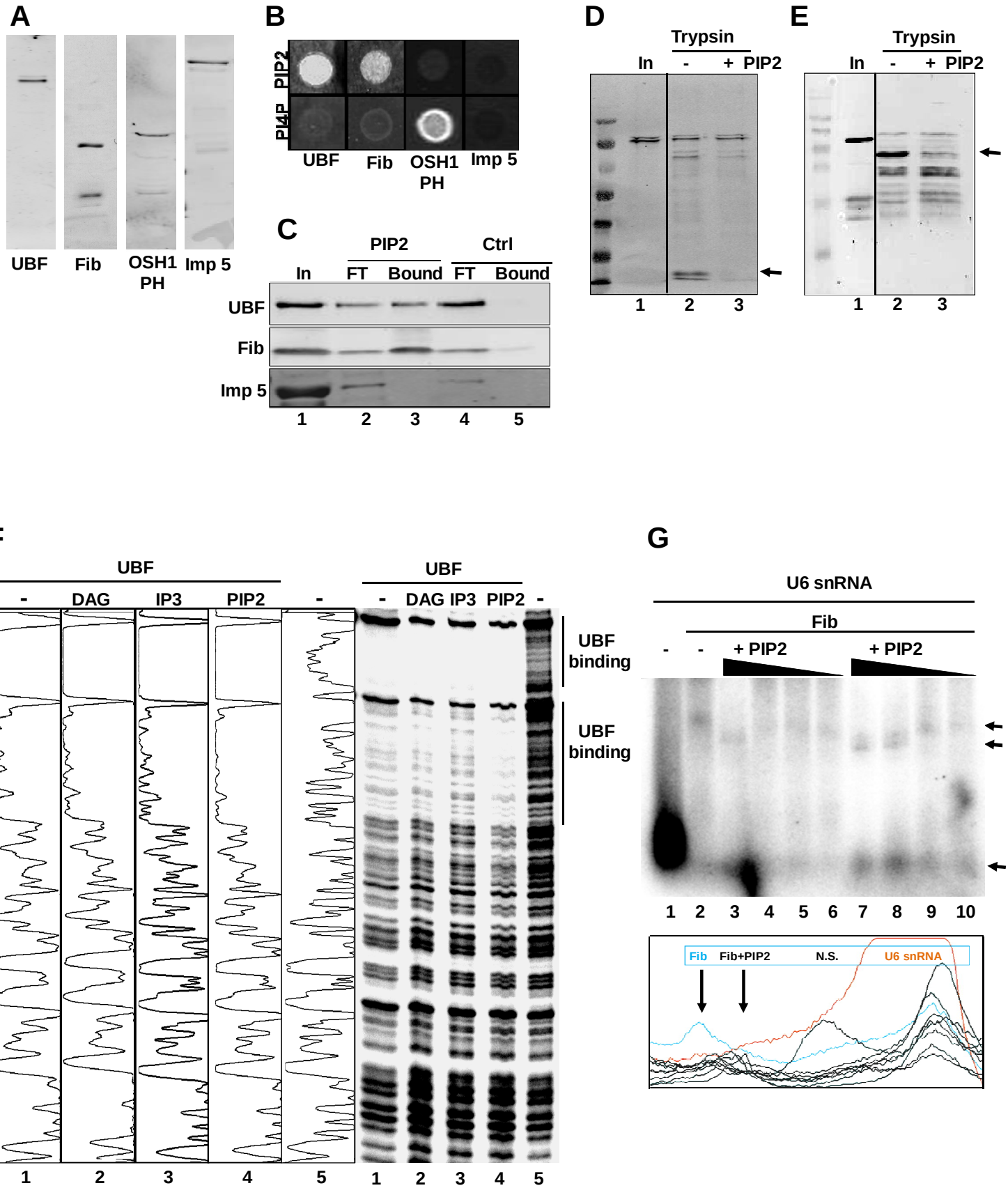
A
UBF
Fib
OSH1 PH
Imp 5
B
PIP2
PI4P
UBF
Fib
OSH1 PH
Imp 5
C
In
PIP2
FT
Bound
Ctrl
FT
Bound
UBF
Fib
Imp 5
1 2 3 4 5
D
Trypsin
In
-
+
PIP2
1 2 3
E
Trypsin
In
-
+
PIP2
1 2 3
F
UBF
- DAG IP3 PIP2 -
UBF
- DAG IP3 PIP2 -
UBF binding
UBF binding
1 2 3 4 5
1 2 3 4 5
G
U6 snRNA
Fib
- - + PIP2 + PIP2
1 2 3 4 5 6 7 8 9 10
Fib
Fib+PIP2
N.S.
U6 snRNA

Fig. 5

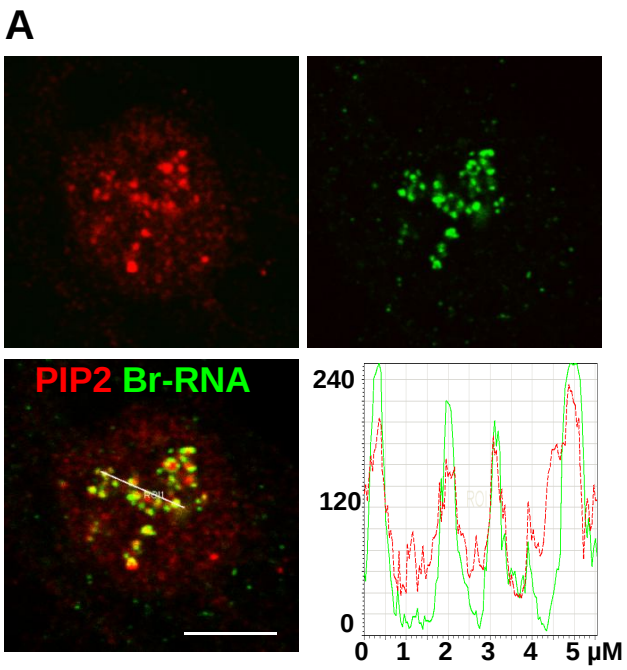

Fig. 6

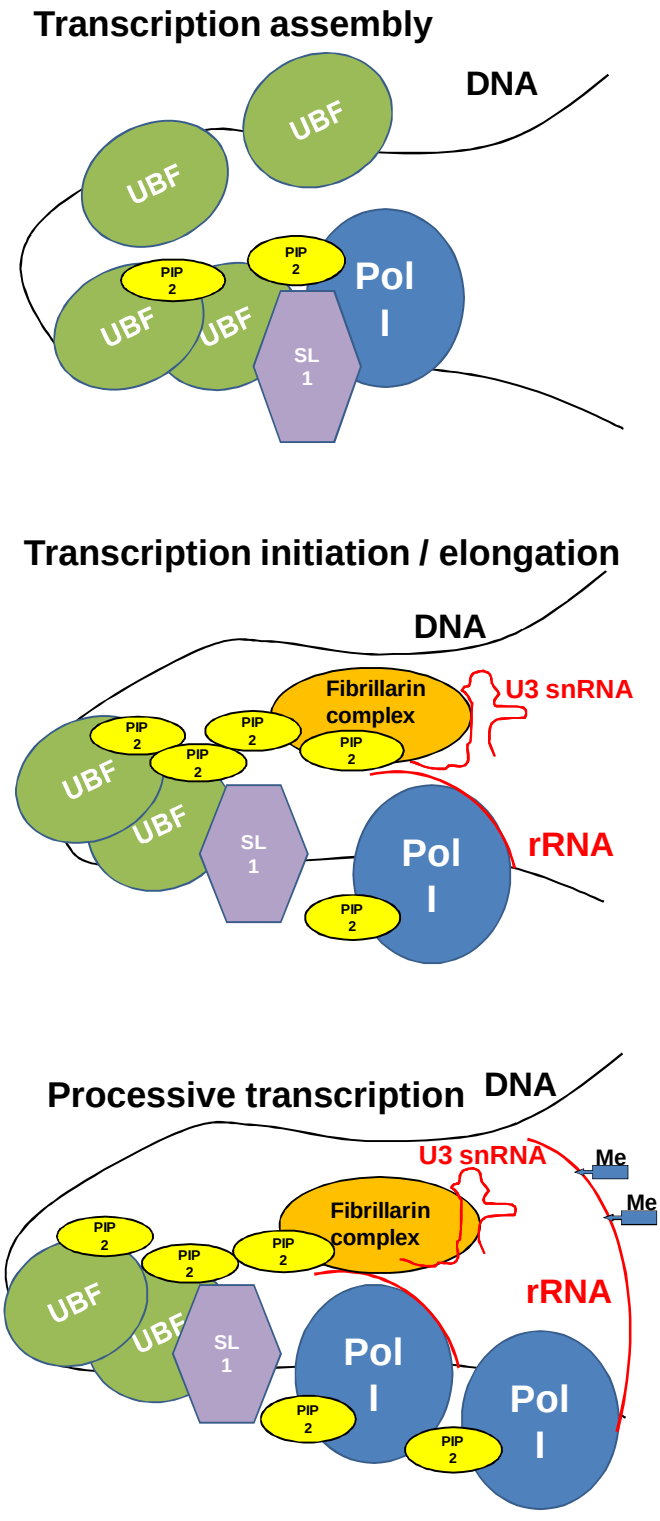
Transcription assembly
DNA
UBF
UBF
UBF
UBF
PIP 2
PIP 2
Pol I
SL 1
Transcription initiation / elongation
DNA
Fibrillarin complex
U3 snRNA
PIP 2
PIP 2
PIP 2
PIP 2
PIP 2
UBF
UBF
SL 1
Pol I
rRNA
Processive transcription
DNA
U3 snRNA
Me
Me
Fibrillarin complex
PIP 2
PIP 2
PIP 2
PIP 2
PIP 2
PIP 2
UBF
UBF
SL 1
rRNA
Pol I
Pol I

Supplementary Figures

Fig. S1

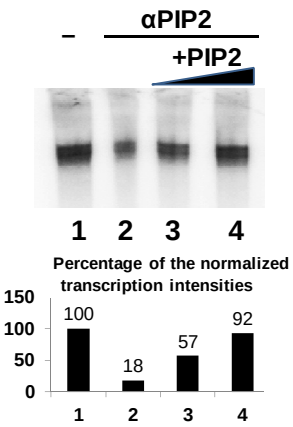

Fig. S2

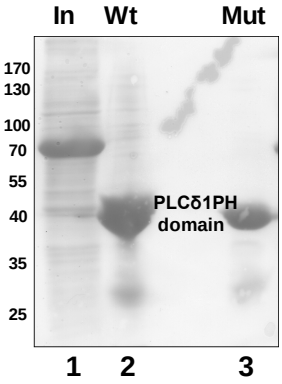

Fig. S3

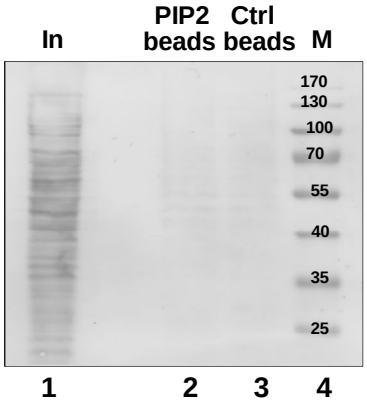

Fig. S4

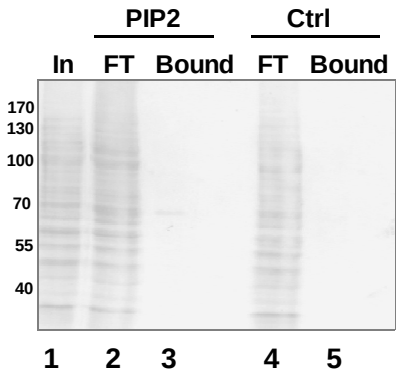

Fig. S5

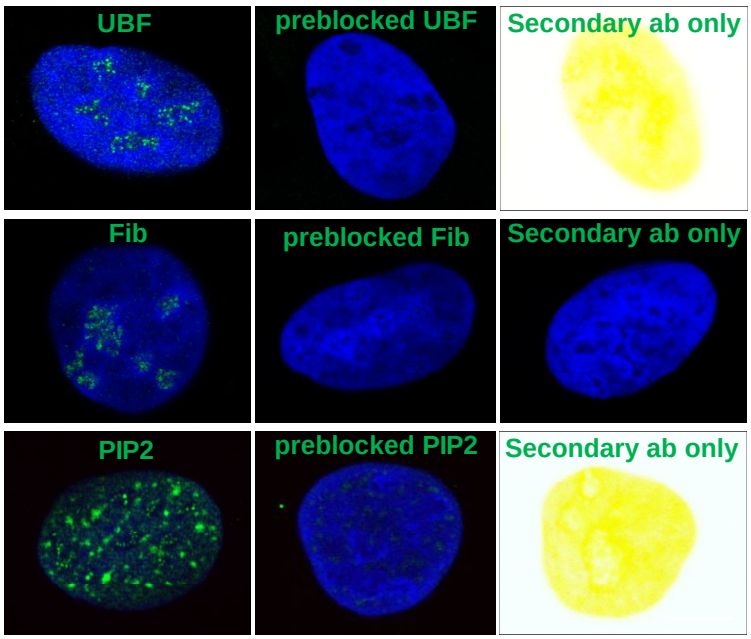

Fig. S6-1

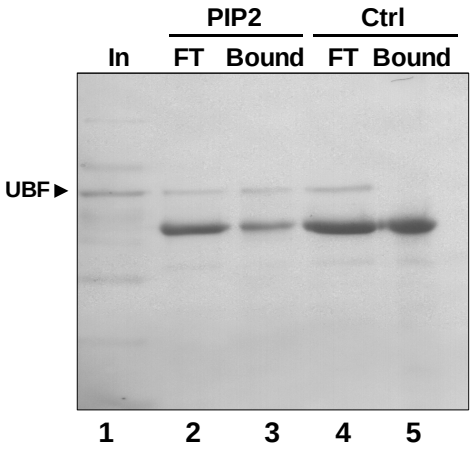

Fig. S6-2

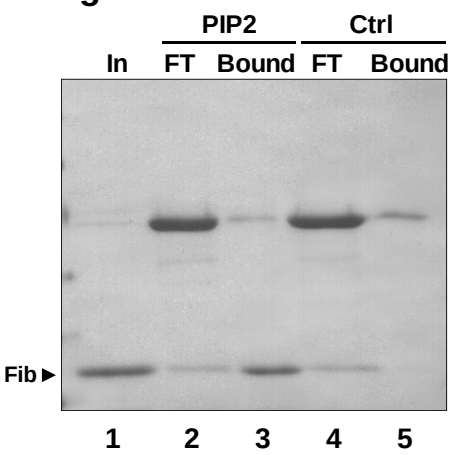

Fig. S6-3

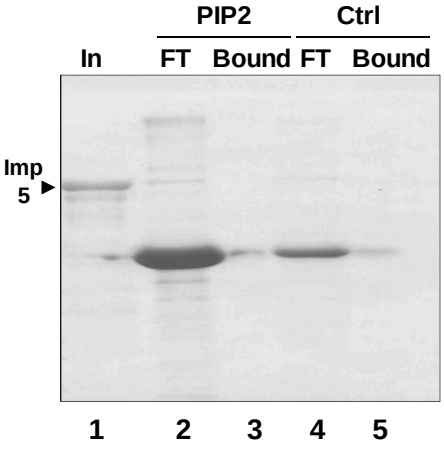

Fig. S7

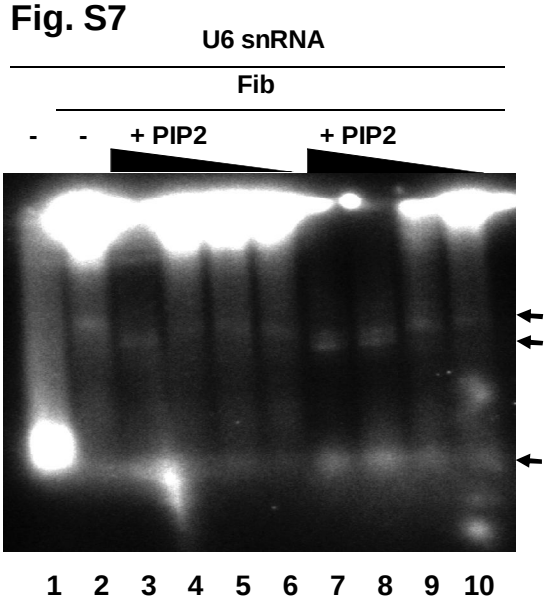

5.3 Mouse nuclear myosin I knock-out shows interchangeability and redundancy of myosin isoforms in the cell nucleus

Venit T, Dzijak R, Kalendová A, Kahle M, Rohožková J, Schmidt V, Rülicke T, Rathkolb B, Hans W, Bohla A, Eickelberg O, Stoeger T, Wolf E, Yildirim AÖ, Gailus-Durner V, Fuchs H, Hrabě de Angelis M, Hozák P

PLOS ONE, 2013, in press
IF: 4,092 (2011)

My contribution to this work:
I generated NM1 KO mice, performed genotyping analysis of all mice and basic phenotyping. I prepared cell lines derived from mice ear explants. I performed proliferation experiments and RT-qPCR experiments. I wrote the manuscript.

Mouse nuclear myosin I knock-out shows interchangeability and redundancy of myosin isoforms in the cell nucleus

Tomáš Venit[1,8], Rastislav Dzijak[1], Alžběta Kalendová[1], Michal Kahle[1], Jana Rohožková[1], Volker Schmidt[2], Thomas Rülicke[2], Birgit Rathkolb[3,5], Wolfgang Hans[3], Alexander Bohla[4], Oliver Eickelberg[4], Tobias Stoeger[4], Eckhard Wolf[5], Ali Önder Yildirim[4], Valérie Gailus-Durner[3], Helmut Fuchs[3], Martin Hrabě de Angelis[3,6,7], Pavel Hozák[1*]

1 Department of Biology of the Cell Nucleus, Institute of Molecular Genetics, ASCR, v.v.i., Prague, Czech Republic

2 Institute of Laboratory Animal Science and Biomodels Austria, University of Veterinary Medicine Vienna, Vienna, Austria

3 German Mouse Clinic, Institute of Experimental Genetics, Helmholtz Zentrum München, German Research Center for Environmental Health, Neuherberg/Munich, Germany;

4 German Mouse Clinic, Comprehensive Pneumology Center and Institute of Lung Biology and Disease, Helmholtz Zentrum München, German Research Center for Environmental Health, Neuherberg/Munich, Germany;

5 Chair of Molecular Animal Breeding and Biotechnology, Gene Center, Ludwig-Maximilians-Universität München, Munich, Germany

6 Chair of Experimental Genetics, Center of Life and Food Sciences Weihenstephan, Technische Universität München, Freising-Weihenstephan, Germany

7 Member of German Center for Diabetes Research (DZD), Neuherberg/Munich, Germany

8 Faculty of Science, Charles University in Prague, Prague, Czech Republic

* corresponding author: hozak@img.cas.cz

Abstract

Background: Nuclear myosin I (NM1) is a nuclear isoform of the well-known “cytoplasmic” Myosin 1c protein (Myo1c). Located on the 11th chromosome in mice, NM1 results from an alternative start of transcription of the Myo1c gene adding an extra 16 amino acids at the N-terminus. Previous studies revealed its roles in RNA Polymerase I and RNA Polymerase II transcription, chromatin remodeling, and chromosomal movements. Its nuclear localization signal is localized in the middle of the molecule and therefore directs both Myosin 1c isoforms to the nucleus.

Methodology/Principal Findings: In order to trace specific functions of the NM1 isoform, we generated mice lacking the NM1 start codon without affecting the cytoplasmic Myo1c protein. Mutant mice were analyzed in a comprehensive phenotypic screen in cooperation with the German Mouse Clinic. Strikingly, no obvious phenotype related to previously described functions has been observed. However, we found minor changes in bone mineral density and the number and size of red blood cells in knock-out mice, which are most probably not related to previously described functions of NM1 in the nucleus. In Myo1c/NM1 depleted U2OS cells, the level of Pol I transcription was restored by overexpression of shRNA-resistant mouse Myo1c. Moreover, we found Myo1c interacting with Pol II. The ratio between Myo1c and NM1 proteins were similar in the nucleus and deletion of NM1 did not cause any compensatory overexpression of Myo1c protein.

Conclusion/Significance: We observed that Myo1c can replace NM1 in its nuclear functions. Amount of both proteins is nearly equal and NM1 knock-out does not cause any compensatory overexpression of Myo1c. We therefore suggest that both isoforms can substitute each other in nuclear processes.

Keywords

Nuclear myosin I, NM1, Myosin 1c, Myo1c, mice knock-out, phenotyping

Introduction

Myosins are unique proteins that have the ability to transform free chemical energy stored in ATP into mechanical force. In comparison to the well-known “conventional” class II myosins found in muscles, there is a variety of other “unconventional” myosins belonging to several groups. Myosin I family members are monomeric, non-processive, slow-rate and low-duty ratio molecular motors. Myosin 1c (Myo1c) was the first single-headed myosin isolated from mammals and it was therefore called mammalian myosin I [1,2]. Based on its similarity to partial myosin sequence from mouse cDNA library, it was later renamed as myosin 1β [3], and finally, after the unification of myosin I nomenclature, myosin 1c [4]. The human MYOIC gene encodes three isoforms. Myosin 1c isoform C is the classic 1063 amino acid “cytoplasmic” form [2]. Myosin 1c isoform B, also known as nuclear myosin 1 (NM1), includes 16 extra N-terminal amino acids arising from an upstream exon -1 [5,6]. The newest isoform is myosin 1c, isoform A, which includes additional 35 amino acids on its N-terminal end from an upstream exon -2 and was described to work in the cell nucleus [7]. In mice there have been only two myosin isoforms described – Myo1c and NM1.

Myosin 1c (isoform C) belongs to a group of molecular motors that link cellular membranes to the actin cytoskeleton, and are involved in membrane tension generation, membrane dynamics, and mechanosignal transduction. In detail, Myo1c was identified to be associated with Neph1 and nephrin proteins. Myo1c mediates their localization to the plasma membrane and its depletion causes defects in tight junctions’ formation and cell migration [8]. In the neuronal growth cone, Myo1c affects lamellipodial motility and is responsible for retention of lamellipodia [9] and retrograde F-actin flow [10]. In *Xenopus laevis,* Myo1c participates in egg activation by coupling dynamic actin to the membranes of cortical granules, and this linkage is essential for their compression and retrieval [11]. Insulin stimulates glucose transport in adipocytes by promoting exocytosis of the population of vesicles containing glucose transporter protein GLUT4. Myo1c enhances exocytosis of GLUT4-containing vesicles to plasma membrane [12,13]. The most extensively studied

function of Myo1c concerns the process of hearing. Sensory cells of the inner ear detect sound and transmit signals representing those stimuli to the central nervous system. Myo1c has a direct function in the adaptation of sensory cells to sustained excitatory deflection, since upon its inhibition the adaptation is slow and inefficient [14]. Moreover, clinical studies revealed 6 missense mutations in Myo1c that were associated with bilateral hearing loss [15].

All these functions connect Myo1c to the plasma membrane and actin filaments. This was further proved by Nambiar et al. (2009) who showed that Myo1c together with other myosin I family members mediate membrane/cytoskeleton adhesion. This makes major contributions to membrane tension, which is one of the main parameters needed in endo- and exocytosis, membrane repair, cell motility, and cell spreading.

Nuclear myosin I (isoform B) was discovered coincidentally by testing of affinity-purified polyclonal antibodies to adrenal myosin 1. The antibody was staining a 120-kDa nuclear protein with ATPase activity, and ATP-, actin- and calmodulin- binding which are the typical features of unconventional myosins [5]. The mass spectrometric analysis of the immunopurified protein showed high homology to the Myo1c protein. Due to the fact that at that time, NM1 was the first myosin found in the cell nucleus, it was called nuclear myosin I [6]. In the nucleus, NM1 associates with nuclear actin and is required for RNA polymerase I (Pol I) and RNA polymerase II (Pol II) transcription [6,16]. Both NM1 and actin co-localize and co-immunoprecipitate with Pol I and Pol II complexes. *In vitro* immunodepletion of NM1 inhibits transcription by both polymerases and the addition of purified NM1 increases the level of transcription in a dose-dependent manner. While both proteins associate with Pol I, actin associates with Pol I regardless of the transcriptional state. In contrast, NM1 only associates with initiation-competent RNA polymerase I complexes through an interaction with the basal transcription factor TIF1A [16]. In addition to transcription initiation, NM1 is needed in further steps during elongation phase where it interacts with chromatin remodeling complex WSTF-SNF2h and facilitates Pol I transcription on chromatin [17]. It is therefore

believed that NM1 bound to TIF-1A is recruited to the pre-initiation complex along with Pol I and associated actin to assemble a functional transcription initiation complex. Recruitment of Pol I to the NM1-TIF-1A complex might facilitate the interaction of NM1 with actin bound to Pol I. Finally, by interacting with NM1, chromatin remodeling complexes join the initiation complex to promote Pol I movement through chromatin [18]. This is also supported by the finding that both actin polymerization and the motor function of NM1 are required for association with the Pol I transcription machinery and transcription activation [19]. Moreover, NM1 was found in interaction with RNA and RNA-protein complexes present in the nucleoplasm and in nucleoli [20]. It participates in the maturation of pre-rRNA, and accompanies rRNA transcripts to the nuclear pore where NM1 decorates actin-rich pore-linked filaments [21]. Aside from its functions in transcription, Chuang et al. (2006) showed that the actin-NM1 complex is needed for long-range directional movement of interphase chromosome sites independently from their engagement in transcription. NM1 is also able to bind DNA directly via its tail domain [22], and NM1 together with gelsolin were identified as key determinants for assembling and/or stabilization of complexes containing estrogen receptor α (ERα) and actin in the nucleus early after receptor activation by its ligands [23].

Both Myo1c and NM1 proteins are shown to be expressed in a wide variety of tissues and cultured cell lines. Their expression pattern is similar but not completely overlapping. Both proteins have the highest level of expression in mouse lungs, followed by intestine, kidney, heart and spleen for NM1, and adrenal gland, stomach, spleen, heart and esophagus for Myo1c. These expression profiles suggested possible tissue-specific functions for both proteins [2,24,25]. However, Myo1c is localized mostly at the cell periphery and at the plasma membrane, particularly at the leading edges of motile cells [2], while NM1 was described to localize mostly in the nucleus where its distribution is dependent on transcriptional activity of the cell [26,27]. The 16 amino acid N-terminal extension of NM1 molecule was thought to be the nuclear localization signal for this protein [6]. However, we recently showed that nuclear localization signal which triggers NM1 to the nucleus is located

in the middle part of the molecule and therefore direct both NM1 and Myo1c to the nucleus. This novel calmodulin-dependent NLS is localized in the second of three IQ domains [24]. Because of the various nuclear functions of NM1, it is important to determine if both isoforms can perform identical functions. We therefore prepared mice lacking NM1 isoform without affecting Myo1c expression and here we describe observed phenotypes in NM1 knock-out mice. Surprisingly, these mice were fully viable and did not show any obvious defects related to previously described functions of NM1 in DNA transcription. Moreover, the ratio between both isoforms in the nucleus and cytoplasm is roughly equal. We therefore tested Myo1c's capability to act in transcription. We found that Myo1c is able to functionally substitute NM1 in Pol I transcription. Moreover, it directly binds to the Pol II CTD domain suggesting it has also a role in Pol II transcription. In conclusion, we suggest that the two isoforms Myo1c and NM1 (isoforms C and B) are mutually redundant in general process of transcription.

Material and methods

Ethics statement

All animal experiments and work with human and mice cell lines conformed to relevant regulatory standards and were approved by the Ministry of Agriculture of the Czech Republic, the ethic committee of the Institute of Molecular Genetics ASCR (animal experiment license no. 40/2009 and 186/2010) and the district government of Upper Bavaria (Regierung von Oberbayern).

The project for the generation of the mutants was discussed and approved by the institutional ethics committee of the Vedmeduni Vienna and animal experiment license granted under no. BMWF-68.205/0084-II/10b/2008. All animal experiments performed in GMC were done with permissions of the appropriate authorities according to the §8 of the German Law for the Protection of Animals.

Plasmids

NM1-Fl and Myo1c-Fl vectors were prepared by cloning of NM1 and Myo1c cDNA into pCDH-CMV-MCS-EF1-Neo (Systems Bio) using SnaBI and EcoRI restriction enzymes in frame with the C-terminal Flag tag. The constructs expressing shRNA-resistant NM1-GFP and Myo1c-GFP was prepared by excision of mouse NM1-GFP and Myo1c-GFP from vectors NM1-GFP and Myo1c-GFP [24] and ligated into pCDH-EF1-Neo (Systems Bio). The NM1-GFP construct has been previously described [24].

Preparation of targeting construct for knock-out mice

For the preparation of conditional NM1 knock-out (KO), the Cre–loxP system and a targeting construct based on pEasyFlox vector was used [28].The short homology arm (SA, ~ 0,9 kb) was prepared by PCR amplification of genomic DNA sequence from -1096 to -166 base pairs from NM1 translation initiation site using primers SA F (5´-gtagagtcgacTATGCCACAAGAGGTGGCAACT-3´) and SA R (5´-gccgaagcttCCGGGCTGGGTGGGAGGGGGTTCG-3´). The long homology arm (LA, ~ 1,7 kb) was prepared by amplification of genomic DNA from + 116 to +1800 base pairs from the NM1 translation initiation site, using primers LA F (5´-ggggatccGGTGGAAGATGTCCCTGAAAGTTG-3´) and LA R (5´-gctgcggccgcGTAGTAACCTGGGCATTGCTGTCC-3´). The floxed part encoding the -1 exon (containing the NM1 start codon); (FP, ~ 0,3 kb) was prepared by amplification of genomic DNA from -165 to +115 base pairs from the NM1 translation initiation site, using primers FP F (5´-cccagtcgacCCAGGCCGGCTGCAGTGGGTCCTA-3´) and FP R (5´-catcttctagaGAAATTCCTGGGCCGCGCCCGCTT-3´) (**Fig. 1A**). All PCR reactions were done using mouse 129/Sv genomic DNA as a template. The SA PCR product was digested and cloned into the pEasyFlox vector via XhoI and HindIII restriction sites, LA by BamHI and NotI and FP via SalI and XbaI restriction sites. For screening of positively electroporated

cells with the targeting construct, we used a neomycin-resistance positive selection marker (Neo) flanked with loxP sites (**Fig. 1B**).

Generation of NM1 knock-out mice

To test the influence of the N-terminal 16 amino acids on NM1 functions, we generated mice lacking exon -1 of *Myo1c* which contains the NM1 start codon [6]. Exon -1, and both the long and the short arm were cloned into the pEasyFlox vector carrying neomycin resistance and thymidyne kinase selection cassettes together with three loxP sites (Fig 1A, 1B, 1C). The linearized NM1 tri-loxP construct was then electroporated into the TBV2 (129S2/SvPas) ES cell line (provided by T. Rülicke) as follows: TBV2 ES cells were cultured in ES cell medium (DMEM with 4.5 g/L glucose, 15% FBS, 1mM Sodium-pyruvate, 2mM glutamine, 1x NEAA, 1x penicillin/streptomycin, 0.1mM 2-mercaptoethanol and 1000u/ml pure leukemia inhibitory factor (Lif)). All ingredients except Lif (Millipore) and 2-mercaptoethanol (Sigma) were purchased from PAA. ES cells were grown on 6cm plates coated with inactivated mouse embryonic fibroblasts (MEF). Ten plates were then pooled and re-suspended in 1ml PBS. About $2x10^7$ cells were mixed with 30µg linearized *Myo1c* targeting construct and chilled on ice before electroporating in a 0.4cm electroporation cuvette using a Gene Pulser Xcell (BioRad); (settings 500µF and 0.23 kV). Electroporated cells were plated onto irradiated neo-resistant MEF cells on ten 6cm plates. Selection with 300µg/ml G-418 sulphate (PAA) was started 24h after electroporation. Neo-resistant colonies were picked after 14 days of G-418 treatment and screened by PCR. PCR-positive clones were confirmed for correct targeting by Southern blot analysis and karyotyped for euploidy. One clone was selected for injection into C57BL/6N blastocysts.

The NM1 tri-loxP conditional mutation (**Fig. 1B**) was induced in the 129/S2 genetic background. Male chimeras with more than 50% ES-derived coat color were bred with C57BL/6NCrl female mice to test for germ-line transmission and the resulting litters with appropriate coat color were genotyped by PCR for the targeted mutation. Heterozygous mutants carrying the NM1 tri-loxP allele were mated with MeuCre40 transgenic mice on

C57BL/6N background in order to excise the floxed neo and exon -1 cassettes [29]. The resulting offspring were screened for the presence of Cre and for the partial recombination of the NM1 tri-lox allele by PCR (**Table 1**). Heterozygous NM1 knock-outs with a partial deletion of either only the neo cassette or the complete deletion of both exon -1 and the neo cassette were back-crossed to C57BL/6N (Charles River Laboratories, Sulzfeld, Germany) for 5 generations. The resulting mutants were designated as B6;129S2-*Myo1c*$^{tm1(flox)\text{Biat}}$ for the conditional allele and B6;129S2-*Myo1c*$^{tm1.1\text{Biat}}$ for the constitutive NM1 knock-out. For all further experiments, mutants (KO) and wild type (WT) controls were produced by mating heterozygous NM1 knock-out mice and their final genotype was proven either by PCR (**Fig. 1D**) or western blot with antibody specific to N-terminal domain (**Fig. 1E**). Mice were housed under standard conditions, (mean room temperature 21+/-1° Celsius, 40-55% relative humidity, 12:12h light-dark cycle) and supplied with standard breeding diet (ssniff Spezialdiäten GmbH, V1126, Germany) and tap water *ad libitum.* Depending on the experiment, all mice used for analysis were aged between 3 to 15 months.

Genotyping of NM1 knock-out mice

Genotypes of ES cells and mice were confirmed by PCR of genomic DNA using consecutive primers. For identification of targeted ES cells, P1 and P2 primers inside the neomycin-resistance gene were used. Homologically recombined targeting constructs were identified with P3 and P4 primers. The presence of Cre recombinase was shown by CreF and CreR primers. Partial recombination of the NM1 tri-lox allele, together with recognition of full NM1 KO, WT and heterozygous mice was done by P5 and P6 specific primers. All primers with sequences are summarized in **Table 1**.

Cell culture and lentivirus work

Primary skin fibroblasts were isolated from ear explants. Skin samples were washed in PBS and incubated with 0,3% trypsin/PBS for 60 min in a 37°C water bath. Samples were then cut into small pieces, placed on the bottom of Petri dish, overlaid by sterile glass

coverslip and supported by complete growth DMEM medium with 10% FBS. Medium was changed every 3 days until cells grew to confluence. Cells were held for a maximum of 10 passages. Stable cell lines were prepared by long-running cultivation of primary cell culture (over 20 passages). All cell types were grown in humidified 5% CO_2/air, 37°C environment.

For testing of interchangeability of the two myosin isoforms, stable knock-down of human NM1 and Myo1c with exogenous expression of mouse NM1 or Myo1c in U2OS cell line (ATCC No. HTB-96) was prepared. U2OS cells were transduced by pCDH-EF1-Neo carrying mouse Myo1c or NM1 and by pLKO1.1 vector expressing shRNA targeting the sequence 5' -GCCCGTCCAGTATTTCAACAA- 3' (Open Biosystems cat No TRCN0000122925 AAO75-C-8). U2OS cells either stably expressing mouse Myo1c-GFP, NM1-GFP or expressing only the endogenous human protein were transduced with recombinant lentiviruses expressing shRNA targeting only human cDNA. 3 days post transduction Pol I transcription rates were compared in WT U2OS cells, U2OS cells expressing shRNA targeting human NM1 and Myo1c and U2OS cells expressing shRNA with exogenous expression of Myo1c-GFP or NM1-GFP by using quantitative PCR. Recombinant lentiviruses were prepared using second generation viral packaging system (Didier Trono Lab).

For immunoprecipitation experiments, a human H1299 cell line (ATCC No. CRL-5803) stably expressing either NM1-FI or Myo1c-FI was prepared by lentivirus transduction of pCDH-CMV-MCS-EF1-Neo vectors carrying NM1-FI or Myo1c-FI constructs.

HeLa cells (ATCC No. CCL-2) were used for defining the protein ratio of the two isoforms in the cell nucleus and cytoplasm.

Antibodies

For western blots and immunofluorescence detection of NM1, rabbit polyclonal antibody specific to N-terminal part of NM1 (M3456, Sigma) or rabbit polyclonal anti-NM1 antibody, which was kindly provided by Piergiorgio Percipalle [20] were used. Polyclonal antibody (R2652) against the tail domain of Myo1c was kindly supplied by Peter G. Gillespie, Oregon

Hearing Research Center and Vollum Institute [30]. All other antibodies used in this study are commercially available: antibody against β-actin (A2066) was purchased from Sigma, anti-GAPDH antibody (clone 6G5) is available from Acris antibodies, anti-FLAG tag antibody (200471) from Stratagene, and anti-RNA polymerase II CTD phospho S2 (H5; ab24758) from Abcam.

Quantification of NM1/Myo1c ratio using LI-COR Odyssey© system

To explore the ratio between both isoforms in the cell nucleus and cytoplasm in HeLa cells, LI-COR Odyssey© fluorescent detection system was used. A polyclonal antibody to the N-terminus and a monoclonal antibody that was generated against the tail domain of NM1/Myo1c (described above) were coupled to infrared dyes IRDye 680 and IRDye® 800CW (LI-COR), which enables quantification of fluorescent signal in two separate channels. To normalize the signal from the two antibodies, we transfected cells with a NM1-GFP construct that has the molecular weight of 170 kDa.

Immunoprecipitation of NM1-Fl and Myo1c-Fl

H1299 cell line stably expressing NM1-Flag or Myo1c-Flag was prepared by lentivirus transduction. For the experiment cells were washed with PBS and extracted with buffer containing 50 mM HEPES pH 8, 300 mM NaCl, 4 mM $MgCl_2$ and 1 % Triton X-100 and sonicated. Extract was cleared by centrifugation and filtered through 0.45 um filter. Clear lysate was incubated 2 hours with 15 ul of pre-equilibrated Flag-M2 agarose (Sigma). As a control, lysates were incubated 2 hours with control IgG from pre-immune serum cross-linked to protein G-agarose beads. After the incubation beads were washed 3 times with buffer containing 50 mM HEPES pH 8, 300 mM NaCl and 4 mM $MgCl_2$. Finally, the bound proteins were boiled for 5 min into SDS-PAGE loading buffer and analyzed by SDS-PAGE.

Phenotyping of mice

A broad phenotype analysis of 50 wild type littermates as controls (29 males, 21 females) and 46 NM1 knock-out mice (27 males, 19 females) was done in collaboration with the

German Mouse Clinic (Helmholtz Zentrum München - Deutsches Forschungszentrum für Gesundheit und Umwelt (GmbH), Neuherberg, Germany). Mice, 9-18 weeks old, were analyzed for irregularities in dysmorphology, behavior, neurology, nociception, eye function, energy metabolism, clinical chemistry and hematology, immunology, allergy reaction, steroid metabolism, cardiovascular and lung function, and pathology according to standardized protocols [31,32].

Bone density analysis

After anesthesia, the weight and length of the mouse were recorded, and the mouse was placed in the pDEXA Sabre X-ray Bone Densitometer (Norland Medical Systems. Inc., Basingstoke, Hampshire, UK). After a scout scan, the area of interest was optimized and the measurement scan started using following settings: scan speed 20 mm/s, resolution 0.5 mm x 1.0 mm, and HAW 0.020. The standard analysis comprises a whole body analysis as well as a whole body analysis excluding the skull. Analysis of quantitative data sets was carried out using StatView software package (SAS Corporation).

Hematology analysis

To investigate the peripheral blood cell count, a blood volume of about 50 µl EDTA-blood was used to measure basic hematological parameters with a blood analyzer, which has been validated for the analysis of mouse blood using the laboratory mouse chip card (ABC-Blutbild-Analyzer, Scil Animal Care Company GmbH; Viernheim, Germany). Number and size of red blood cells were measured by electrical impedance, and hemoglobin by spectrophotometry. Mean corpuscular volume (MCV) was calculated directly from the cell volume measurements. The hematocrit (HCT) was assessed by multiplying the MCV with the red blood cell count. Mean corpuscular hemoglobin (MCH) and mean corpuscular hemoglobin concentration (MCHC) were calculated from hemoglobin/red blood cell count and hemoglobin/hematocrit respectively. Data were statistically analyzed using an R-Script, applying ANOVA (testing effects of genotype, sex and the interaction of both) and subsequent pair-wise comparisons using the Tukey *post hoc* test, and the Wilcoxon Rank

Sum Test on genotype differences separately for each sex and over all, with the level of significance set at $p<0.05$.

Pulmonary function analysis

All mice were anesthetized by i. p. injection of ketamine (137 mg/kg body weight) and xylazin (6.6 mg/kg body weight). After opening the trachea by a small incision, an 18 gauge cannula was inserted and fixated by ligation. The mice were then placed in a FinePointe RC system (Buxco Research Systems; Wilmington, NC, USA). In a heated plethysmograph chamber, mice were ventilated at an average rate of 160 breaths per minute, and flow and mouth pressure and heart rate were monitored to measure resistance and dynamic compliance. Beginning with an initial acclimation period of three minutes, a two-minute measurement was performed. After the resistance (R) and compliance (Cdyn) measures, mice were transferred to a forced pulmonary maneuvers system (Buxco Research Systems; Wilmington, NC, USA). Here, the forced residual capacity (FRC) was determined during spontaneous breathing of the mouse using Boyle's Law, then quasistatic pressure volume (PV) and fast flow volume (FV) maneuvers were run three times each and averaged to obtain all lung volume and flow parameters. The PV test uses a slow expiration phase after inflating the mouse to total lung capacity (TLC) to obtain quasistatic chord compliance (Cchord), TLC, expiratory reserve volume (ERV), residual volume (RV) and inspiratory capacity (IC). The FV test applies a fast expiration after inflation to TLC, thereby measuring forced vital capacity (FVC), peak expiratory flow (PEF) and forced expiratory volume at 100 ms (FEV100).
Measurements were always performed between 8 a.m. and 1 p.m. The system was set up in a quiet room where temperature and humidity were kept constant throughout the measurements. Statistical analyses were performed using R-scripts implemented in the database (MausDB). Differences between genotypes were evaluated by Wilcoxon test. Statistical significance was assumed at $p<0.05$. Data are presented as mean values ± standard deviation (SD).

Cell proliferation rate

Cells were seeded on a 6-well culture plate at a 20% confluence and left to grow for six days in full DMEM medium, and then the number of cells was counted. For quantitative analysis of cell viability and cell proliferation, we also used the redox indicator dye alamarBlue® (life technologies), which yields a colorimetric change in a response to a metabolic activity. For all the experiments primary as well as stable skin fibroblast derived from mice ear explants were used.

RNA isolation and RT-qPCR

Total RNA from cells was isolated with GeneElute Mammalian total RNA Miniprep Kit (Sigma) according to manufacturer's protocol. The cells were lysed directly on cultivation plates. Concentration of RNA was measured by spectrophotometry and the integrity of RNA was checked on an agarose gel. 50 ng of total RNA was reverse transcribed and single-step real-time qPCR was performed with TaqMan® Reverse Transcription Reagents and PowerSYBR® Green PCR Master Mix (Applied Biosystems, Roche). RT-qPCR was performed in ABI Prism 7300 instrument (Applied Biosystems). For detection of mRNA of Myo1c and 45S pre-rRNA and GAPDH genes, the following primers were used: Myo1c CGATCACCCGAAGAACCA and GCGCTCTCCATGGTCACT, 45S pre-rRNA GGAGTGGGGGGTGGCCGG and GGGGAGAGGAGCAGACGAG, and GAPDH GGAAGGGCTCATGACCACAG and GCCATCCACAGTCTTCTGGG. Expression levels of 45S pre-rRNA and Myo1C were evaluated relative to GAPDH expression level.

Results

NM1 knock-out mice are viable and fertile.

Because of the different expression pattern of NM1 in different tissues and the important roles of this protein in transcription [6,16], chromatin remodeling [17], and chromosome movements [33], one would assume that NM1 knock-out would have lethal

effect early during embryonic development or would have severe developmental defects. However, NM1 KO mice were fully viable with no significant differences from WT mice. They had a normal number of littermates and sex rate. 320 offspring from heterozygous mating have been checked: there were 157 males (49%) and 163 females (51%); 83 animals were wild type (25.9%), 159 heterozygous (49.7%) and 78 animals homozygous mutants (24.3%); the mean litter size was 6.09 pups per litter. These data indicate no major deviations from the expected numbers according to the Mendelian laws suggesting normal fertility of the heterozygous mice and viability of the homozygous mutants.

NM1 knock-out mice did not show significant differences in weight, size or physical condition, and haven´t shown any obvious behavior deviations or defects, or any pathology differences (data not shown). 50 wild type controls (29 males, 21 females) and 46 NM1 -/- mice (27 males, 19 females) have been analyzed for irregularities in dysmorphology, behavior, neurology, nociception, eye function, energy metabolism, clinical chemistry and hematology, immunology, allergy reaction, steroid metabolism, cardiovascular and lung function, and pathology in a comprehensive phenotypic screen in cooperation with the German Mouse Clinic.

In previous experiments, Kahle et al. (2007) have determined the expression profile of NM1 in different mouse tissues, with the highest NM1 protein levels in the lungs. Therefore, first we evaluated the qualitative aspects of lung function. Several parameters have been tested in female NM1 -/- mutants and then compared to wild type littermates (Tidal Volume, Inspiratory Capacity, Expiratory Reserve Volume, Vital Capacity, Functional Residual Capacity, Total Lung Capacity, Forced Vital Capacity, Flow Parameters, Forced Expiratory Volume, Peak Expiratory Flow, Static Lung Compliance, Dynamic Lung Compliance, and Lung Resistance). However, no significant genotype-specific differences in volumetric, flow or mechanical lung function parameters were found (**Table 2**). Therefore, despite high NM1 expression in lungs, the NM1 knock-out has no significant effect on pulmonary function *per se*.

Further tests on NM1 knock-out evaluating deviations or pathological changes in different screens described above did not show any significant change between NM1 WT and KO animals (data will be given upon request).

One group of tests evaluated bone and weight-related quantitative parameters of mature mice at the age of 14 weeks. Here NM1 -/- male mice had significantly ($p \leq 0.05$ without correction due to multiple testing) increased bone mineral density in comparison to wild type mice (+/+: 45±4 mg/cm^2, n=10; -/-: 51±5 mg/cm^2, n=9). Other parameters such as bone mineral content, body weight, body length, fat and lean mass showed no significant change or deviation in comparison to the control littermates (**Table 3**). Finally, hematology screening results indicated mild macrocytosis in mutant animals associated with a trend towards an increased hemoglobin content in erythrocytes, which was accompanied by slightly reduced red blood cell counts and corpuscular hemoglobin concentration in males. Number of red blood cells was slightly decreased (**Fig. 2A**), the mean corpuscular volume (**Fig. 2B**) and mean corpuscular hemoglobin (**Fig. 2C**) were significantly increased. This observation might indicate impaired cell division during erythropoiesis [34].

Taken together, these data show that knock-out of NM1 gene has no effect on mice viability and fertility, and broad phenotyping uncovered some minor but significant changes in bone mineral density and red blood cells parameters without any obvious pathological defects during mice proceeding.

NM1 knock-out has no effect on cell viability, proliferation and transcription activity.

For further experiments, we prepared primary and stable fibroblast cell lines from NM1 KO and WT mice skin explants. These cell lines were used for evaluation of influence of NM1 deficiency at the cellular level. Typically, the condition of a cell highly correlates with the level of transcription activity. Therefore, we examined cell proliferation and viability by measuring the number of cells at different time points after seeding. After six days of growing, numbers of NM1 +/+ and NM1 -/- cells were the same, suggesting that cell proliferation and viability in NM1 KO cells was not affected (**Fig. 3A**). We also performed

alamarBlue® assay to measure proliferation rate by colorimetric change in a response to a metabolic activity of the cells. The data re-confirmed the observations from the proliferation assay (data not shown).

Because of described functions of NM1 in RNA Pol I transcription, we directly explored whether NM1 knock-out has some effect on this process. We isolated RNA from NM1 WT and KO skin fibroblasts in the exponential growth phase, and measured the overall level of 45S pre-rRNA expression by RT-qPCR. NM1 knock-out had no effect on RNA Pol I transcription (**Fig. 3B**), and the expression level of 45S pre-rRNA in both cell lines was comparable.

Considering the connection between NM1 functions in Pol I transcription and the results described above, we can suggest that the function of NM1 protein in knock-out mice and cell lines is supplemented by functioning of other myosin protein or proteins.

NM1/Myo1c expression is nearly equal in tissues and cell lines

We have previously shown that Myo1c protein differs from NM1 in just the first 16 amino acids [6]. Both proteins contain an identical NLS and both are able to enter the nucleus [24]. We therefore asked whether Myo1c would be able to substitute for the nucleus-related functions of NM1.

Firstly, we explored the ratio between both isoforms in the cell nucleus and cytoplasm in HeLa cells. Because the molecular weight of NM1 and Myo1c are very close to each other, we were unable to separate the two isoforms efficiently enough to quantify their amounts directly on western blots. We therefore used LI-COR Odyssey© fluorescent detection system that enables quantification of fluorescent signal in two separate channels. The intensities of NM1 and Myo1c were compared in the cytosolic and nuclear extracts of HeLa cells. We found that in this cell line, the ratio between NM1 and Myo1c was nearly 1:1 in both cellular compartments (**Fig. 4A**). To confirm this result, we used NM1 knock-out skin fibroblasts in which the expression of NM1 is ablated and only Myo1c is expressed. We compared the

level of total protein NM1+Myo1c using western blot. In KO cells, we observed about 50% reduction of signal intensity as compared to the wild type cells **(Fig. 4B)**. Similar reduction in fluorescent signal was observed using immunofluorescent labeling with an antibody against NM1/Myo1c (data not shown). We also repeated the quantification of NM1 and Myo1c using lungs and stomach tissues from NM1 KO in comparison to WT ones. Here the ratio of NM1 versus Myo1c was shifted more toward the Myo1c (~55% in lungs, ~64% in stomach tissue); (**Fig. 4C**).

Taken together, in cell types such as the primary fibroblasts and immortal cell lines, the NM1 isoform comprises about 50% of total NM1+Myo1c, while the ratio appears to be shifted toward the Myo1c isoform in mouse lungs and stomach (**Fig. 4D**).

Myo1c is able to functionally substitute NM1

Since the cellular distribution and expression levels of NM1 and Myo1c are similar, we also explored the possible functional similarities between these isoforms. Previous experiments showed that NM1 depletion decreased RNA polymerase I transcription rate [16]. To test whether Myo1c is able to functionally substitute NM1 in RNA pol I transcription, we used shRNA mediated depletion of NM1/Myo1c in U2OS cells. After decreasing Pol I transcription rate, we were able to reconstitute the phenotype by overexpressing mouse Myo1c that was resistant to the RNAi. Overepression of Myo1c similarly to restored Pol I transcription rate back to almost endogenous level in RNAi depleted cells (**Fig. 5A**). Moreover, NM1 was found to be a component of Pol II transcription machinery and was found to bind to Pol II [6]. We already showed that Myo1c appears to have the same function in Pol I transcription as NM1. To prove if Myo1C would also mimic the function of NM1 with Pol II, we explored possible interacting partners which would belong to molecular components of Pol II transcriptional complex. When immunoprecipitating NM1 or Myo1c proteins tagged with Flag-tag, we succeeded in co-precipitating the CTD domain of Pol II (**Fig. 5B**). This together with previous results showing no significant differences in cell

proliferation and viability in NM1 KO cells suggests a role for Myo1c also in Pol II transcription.

Knock-out of NM1 protein has no effect on Myo1c expression

In a previous experiment, we claimed that Myo1c seems to be able to functionally substitute NM1 in Pol I transcription. To test whether NM1 knock-out leads to a compensatory overexpression of Myo1C, we isolated RNA from NM1 WT and KO skin fibroblasts in the exponential phase of growth, and measured Myo1c expression by RT-qPCR. All experiments were done in triplicates, and we used primers specifically amplifying just the Myo1c coding region. However, the level of expression of Myo1c in both cell lines was comparable (**Fig. 5C**). This result suggests that the amount of Myo1C in the nucleus is sufficient to fulfill the roles in Pol I and Pol II transcription by itself.

Taken together, Myo1c is able to compensate for the loss of NM1. Because the amount of Myo1c is equal to NM1 and there is no compensatory overexpression of Myo1c in NM1 KO cells, we suggest that both isoforms are redundant to each other and can have same functions in Pol I transcription. Moreover, Myo1C is able to bind to CTD domain of Pol II suggesting that these proteins also have identical roles in Pol II transcription.

Discussion

Nuclear myosin I (Myo1c isoform B), the first molecular motor protein which has been discovered in the cell nucleus, has brought a revolution into the myosin field. In comparison to conventional class I myosins which were described in different functions related to plasma membrane and cytoskeleton, endo- and exo- cytosis, cell motility and cell spreading [35], NM1 was found to be directly involved in processes of RNA Pol I and RNA Pol II transcription, chromatin remodeling and chromosome movements in the cell nucleus. Since its discovery in 1997, 5 others myosins have been observed in the cell nucleus (myosin VI, Va, Vb, XVIb, and XVIIIb); [36]. Recently, a new isoform of human myosin 1c protein - isoform A - was discovered and found to localize to the nucleus. Similar to NM1, this isoform contains a unique N-terminal peptide sequence and co-localizes with RNA polymerase in the

nucleoplasm. However, unlike NM1, upon exposure to inhibitors of RNA polymerase II transcription, the newly identified isoform translocates to nuclear speckles. Furthermore, in contrast to NM1, this new isoform is absent from nucleoli and does not co-localize with RNA polymerase I [7].

We showed previously that the “cytoplasmic” Myo1c protein (isoform C) is also able to localize to the nucleus in the same manner as the other isoforms via NLS signal localized in the middle part of molecule [24]. To test the influence of the specific N-terminal 16 amino acids on NM1 functions, we prepared knock-out mice lacking the exon -1 which contains the NM1 start codon. The resulting mRNA only contains the downstream start of translation which gives rise to Myo1c isoform C protein. Surprisingly, knock-out mice were without any obvious phenotype, and proliferation assays together with RT-qPCR of 45S pre-rRNA did not show any differences or aberrance in RNA Pol I and Pol II transcription. This could be explained by compensatory expression of other myosin motor protein, acting in transcription, or by the fact that the overall level of myosin motor proteins in the nucleus is redundant and therefore a depletion of one isoform does not affect transcription. To test these hypotheses, we depleted Myo1c isoforms from U2OS cells by shRNA in order to decrease Pol I transcription. We then measured the reconstitution of transcription after overexpression of mouse Myo1c that was unsusceptible to the RNAi. Exogenously expressed Myo1c was able to restore the Pol I transcription rate to nearly the endogenous level, apparently compensating for the loss of NM1. Moreover, we found that the ratio between both isoforms in the nucleus of WT cells is equal and there is no compensatory change in expression of Myo1c in NM1 KO cells, suggesting that Myo1c is transported to the nucleus normally and its amount in nucleus is sufficient to fulfill myosin functions in transcription by itself. In conclusion, the two different isoforms (B and C) in the nucleus seem to be redundant for effective Pol I transcription. Moreover, Myo1c is able to bind to CTD domain of Pol II suggesting its same role also in Pol II transcription.

However, as mentioned above, the third Myo1c isoform - isoform A - carrying different and longer N-terminal extension has slightly different cytoplasmic and nuclear localization in comparison to NM1 [7], and we also noted previously that localization pattern of exogenously expressed NM1 and Myo1c do not fully overlap [24]. This could suggest different roles for each isoform, dependent on their N-terminal extensions, but most probably without affecting the general process of transcription by Pol I or Pol II. Because we did not detect changes in Pol I transcription in NM1 KO cells, it is possible that different N-terminal extensions will have a role in a fine tuning of myosin functions under special conditions or in specialized cell types. It would be therefore interesting to explore these three isoforms under various stress conditions (i.e. UV, starvation, heat shocks) and in different tissues and cell lines. However, to come to a definitive conclusion, conditional knock-out mouse and derived cell lines lacking all three isoforms are needed.

Studies of NM1 function in tissue and at a whole body level did not show any obvious deviations in comparison to WT mice. However, we discovered minor differences in bone mineral density of KO mice, and discovered several genes with changed expression profiles in NM1 KO mice in relation with lipid metabolism in adipocytes (data not shown). This could relate bone metabolism with insulin signaling and energy metabolism as was described previously [37,38], but the function of NM1 in this process is not known and has to be further studied. However, it was shown that Myo1c is highly expressed in adipocytes and is responsible for movements of GLUT-4 containing vesicles upon insulin stimulus [13]. Therefore we cannot exclude the possibility that NM1 is also playing some role in these processes, but we suppose that its function would be related to the cytoplasmic rather than to nuclear functions. However, to support this speculation, future biochemical analysis of pathways of the insulin signaling in NM1 KO mice are required.

Experiments monitoring physiological changes included also hematology analysis which revealed mild hyperchromic macrocytosis of red blood cells in mutant males characterized by larger red blood cells containing a higher amount of hemoglobin. This

phenotype suggest an impaired cell division during erythropoiesis [34]. Although, in cell culture cell function of the cell cycle machinery did not show a detectable effect, rate limitation concerning proliferation might occur in vivo on a high level due to decreased amounts of Myo1c being available in the nucleus. This could results in mild detectable effects in hematopoiesis since hematopoietic tissue has an extremely high proliferation rate. This would be comparable to the effect of some missense mutations in ribosomal protein S19, which can be associated with macrocytosis as the only or one of some mild symptoms in the heterozygous state in men and mice [39,40]. Another possible explanation is that red blood cells in NM1 knock-out mice have partially impaired linkage between plasma membrane and cytoskeleton, and therefore they could show increased mean corpuscular volume. This suggestion is in agreement with previous data on different members of Myosin I family, which were shown to work as a dynamic link between plasma membrane and cytoskeleton [41]. In particular; class I myosins mediate membrane/cytoskeleton adhesion and thus they make major contribution to membrane tension. Their study showed that class I myosins directly control the mechanical properties of the cell membrane and are master regulators of cellular events involving membrane deformation. Microarray analysis from NM1 KO mice and co-immunoprecipitation experiments, which identified mostly cytoplasmic and membranous proteins link NM1 to similar processes, described for the other members of Myosin I family (Kalendova and Venit, in preparation). However, results mentioned above suggest some new role of NM1 on the cell membrane and in cytoplasmic shuttling but not in nucleus/nucleolus.

In conclusion, we prepared mice lacking functional nuclear myosin 1 protein, which has been described as a key player in Pol I and Pol II transcription. Knock-out mice do not show any obvious pathological phenotype, which can be explained by functioning of “cytoplasmic” Myo1c isoform in nucleus in general process of transcription. Both proteins have nearly equal expression levels and distribution in the cell and a knock-out of NM1 does not cause any compensatory changes in Myo1c expression. Therefore, we suggest that both isoforms are interchangeable and redundant with each other in the cell nucleus. This data raises additional interesting questions: What is the functional significance of the different N-

terminal regions of the myosin molecules in nuclear and cytoplasmic processes? What are the functions of NM1 in the cytoplasm and on plasma membrane? What is the relationship between these isoforms in the different cell types or tissues? Obviously, some further investigation and preparation of new tools will be needed to understand the interplays of Myosin 1c isoforms.

Acknowledgments

We are very grateful to Prof. Peter Gillespie and Prof. Piergiorgio Percipalle for providing the antibodies, and Pavel Kříž and Iva Jelínková for technical assistance. Moreover, we want to thank Reinhard Seeliger, Birgit Frankenberger, Christine Hollauer, Elfi Holupirek, Susanne Wittich, and Anja Wohlbier, as well as the GMC animal caretaker team for sophisticated technical assistance in mouse phenotyping.

This study has been supported by the Grant Agency of Czech Republic (Reg. No. 204/09/4048 and Reg. No. P305/11/2232), by the Technology Agency of Czech Republic (Reg. No. TE01010118), by the Ministry of Education, Youth and Sports of the Czech Republic (Reg. No. LH12143), by the institutional grant AV0Z50520514, by the Grant Agency of the Charles University (Reg. No. 253189) and by the Austrian Federal Ministry of Science and Research (BM.W_Fa, GEN-AU II/III “Austromouse”). Phenotyping of NM1 KO mice in the German Mouse Clinic has been supported by grants from the European Community (EUMODIC LSHG-2006–037188) and from the Bundesministerium für Bildung und Forschung (NGFN-Plus: 01GS0850, 01GS0851; Infrafrontier 01KX1012) to the GMC and to the German Center for Diabetes Research (DZD e.V.).

Figures:

Figure 1. Preparation of NM1 knock-out cassette. (**A**) WT genomic locus of *Myo1c* gene. Short homology arm (SA), floxed part (FP), and long homology arm (LA) of appropriate length (0.9; 0.3; 1.7 kb respectively), were cloned to pEasyFlox vector carrying neomycin

(NeoR) and thymidine kinase (ThK) selection genes (**B**). Black lines represent genomic sequences; red line represents sequences derived from pEasyFlox vector. (**B**). (**C**) Genomic loci of *Myo1c* gene with excision of exon -1; P1 – P6 represent different primers needed for genotyping of ES cells and knock-out mice, yellow triangles represent loxP recombination sites. (**D**) Genotyping of NM1 knock-out mice by PCR. P5 and P6 primers were used to distinguish between wild type (+/+), heterozygous (+/-) and knock-out (-/-) animals. (**E**) Western blot analysis of NM1 levels in NM1 wild type (+/+) and knock-out (-/-) mice. Fifteen micrograms of protein per lane was loaded, and probed for NM1. Equal loading was monitored by Coomassie Brilliant Blue staining of the band corresponding to actin.

Figure 2. Red blood cells related phenotype in NM1 knock-out mice. (**A**) Comparison of red blood cell counts (RBC) between NM1 KO (-/-) and WT (+/+) male (m) and female (f) mice. Male mice show slightly lower number of red blood cells. (**B**) Comparison of mean corpuscular volume (MCV) in WT and KO animals shows increased cell volume in KO males and females. (**C**) NM1 KO animals have increased mean corpuscular hemoglobin (MCH) level in comparison to WT males. Data are presented as mean +/- SD. * $p<0.1$; ** $p<0.05$, *** $p<0.01$, **** $p<0.001$.

Figure 3. NM1 knock-out has no effect on cell proliferation and Pol I transcription. (**A**) Proliferation of NM1 KO cells (NM1 -/-) is not altered in comparison to WT cells (NM1 +/+). $1x10^5$ cells were seeded on plates (20% confluence; day 0) and let to grow for six days when number of cells was counted again (day 6). (**B**) Pol I transcription rate in NM1 KO (NM1 -/-) and WT (NM1 +/+) cells is equal. RNA from exponentially growing cells was isolated and expression of 45S pre-rRNA was measured by RT-qPCR. Expression of 45S pre-rRNA is compared relatively to GAPDH expression. Data are presented as mean +/- SD.

Figure 4. Ratio between NM1 and Myo1c is nearby equal. (**A**) HeLa cells were fractionated into cytosolic and nuclear fractions. NM1 and Myo1c amounts were quantified using double fluorescent labeling of western blot membranes after normalization to NM1-GFP band. (**B**) Total amounts of NM1 + Myo1c were compared in mouse skin fibroblasts

derived from NM1 knock-out and NM1 wild type mouse. Beta actin signal was used as loading normalizer. (**C**) Total amounts of NM1 + Myo1c were compared in lungs and stomach from NM1 knock out and NM1 wild type mouse. GAPDH signal was used as loading normalizer. (**D**) The graph shows the amount of NM1 and Myo1c after densitometric quantification of bands from figures 4B and 4C showing the ratio between NM1 and Myo1c as compared to actin/GAPDH expression.

Figure 5. Myo1C is able to function in Pol I and Pol II transcription without changes in its expression level. (**A**) The level of nascent rRNA was decreased to 80% of WT levels in NM1/Myo1c knock-down cells (U2OS+C8). An overexpression of mouse NM1 (U2OS+C8+NM1) or Myo1c (U2OS+C8+M1c) resistant to shRNA causes restoration of Pol I transcription to almost endogenous levels. As a negative control were used U2OS cells with transduced empty pLKO1.1 vector (U2OS+NC). (**B**) Both NM1-Flag and Myo1c-Flag interact with Pol II. Extracts from cells overexpressing NM1-Flag and Myo1c-Flag were co-immunoprecipitated with Flag antibody and control IgG. Immunoprecipitates were analyzed by western blotting with antibodies against Flag, Pol II CTD subunit and Myo1c (tail domain recognizing both NM1 and Myo1c). (**C**) NM1 knock-out does not cause compensatory changes in expression of Myo1c. Expression of Myo1c was measured by RT-qPCR and compared relative to GAPDH expression. Data are presented as mean +/- SD. *** $p<0.001$.

References

1. Barylko B, Jung G, Albanesi JP (2005) Structure, function, and regulation of myosin 1C. Acta Biochim Pol 52: 373-380.
2. Wagner MC, Barylko B, Albanesi JP (1992) Tissue distribution and subcellular localization of mammalian myosin I. J Cell Biol 119: 163-170.
3. Reizes O, Barylko B, Li C, Sudhof TC, Albanesi JP (1994) Domain structure of a mammalian myosin I beta. Proc Natl Acad Sci U S A 91: 6349-6353.
4. Gillespie PG, Albanesi JP, Bahler M, Bement WM, Berg JS, et al. (2001) Myosin-I nomenclature. J Cell Biol 155: 703-704.
5. Nowak G, Pestic-Dragovich L, Hozak P, Philimonenko A, Simerly C, et al. (1997) Evidence for the presence of myosin I in the nucleus. J Biol Chem 272: 17176-17181.
6. Pestic-Dragovich L, Stojiljkovic L, Philimonenko AA, Nowak G, Ke Y, et al. (2000) A myosin I isoform in the nucleus. Science 290: 337-341.

7. Ihnatovych I, Migocka-Patrzalek M, Dukh M, Hofmann WA (2012) Identification and characterization of a novel myosin Ic isoform that localizes to the nucleus. Cytoskeleton (Hoboken) 69: 555-565.
8. Arif E, Wagner MC, Johnstone DB, Wong HN, George B, et al. (2011) Motor protein Myo1c is a podocyte protein that facilitates the transport of slit diaphragm protein Neph1 to the podocyte membrane. Mol Cell Biol 31: 2134-2150.
9. Wang FS, Wolenski JS, Cheney RE, Mooseker MS, Jay DG (1996) Function of myosin-V in filopodial extension of neuronal growth cones. Science 273: 660-663.
10. Diefenbach TJ, Latham VM, Yimlamai D, Liu CA, Herman IM, et al. (2002) Myosin 1c and myosin IIB serve opposing roles in lamellipodial dynamics of the neuronal growth cone. J Cell Biol 158: 1207-1217.
11. Sokac AM, Schietroma C, Gundersen CB, Bement WM (2006) Myosin-1c couples assembling actin to membranes to drive compensatory endocytosis. Dev Cell 11: 629-640.
12. Bose A, Guilherme A, Robida SI, Nicoloro SM, Zhou QL, et al. (2002) Glucose transporter recycling in response to insulin is facilitated by myosin Myo1c. Nature 420: 821-824.
13. Bose A, Robida S, Furcinitti PS, Chawla A, Fogarty K, et al. (2004) Unconventional myosin Myo1c promotes membrane fusion in a regulated exocytic pathway. Mol Cell Biol 24: 5447-5458.
14. Stauffer EA, Scarborough JD, Hirono M, Miller ED, Shah K, et al. (2005) Fast adaptation in vestibular hair cells requires myosin-1c activity. Neuron 47: 541-553.
15. Zadro C, Alemanno MS, Bellacchio E, Ficarella R, Donaudy F, et al. (2009) Are MYO1C and MYO1F associated with hearing loss? Biochim Biophys Acta 1792: 27-32.
16. Philimonenko VV, Zhao J, Iben S, Dingova H, Kysela K, et al. (2004) Nuclear actin and myosin I are required for RNA polymerase I transcription. Nat Cell Biol 6: 1165-1172.
17. Percipalle P, Fomproix N, Cavellan E, Voit R, Reimer G, et al. (2006) The chromatin remodelling complex WSTF-SNF2h interacts with nuclear myosin 1 and has a role in RNA polymerase I transcription. EMBO Rep 7: 525-530.
18. Grummt I (2006) Actin and myosin as transcription factors. Curr Opin Genet Dev 16: 191-196.
19. Ye J, Zhao J, Hoffmann-Rohrer U, Grummt I (2008) Nuclear myosin I acts in concert with polymeric actin to drive RNA polymerase I transcription. Genes Dev 22: 322-330.
20. Fomproix N, Percipalle P (2004) An actin-myosin complex on actively transcribing genes. Exp Cell Res 294: 140-148.
21. Obrdlik A, Louvet E, Kukalev A, Naschekin D, Kiseleva E, et al. (2010) Nuclear myosin 1 is in complex with mature rRNA transcripts and associates with the nuclear pore basket. FASEB J 24: 146-157.
22. Hofmann WA, Johnson T, Klapczynski M, Fan JL, de Lanerolle P (2006) From transcription to transport: emerging roles for nuclear myosin I. Biochem Cell Biol 84: 418-426.
23. Ambrosino C, Tarallo R, Bamundo A, Cuomo D, Franci G, et al. (2010) Identification of a hormone-regulated dynamic nuclear actin network associated with estrogen receptor alpha in human breast cancer cell nuclei. Mol Cell Proteomics 9: 1352-1367.
24. Dzijak R, Yildirim S, Kahle M, Novak P, Hnilicova J, et al. (2012) Specific nuclear localizing sequence directs two myosin isoforms to the cell nucleus in calmodulin-sensitive manner. PLoS One 7: e30529.
25. Kahle M, Pridalova J, Spacek M, Dzijak R, Hozak P (2007) Nuclear myosin is ubiquitously expressed and evolutionary conserved in vertebrates. Histochem Cell Biol 127: 139-148.
26. Kysela K, Philimonenko AA, Philimonenko VV, Janacek J, Kahle M, et al. (2005) Nuclear distribution of actin and myosin I depends on transcriptional activity of the cell. Histochem Cell Biol 124: 347-358.
27. Philimonenko VV, Janacek J, Harata M, Hozak P (2010) Transcription-dependent rearrangements of actin and nuclear myosin I in the nucleolus. Histochem Cell Biol 134: 243-249.
28. Schenten D, Gerlach VL, Guo C, Velasco-Miguel S, Hladik CL, et al. (2002) DNA polymerase kappa deficiency does not affect somatic hypermutation in mice. Eur J Immunol 32: 3152-3160.

29. Leneuve P, Colnot S, Hamard G, Francis F, Niwa-Kawakita M, et al. (2003) Cre-mediated germline mosaicism: a new transgenic mouse for the selective removal of residual markers from tri-lox conditional alleles. Nucleic Acids Res 31: e21.
30. Gillespie PG, Wagner MC, Hudspeth AJ (1993) Identification of a 120 kd hair-bundle myosin located near stereociliary tips. Neuron 11: 581-594.
31. Fuchs H, Gailus-Durner V, Adler T, Aguilar-Pimentel JA, Becker L, et al. (2011) Mouse phenotyping. Methods 53: 120-135.
32. Gailus-Durner V, Fuchs H, Adler T, Aguilar Pimentel A, Becker L, et al. (2009) Systemic first-line phenotyping. Methods Mol Biol 530: 463-509.
33. Chuang CH, Carpenter AE, Fuchsova B, Johnson T, de Lanerolle P, et al. (2006) Long-range directional movement of an interphase chromosome site. Curr Biol 16: 825-831.
34. Aslinia F, Mazza JJ, Yale SH (2006) Megaloblastic anemia and other causes of macrocytosis. Clin Med Res 4: 236-241.
35. McConnell RE, Tyska MJ (2010) Leveraging the membrane - cytoskeleton interface with myosin-1. Trends Cell Biol 20: 418-426.
36. Simon DN, Wilson KL (2011) The nucleoskeleton as a genome-associated dynamic 'network of networks'. Nat Rev Mol Cell Biol 12: 695-708.
37. Ferron M, Wei J, Yoshizawa T, Del Fattore A, DePinho RA, et al. (2010) Insulin signaling in osteoblasts integrates bone remodeling and energy metabolism. Cell 142: 296-308.
38. Fulzele K, Riddle RC, DiGirolamo DJ, Cao X, Wan C, et al. (2010) Insulin receptor signaling in osteoblasts regulates postnatal bone acquisition and body composition. Cell 142: 309-319.
39. McGowan KA, Li JZ, Park CY, Beaudry V, Tabor HK, et al. (2008) Ribosomal mutations cause p53-mediated dark skin and pleiotropic effects. Nat Genet 40: 963-970.
40. Willig TN, Draptchinskaia N, Dianzani I, Ball S, Niemeyer C, et al. (1999) Mutations in ribosomal protein S19 gene and diamond blackfan anemia: wide variations in phenotypic expression. Blood 94: 4294-4306.
41. Nambiar R, McConnell RE, Tyska MJ (2009) Control of cell membrane tension by myosin-I. Proc Natl Acad Sci U S A 106: 11972-11977.

Tables:

Table 1. PCR primers for genotyping of ES cells and mice mutants

Name	Sequence 5' - 3'
P1	AGACAATCGGCTGCTCTGAT
P2	CTCGTCCTGCAGTTCATTCA
P3	GGGTAGTAGTGGTGTTGATGGCTTGG
P4	TGTTCCACATACACTTCATTCTCAG
P5	TTCCTCCTGGAAAACCTGACTC
P6	CTCTGCTTCTCCGTCACCC
CreF	CTGGAAAATGCTTCTGTCCG
CreR	CAGGGTGTTATAAGCAATCCC

Table 2. Lung function parameters tested in NM1 knock-out and wild type mice

Parameter		**Female WT**	**Female KO**	**p-value**
		n=6	**n=6**	
Body Mass	[g]	28.2 ± 2.5	26.1 ± 3.3	0.223
Volumetric Parameters				
Tidal Volume	[ml]	0.203 ± 0.005	0.206 ± 0.007	0.665
Inspiratory Capacity	[ml]	0.88 ± 0.087	0.841 ± 0.119	0.394
Expiratory Reserve Volume	[ml]	0.27 ± 0.06	0.3 ± 0.04	0.294
Vital Capacity	[ml]	1.15 ± 0.13	1.14 ± 0.16	0.851
Functional Residual Capacity	[ml]	0.257 ± 0.028	0.266 ± 0.027	0.316
Total Lung Capacity	[ml]	1.137 ± 0.094	1.107 ± 0.131	0.394
Forced Vital Capacity	[ml]	1.052 ± 0.102	1.028 ± 0.156	0.394
Flow Parameters				
Forced Expiratory Volume	[ml]	1.024 ± 0.095	0.999 ± 0.151	0.416
Peak Expiratory Flow	[ml/sec]	29.9 ± 0.6	28.5 ± 1.7	0.197
Mechanical Parameters				
Static Lung Compliance	[ml/cm H2O]	0.0694 ± 0.0084	0.0678 ± 0.0104	0.732
Dynamic Lung Compliance	[ml/cm H2O]	0.0262 ± 0.0028	0.0278 ± 0.0042	0.818
Lung Resistance (R)	[cm H2O/ml/sec]	1.35 ± 0.08	1.31 ± 0.09	0.563

Table 3. Overall body and bone parameters in NM1 knock-out and wild type mice

Parameter		**Male WT**	**Male KO**	**p-value**
		n=10	**n=9**	
Bone mineral density	[mg/cm^2]	45 ± 4	51↑ ± 5	0.01
Bone mineral content	[mg]	350 ± 95	286 ± 86	0.147
Bone content	[%]	1.24 ± 0.31	1.01 ± 0.31	0.134
Body length	[cm]	9.68 ± 0.22	9.70 ± 0.18	0.835
Body weight	[g]	28.07 ± 1.34	28.28 ± 0.93	0.703
Fat Mass	[g]	2.73 ± 2.01	2.13 ± 1.28	0.459
Lean Mass	[g]	19.59 ± 2.43	20.22 ± 2.15	0.564

Fig 1.

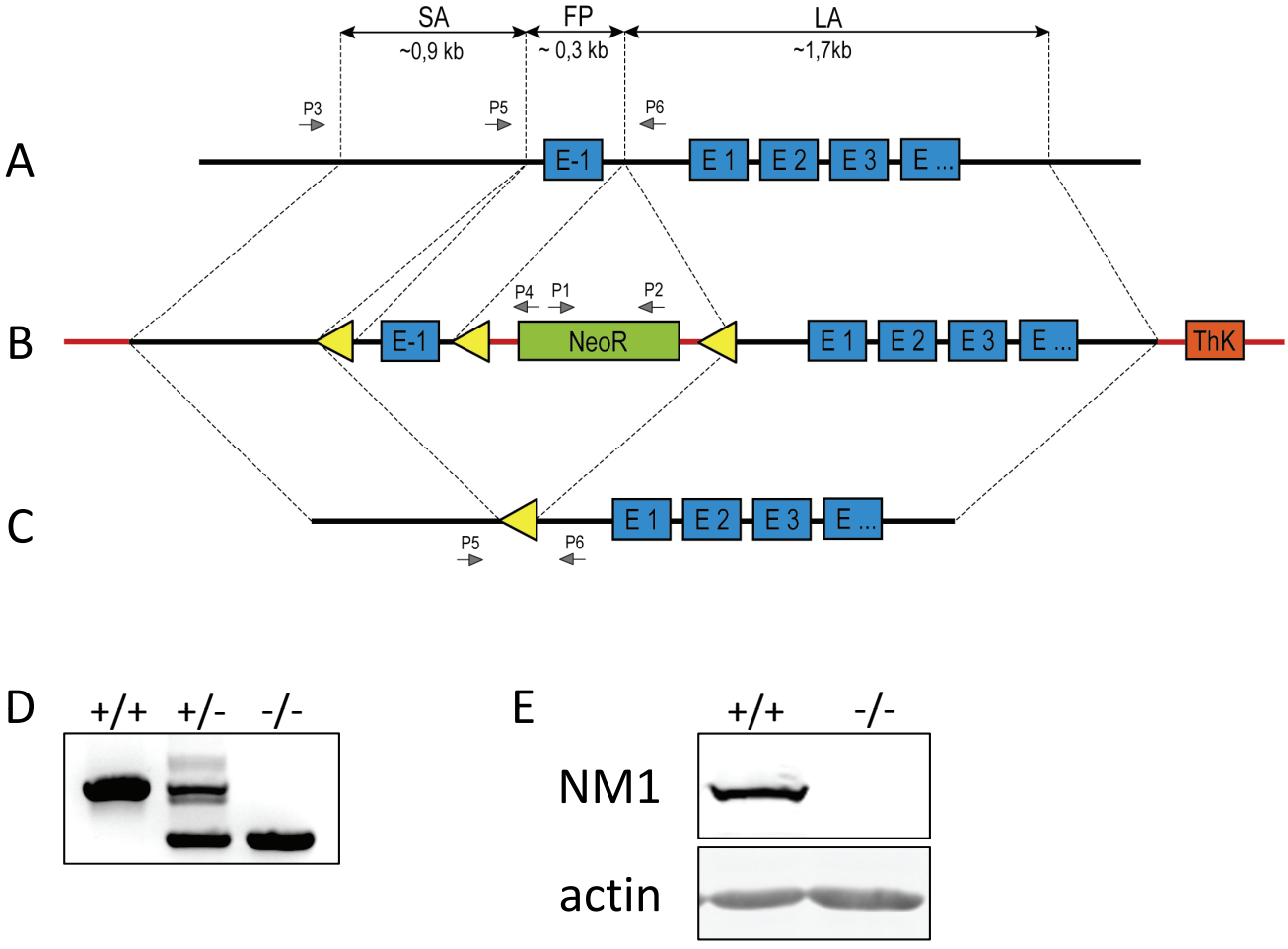
SA
~0,9 kb
FP
~ 0,3 kb
LA
~1,7kb
P3
P5
P6
A
E-1
E 1
E 2
E 3
E ...
P4
P1
P2
B
E-1
NeoR
E 1
E 2
E 3
E ...
ThK
C
E 1
E 2
E 3
E ...
P5
P6
D
+/+
+/-
-/-
E
+/+
-/-
NM1
actin

Fig. 2

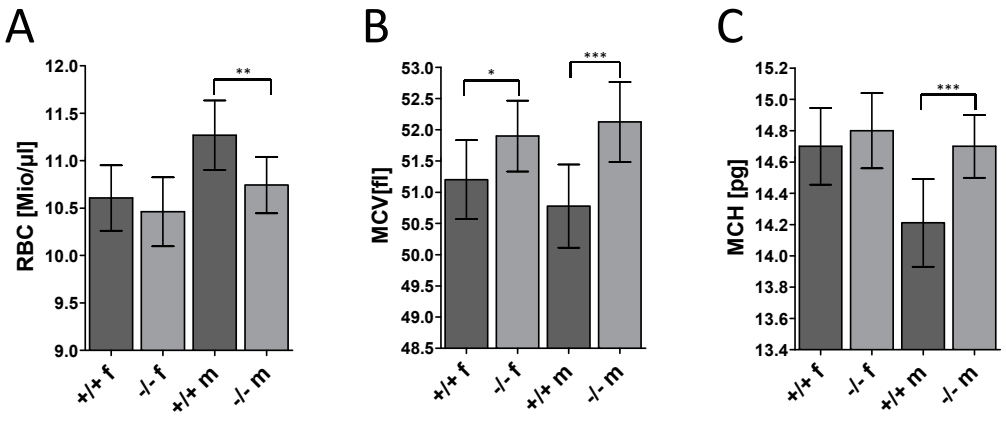

Fig. 3

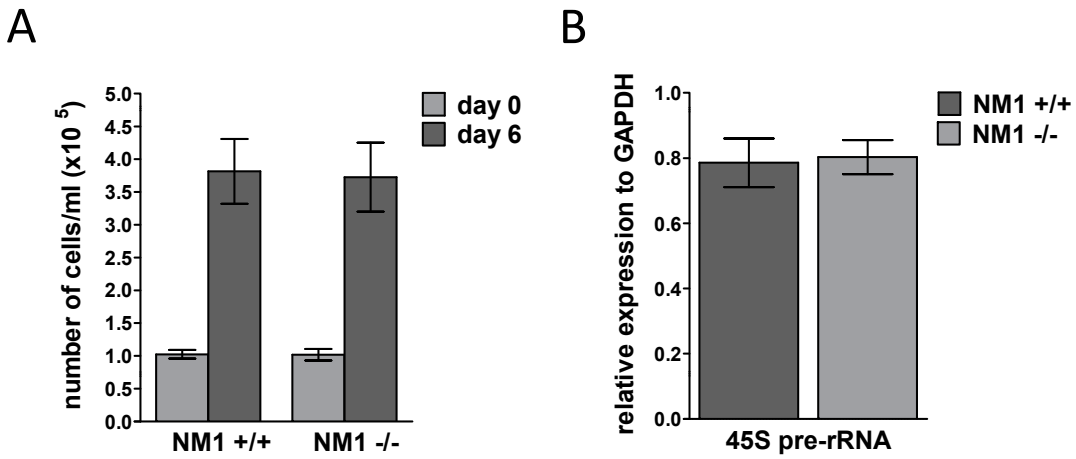
A
number of cells/ml (x10 5)
5.0
4.5
4.0
3.5
3.0
2.5
2.0
1.5
1.0
0.5
0.0
day 0
day 6
NM1 +/+
NM1 -/-
B
relative expression to GAPDH
1.0
0.8
0.6
0.4
0.2
0.0
NM1 +/+
NM1 -/-
45S pre-rRNA

Fig. 4

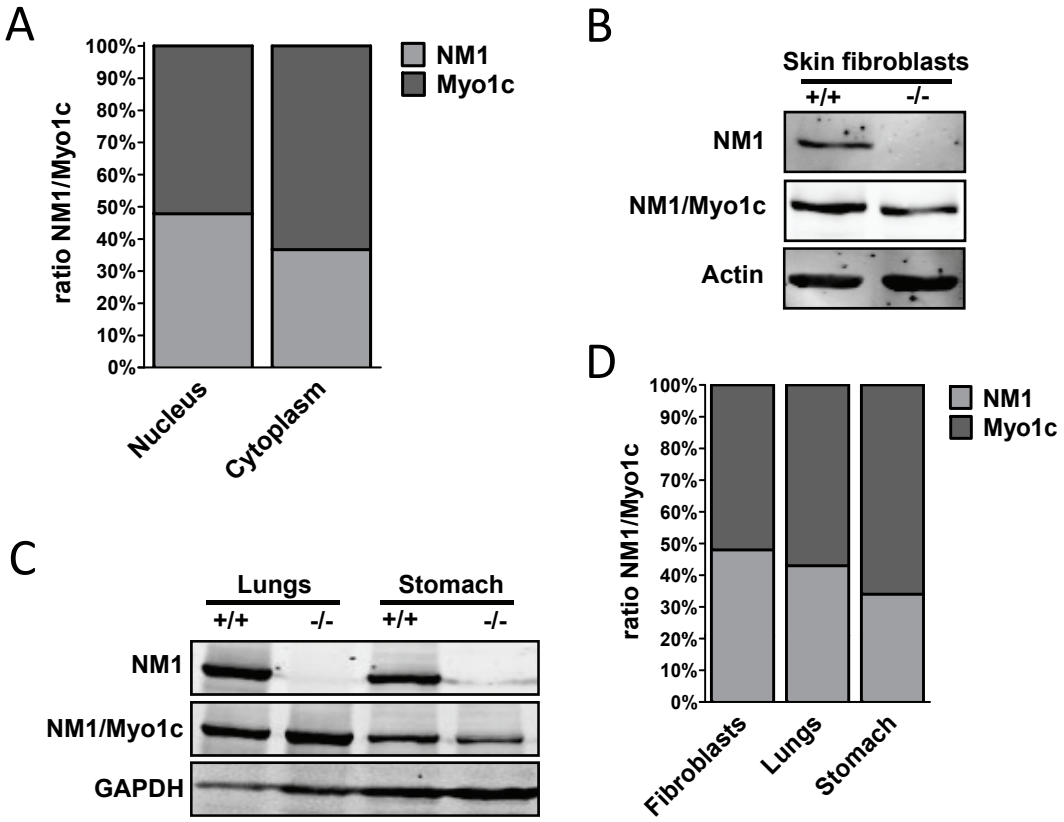
A
100%
90%
80%
70%
60%
50%
40%
30%
20%
10%
0%
ratio NM1/Myo1c
NM1
Myo1c
Nucleus
Cytoplasm
B
Skin fibroblasts
+/+
-/-
NM1
NM1/Myo1c
Actin
C
Lungs
Stomach
+/+
-/-
+/+
-/-
NM1
NM1/Myo1c
GAPDH
D
100%
90%
80%
70%
60%
50%
40%
30%
20%
10%
0%
ratio NM1/Myo1c
NM1
Myo1c
Fibroblasts
Lungs
Stomach

Fig. 5

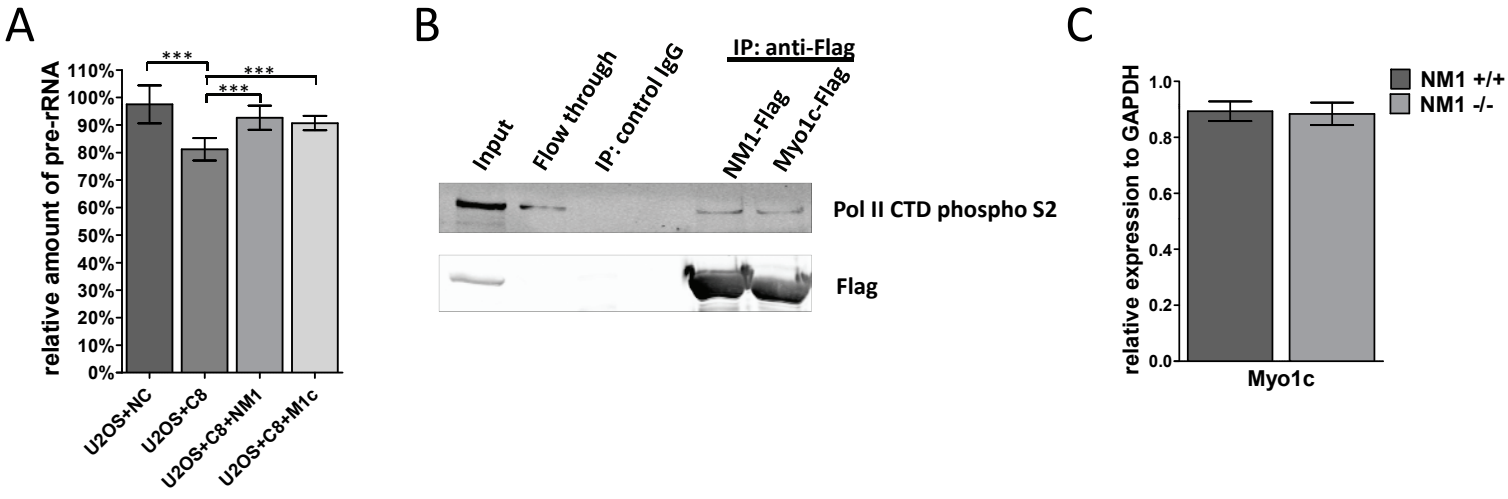
A
relative amount of pre-rRNA
110%
100%
90%
80%
70%
60%
50%
40%
30%
20%
10%
0%
***
***
***
U2OS+NC
U2OS+C8
U2OS+C8+NM1
U2OS+C8+M1c
B
IP: anti-Flag
Input
Flow through
IP: control IgG
NM1-Flag
Myo1c-Flag
Pol II CTD phospho S2
Flag
C
relative expression to GAPDH
1.0
0.8
0.6
0.4
0.2
0.0
NM1 +/+
NM1 -/-
Myo1c

5.4 Cytoplasmic functions for nuclear myosin I

Kalendová A and Venit T, Dzijak R, Rohožková J, Petr M, Hozák P

Manuscript

My contribution to this work:

I prepared NM1 WT and KO cell lines expressing NM1 or GFP. I performed microarray analysis of selected organs and skin fibroblast from NM1 KO and WT mice. I phenotyped WT and KO cell lines and perform hypotonic stress experiments. Finally, I contribute to writing of the manuscript.

Functions of nuclear myosin 1 in cytoplasm

Alžběta Kalendová[1+], Tomáš Venit[1+], Rastislav Dzijak[1], Jana Rohožková[1], Martin Petr[1] and Pavel Hozák[1*]

[1]Department of Biology of the Cell Nucleus, Institute of Molecular Genetics, AS CR, v.v.i., Videnska 1083, 142 20 Prague, Czech Republic

* Corresponding author: hozak@img.cas.cz

[+]These authors contributed equally to this work

Abstract

Myosins are molecules that utilize energy stored in ATP to generate mechanical force during a power stroke cycle. Myosin head binds and releases from the actin while undergoing conformational changes which results in a movement of cargo bound to the myosin tail. Because vertebrate class 1 myosins can bind acidic phospholipids by tail, they serve as a dynamic links between membranes and actin cytoskeleton. They participate in control of membrane tension, cell adhesion and various steps of endocytosis. Surprisingly, two isoforms of a class 1 member myosin 1c (Myo1c, isoform C) termed nuclear myosin 1 (NM1) and Myo1c isoform A have been described as nuclear proteins promoting transcription, chromatin remodelling and ribosomal particles assembly. Recent works however demonstrated that all the three isoforms can be found both in cytoplasm and nucleus and that the function of NM1 and Myo1c in transcription is redundant. In this paper we show that both NM1 and Myo1c predominantly reside in the cytoplasm which suggests some yet unknown cytoplasmic functions of NM1. Skin fibroblasts derived from NM1 knock-out mouse do not show any defects in behaviour under normal conditions. However, when challenged by hypotonic shock, they exhibit increased ability to resist immediate changes in the cell volume. This trend is further strengthened when fibroblasts overexpress NM1-Flag. Co-immunoprecipitations revealed novel NM1 interacting partners: filamin A, annexin A2, myosin 1b and alpha-actinin 4. They co-localize with NM1 especially at the leading edge of the cell where cytoskeleton and cortical actin are dynamically remodelled. When fibroblasts, lung and heart tissues were subjected to expression profiling on microarrays, 222 proteins with altered expression were detected. A vast majority of those are cytoplasmic, membranous and extracellular proteins. These observations point out the specialized functions of NM1 in the cytoplasm, which can not be mimicked by Myo1c. Based on our data

we suggest that NM1 may as well as the other class 1 myosins connect plasma membrane with cytoskeleton, which is reflected in the differential behaviour under hypotonic conditions. Alternatively, NM1 might assist in opening and closure of various transmembrane channels as well as maintain structure of extracellular matrix during assembly of cells into tissues.

Key words

Nuclear myosin 1, NM1, myosin 1c, Myo1c, hypotony, cytoplasm

Introduction

Myosins are proteins that are able to convert chemical energy into mechanical force. This is achieved by the architecture of myosin molecule comprising of a 3 functionally important domains: a head or motor domain, which possesses ATPase activity and therefore regulates binding to actin; neck, where light chains bind in order to provide the necessary stiffness and finally tail, which binds various cargos or enables myosins to polymerize via coiled-coil domains. Based on comparative genomic analysis of the motor domains myosins can be grouped into 35 classes (Odronitz and Kollmar 2007). Class 2 is traditionally called 'conventional' although its members have highly specialized functions among the myosin superfamily (Woolner and Bement 2009).

The unconventional myosin 1 is believed to be one of the myosin ancestors (Foth et al. 2006; Richards and Cavalier-Smith 2005) as members of the class 1 were found in almost all organisms (Odronitz and Kollmar 2007). In vertebrate genome, eight myosin 1 genes termed MYO1A to 1G have been found (Berg et al. 2001). In contrast to conventional ones, myosins 1 are monomeric molecules with a relatively short tails through which they interact with cargos and other proteins. All vertebrate myosins 1 share the same features: they bind actin by the head domain and acidic phospholipids by tail domain. This implicates their physiological functions – linking actin to membranes and membranous structures (Adams and Pollard 1989; Nambiar et al. 2009; Olety et al. 2010). Both human Myo1a and Myo1b control membrane tension and facilitate the initial steps of endocytic vesicle formation (Almeida et al. 2011; McConnell et al. 2009; McConnell and Tyska 2007). Myo1d participates in transfer of recycling vesicles (Huber et al. 2000), whereas Myo1e has been suggested not only to promote vesicles formation, but also to assists in their transport, scission and uncoating (Krendel et al. 2007). Myo1f is important for immune cells adhesion and motility

(Kim et al. 2006) similarly to Myo1g, which assists in receptor-mediated phagocytosis in macrophages (Dart et al. 2012) and lysosomal trafficking in a breast cancer cell line (Groth-Pedersen et al. 2012).

Like the other myosins-1, Myo1c mediates trafficking of vesicles rich in various molecules such as GLUT4 (Bose et al. 2002), VEGFR (Tiwari et al. 2013), lipid raft-associated proteins (Brandstaetter et al. 2012) or aquaporin-2 (Barile et al. 2005). Myo1c is present at the cell periphery, where it maintains proper arrangement of actin-rich structures (Bose et al. 2004; Fan et al. 2012; Hagan et al. 2008; Maravillas-Montero et al. 2011), it affects their dynamics (Diefenbach et al. 2002) and maintains intracellular tension (Coluccio and Geeves 1999). Taken together, Myo1c plays a role in cell growth, spreading, migration and transport of vesicles. Besides that, Myo1c is essential in hearing, where it participates in opening and re-closure of transmembrane ion channels during the process of adaptation to external stimuli (Dumont et al. 2002; Gillespie and Cyr 2004; Gillespie and Muller 2009).

Alternative splicing of MYO1C gene in combination with alternative start of transcription gives rise to three proteins differing in their N-terminal parts: the shortest Myo1c isoform C (Myo1c), Myo1c isoform B termed nuclear myosin 1 (NM1, NM1β) that has additional 16 amino acids at the N-terminus, and the longest Myo1c isoform A (Myo1c-isoA) having 36 amino acids at the N-terminus (Fig. 1). Isoform A is not expressed in mouse, because it lacks transcription start site. In human the expression of isoform A is low in comparison to the other isoforms, whereas it is highly expressed in African green monkey (Ihnatovych et al. 2012).

Even though the isoforms differ only in their N-terminal parts, their functions seemed to be completely different. While Myo1c has been described as exclusively cytoplasmic protein, NM1 has been shown to work in the nucleus and nucleolus (Nowak et al. 1997;

Philimonenko et al. 2004). NM1 maintains chromosomal organization of the nucleus (Hu et al. 2008; Chuang et al. 2006) and actively participates in some crucial nuclear processes such DNA transcription by polymerases I and II (Hofmann et al. 2006; Philimonenko et al. 2004; Ye et al. 2008), chromatin remodelling (Percipalle and Farrants 2006), ribosomal subunits biogenesis (Cisterna et al. 2006), and mRNA export from the nucleus (Obrdlik et al. 2010). Moreover, NM1 is in the nucleus engaged in lipoprotein complexes via interaction with PIP2 (Yildirim et al., unpublished). The longest Myo1c-isoA can be found both in the cytoplasm and in the nucleus, but it is absent from the nucleolus, therefore it has a role in transcription by polymerase II only (Ihnatovych et al. 2012). Because of different localisation pattern of each isoform, it was suggested that the nuclear localisation signal (NLS) directing the two longer isoforms to the nucleus is localised in the N-terminal domain (Pestic-Dragovich et al. 2000). However, our recent study demonstrated that the NLS is localized in the neck region of NM1 (Dzijak et al. 2012) and therefore can direct all the three isoforms to the nucleus. Moreover, both NM1 and Myo1c are present in the cytoplasm (Venit et al. 2013). This observation led to a question whether the three isoforms serve in the same cellular compartment identical functions or whether they are functionally unique. In order to address this question, Venit et al. (2013) prepared an NM1 knock-out mouse, in which the expression of NM1 is abolished, while Myo1c expression is unaffected. Despite of previously described involvement of NM1 in many key cellular processes, the knock-out mice are fully viable and do not show any severe phenotype. Considering the recent findings about the ability of NM1 and Myo1c to translocate into the nucleus, it was concluded that these isoforms are interchangeable in nuclear processes (Venit et al. 2013). However, the cytoplasmic pool of NM1 has not been inspected yet. In this paper, we show that NM1 is as

well as Myo1c involved in cytoplasmic processes and in addition, its deletion causes changes in cell viability under particular conditions.

Results

NM1 and Myo1c are predominantly localized in the cytoplasm

At the beginning, we were interested in cellular distribution of NM1 and Myo1c. In the previous study we have shown that from the quantitative point of view, there is the same amount of NM1 and Myo1c in the nucleus. The identical balance between these two proteins exists also in the cytoplasm (Venit et al. 2013). However, the predominant localization in cellular compartments remained unclear. To answer this question, we prepared nuclear and cytoplasmic fractions from suspension HeLa cells and check for the presence of NM1 and Myo1c by western blotting (Fig. 2). Using two antibodies specific for the N-terminal peptide and the tail domain enabled us to distinguish between NM1 and Myo1c isoform. The result indicates that within the cell there is 80 % of the total amount of NM1 and Myo1c present in the cytoplasm, whereas only 20 % resides in the nucleus. The same distribution applies also for NM1 protein alone.

Knock-out of NM1 causes increased resistance of mouse skin fibroblasts to hypotonic environment

We took advantage of the NM1 knock-out mouse prepared previously, which lacks the NM1, while retaining Myo1c (Venit et al. 2013). We derived adult skin fibroblasts from both knock-out (KO) and wild-type (WT) mice (Fig. 3A). It is known from the recent work, that even though NM1 is involved in crucial nuclear processes, neither the mice nor the fibroblasts show any phenotype under physiological conditions (Venit et al. 2013). Therefore

we tried to induce phenotypical alterations in fibroblasts by challenged conditions. We challenged them under various stress conditions such as UV light or heat shock and tested their wound healing ability. None of these revealed any significant difference in behaviour between KO and WT fibroblasts (data not shown). Surprisingly, under hypotonic conditions ranging from 1 to 7 min, KO fibroblasts had higher ability to survive in comparison to WT (Fig. 3B). This observation points out to the involvement of NM1 in mechano-chemical processes of the cell, as previously described for Myo1c.

Overexpression of NM1 in KO cells rescues the hypotonic phenotype

To further prove that the hypotony effect observed on fibroblasts is indeed caused by NM1, we performed the rescue experiments. We prepared KO and WT fibroblasts stably expressing NM1-Flag or control GFP (Fig. 4A) and subjected them to hypotony for 1 min (Fig. 4B). In agreement with the previous experiment, survival of WT fibroblasts in comparison to KO was decreased by 25 %. Moreover, when NM1-Flag is expressed in WT fibroblasts, the survival is further reduced by 30 %. KO fibroblasts expressing NM1-Flag show the identical ability to resist hypotony as WT, which reflects the fact, that the level of NM1 expressed in both cell lines is endogenous. Taken together these data suggest that NM1 plays a role in a process of maintenance of appropriate volume and osmotic pressure of the cell.

NM1 knock-out affects expression of various cytoplasmic and plasma membrane proteins

When the cell experiences decrease or increase in a volume resulting from changes in osmotic pressure of surrounding environment, various processes are triggered. These processes are consequences of sterical alterations between molecules, changes in concentrations of various ions and modifications in structure of plasma membrane.

Therefore wide range of biomolecules can serve as “molecular osmosensors”, which set off diverse cascades in order to deflect osmotic perturbations. Transmembrane molecules (integrins, ion channels, growth factor receptors), enzymes involved in lipid metabolism, phospholipids, cytoskeletal proteins, GTP-binding proteins can be considered as such osmosensors (Hoffmann et al. 2009).

In order to better understand pathways, in which NM1 is active, we tried to identify proteins that are affected by its absence. For this purpose we have chosen mouse organs with the highest expression of NM1 (Kahle et al. 2007) - lungs, heart and skin fibroblasts – and compare their expression profile in WT and KO mice by microarray analysis. The analysis revealed that there are 222 statistically significant genes ($p<0.05$) with at least 2-fold change in expression, from which 23 were found in lungs, 102 in heart and 97 in cells (Fig. 5A). Only known genes were taken into account, all the predicted or non-identified genes were omitted. We performed a screening of the functions of all 222 genes using Onto-express gene ontology software (Intelligent systems and bioinformatics laboratory, Department of Computer Science, Wayne State university, Detroit) and also manually verified the results in gene databases Uniprot and NCBI-NLM-NIH. Firstly, we classified the gene products according to their localization within the cell (Fig. 5B). Approximately one quarter (23 %) of the gene products is located to the nucleus and nucleolus, where they act as transcription factors affecting development, differentiation and proliferation of various types of cells, especially of immune and nervous systems. Nearly the equal portion (28 %) is composed of membrane or transmembrane proteins. Many of them are receptors on the outer side of plasma membrane which are coupled with G-proteins and trigger downstream signalling. Importantly, there are molecules which mediate cell-cell or cell-matrix adhesion and affect cell motility (15 proteins). 12 proteins are ion channels or channels-associated proteins that

transport various ions or molecules across the plasma membrane. Huge portion of proteins is cytoplasmic (22 %), playing role in various processes such as cytoskelet assembly, protein processing, signalling events or molecular trafficking. There is 11 % of proteins located in either endoplasmatic reticulum, Golgi complex or mitochondria. These are the enzymes of lipid metabolism, proton transporters and proteins involved in vesicle trafficking. Proteins that localize in the extracellular space compose 19 % of the genes changed. These proteins are extracellular matrix components, which helps in the assembly of cells into the tissues and in maintenance of their functions in connection to surrounding environment. Besides, there are also various ligands that after membrane receptor binding trigger various pathways and are important in development, growth and proliferation.

NM1 interacts with various cytoplasmic proteins

Previous studies widely focused on identification of NM1-interacting partners in the nucleus and limited attention was brought to its cytoplasmic or membrane-associated partners. Here we tried to find novel candidates that can help us to understand in which cytoplasmic processes NM1 is involved. Since we knew that lungs are the tissue with highest expression of NM1 (Kahle, 2007), we performed co-immunoprecipitations of endogenous NM1 from mouse lung tissues, A549 lung cell line and Hela cells using three different antibodies raised specifically against N-terminal extension of NM1 (Table 2A). Moreover, we tracked interactions of NM1-Flag stably expressed in A549 or H1299 lung cell lines and HUVEC endothelial cell line (Table 2B). For the experiments, whole cell extracts were prepared by using optimized buffer compositions that enabled us to capture the proteins, which interact with NM1 either via actin or lipid-binding domain. Use of various detergents allowed us to extract different pools of NM1 – digitonin extracts the cytosolic

NM1; Triton X-100 extracts the lipid-bound NM1; and Tween-20 after sonication solubilizes total cellular NM1 omitting the lipid-bound portion. Proteins binding specifically to the antibody in comparison to negative control were analyzed by MALDI-FT-ICR.

Under all conditions we identified actin and calmodulin, well-known proteins that bind to nearly all myosins promoting the power stroke. Apart from these, filamin A, alpha-actinin 4, annexin A2 and even myosin 1b were detected. Filamin A is a crosslinker of cortical actin and is necessary for stabilization of cell surface and promoting of cellular translocation. Similarly, annexin A2 serves as a linker of plasma membrane-associated proteins with cytoskeleton. It's also involved in endocytosis, ion channel formation and cell matrix interactions. Alpha-actinin 4 is in non-muscle cells localized along microfilament bundles and adherens-type junctions, therefore binding actin to the membranes. myosin 1b is similarly to annexin A2 involved in initial steps of endocytic vesicle formation. Functions of these proteins, ineracting partners of NM1, strongly suggest that NM1 is in a similar way as other myosins-1 involved in control of membrane tension, organization of cytoskeleton and its attachment to membranes.

NM1 co-localizes with filamin A, alpha-actinin 4, annexin A2 and myosin 1B at the leading edge

In the previous experiment we have found filamin A, alpha-actinin 4, annexin A2 and myosin 1b in interaction with NM1 in the lungs and lung cell lines. To define at which cellular compartments these proteins precisely co-localize with NM1, we performed immunostaining of endogenous proteins in A549 lung cells using antibodies against tail domain of NM1/Myo1c (Fig. 6). We found that filamin A, alpha-actinin 4, annexin A2 and myosin 1b co-localized with NM1/Myo1c in the cytoplasm. Moreover the co-localization is most

prominent at the leading edge of the cell. This observation further proves that NM1 is engaged in cytoskeleton dynamics in actively moving cells.

Discussion

NM1 was known as a nuclear isoform of cytoplasmic Myo1c. However, recent studies revealed that not only Myo1c can enter the nucleus, but also NM1 is a cytoplasmic protein (Dzijak et al. 2012). Moreover it is now clear that either in the nucleus or in the cytoplasm the ratio between NM1 and Myo1c is equal (Venit et al. 2013). Our data revealed that both isoforms are enriched in the cytoplasm (Fig. 2). From the total cellular content, 80 % of both NM1 and Myo1c is localized to the cytoplasm, whereas only 20 % resides in the nucleus. This finding suggests that there is also some functional relevance of NM1 in the cytoplasm, which has not been described yet, because all the studies performed up to date have focused only on the nuclear portion of NM1. We took advantage of the NM1 KO mouse, which lacks the expression of NM1, and derived skin fibroblasts. The KO mouse doesn't have any phenotype and no aberrancy was observed in fibroblast viability and proliferation when cultured under standard conditions (Venit et al. 2013). However, when we challenged fibroblasts to various stress condition, survival under hypotonic conditions was increased in KO (Fig. 3B). In addition, survival of WT fibroblasts expressing NM1-Flag declined even more, whereas KO fibroblasts expressing NM1-Flag were able to resist hypotony to the same extent as the WT (Fig. 4). Since NM1 deletion seems to enhance survival in hypotony, it implies NM1 for being a negative regulator of regulatory volume decrease, which is the mechanism, by which cell tend to balance perturbations in its volume. However, the pathways triggered after cell swelling are quite complex and variable including various ion channels, aquaporins, cell-adhesion molecules, cytoskeletal proteins, growth factor receptors, molecules remodelling

membranes and GTP-binding proteins (reviewed in Hoffmann EK, 2009). In order to identify molecules that can be responsible for augmented reaction for hypotony or generally any other cytosolic process, we subjected two mouse organs most abundant in NM1 (lungs, heart) and skin fibroblasts to microarray expression profiling. We selected the genes that were statistically significant ($p<0.05$) and whose expression was changed more than twice (total 222). Surprisingly, only 23 % of the gene products affected by NM1 depletion are nuclear and as much as 60 % are cytosolic, membrane or transmembrane proteins (including mitochondria, ER, GA; Fig. 5). Proteins localized to the nucleus are mainly transcription factors, whereas the membrane proteins are various receptors (including growth factor receptors) coupled to G-proteins, cell-cell or cell-to-matrix adhesion proteins that affect cell motility (15 proteins). Ion channels or channels-associated proteins were also identified (12 proteins) as well as proteins playing roles in cytoskeleton organization and dynamics. Proteins identified to be in GA or ER are enzymes of lipid metabolism and vesicle trafficking. Taken together, ion channels, cell-adhesion and cytoskeletal proteins might contribute to pathways triggered after hypotonic shock in the cells. Myo1c has already been shown to participate in trafficking of vesicles containing VEGFR (Tiwari et al. 2013) and other lipid-raft-anchored proteins (Brandstaetter et al. 2012), which affect rigidity of plasma membrane. Absence of such a process would definitely lead to altered response to a hypotonic shock. Myo1c assists in opening and re-closure of ion channels in the inner ear (Dumont et al. 2002) and mediates trafficking of aquaporin vesicles in kidney (Barile et al. 2005). Alteration of such processes would also change the osmosensitivity and water permeability of a cell. It is highly probable that NM1 in the cytoplasm also mimic the functions of Myo1c. Myo1c is known to organize cytoskeleton at the cell periphery (Bose et al. 2004) and together with other myosin 1 family members mediates membrane-cytoskeleton adhesion. Downregulation of any

isoform causes reduction in rigidity of the plasma membrane (Nambiar et al. 2009). One possibility is that NM1 as well creates a dynamic link between plasma membrane and cytoskeleton and thus make major contributions to membrane tension. This would suggest that all myosin 1 molecules on plasma membrane contribute to linkage between membrane and cytoskeleton together.

As a consequence, the overall number of myosin molecules on plasma membrane of NM1 KO cells is reduced, less tight bonding of cytoskeleton to membrane is achieved and the cells are more accessible for swelling, because the plasma membrane can remodel more effectively. In contrary, cells with exogenous overexpression of NM1 have overall higher levels of myosin 1 molecules on the plasma membrane and the link between membrane and cytoskeleton is therefore more rigid and more sensitive to cell swelling. We therefore suggest that in the steady state, the overall number of myosin 1 molecules in the cytoplasm is sufficient for normal proceeding in NM1 KO cells, but after exposure to strong stress conditions, differences in mechanical properties of the cells can be seen. It is plausible that various pathways make contributions to the phenotype observed under stress conditions.

To find the interaction partners of NM1 in a more direct way, we firstly performed co-immunoprecipitations of endogenous NM1 from lungs and two lung cell lines (A549, H1299) as well as endothelial line (HUVEC). We also used lung cell lines overexpressing NM1-Flag for co-immunoprecipitations via Flag antibody. Besides actin and calmodulin, well-known NM1 binding partners, we identified filamin A, annexin A2, alpha-actinin 4 and myosin 1b by mass spectrometry. These proteins are in cells responsible for processes in focal adhesions and leading edge: organization of cortical actin and its binding to membrane, which is crucial for cell motility, endocytosis and maintenance of proper membrane tension. We further confirmed that NM1 co-localizes with these proteins at the leading edge of the cell by

immunostaining using respective antibodies. This observation further strengthens our hypothesis that NM1 along with other myosin 1 molecules links cytoskelet to plasma membrane. Leading edge of a cell is a place where rapid and frequent actin filaments formation takes place in order to provide the force that triggers movement of a cell. The newly synthesized actin filaments require vast and tight interaction with plasma membrane, which can be accomplished via NM1.

It is now obvious that besides its nuclear role, NM1 is also active in various processes in cytoplasm and even at the plasma membrane. The absence of dramatic phenotype in the NM1 KO mouse (Venit, 2013) might be a consequence of partial redundancy of NM1 and Myo1c especially in case when one isoform is missing. However, challenged conditions might help to uncover weaknesses in cell behaviour caused by NM1 absence as shown in this paper. It appears from the published data that compensation of specific myosin functions by other member from the same or different family is not rare. After deletion of Myo1a, the most abundant brush border myosin, Myo1d, Myo1e and Myo1c can compensate for the loss, but the rescue effect of Myo1c and Myo1e is less prominent (Tyska 2005, Benesh 2010). It has been also reported that after loss of myosin 2a, myosin 2b can functionally substitute (Even-Ram, 2007) and deletion of myosin 5a is probably compensated by myosin from other family (Takagishi, 2005).

Since it is now clear that NM1 holds for various cytoplasmic and plasma membrane functions, it remains unclear whether those are identical with functions of Myo1c or whether any specific process requires specific presence of N-terminal domain. The important question also remains, if NM1 would be able to rescue for the loss of Myo1c. More detailed information on roles of NM1 and Myo1c and their cross-talk might be obtained after generation of KO mouse with both isoforms deleted.

Materials and methods

Plasmids and cell lines

U2OS, H1299 and A549 cell lines were obtained from ATCC. All cell lines were cultured in Dulbecco's modified Eagle medium supplemented with 10 % fetal bovine serum (Invitrogen) and gentamicin 40 ug/ml, in humidified incubator at 37 °C, 5 % CO2. , Suspension Hela cells were cultured in minimum essential Eagle medium modified for spinner culture supplemented with 5 % fetal bovine serum and 40 ug/ml gentamicin in humidified incubator at 37 °C with 5 % CO2. Mouse skin fibroblasts were derived (Venit et al. 2013) from the WT and KO mice and cultured in Dulbecco's modified Eagle medium supplemented with 10 % fetal bovine serum (Invitrogen) and gentamicin 40 ug/ml, in humidified incubator at 37 °C, 5 % CO2. NM1 with C-terminal Flag tag was cloned into pCDH-CMV-MCS-EF1-Neo using SnaBI and EcoRI. Lentivirus, generated using pMD2.G and psPAX2 packaging plasmids, was used for transduction of A549, H1299 and mouse skin fibroblasts. Stable recombinants were selected using neomycin.

Cell fractionation

Cells were fractionated as described previously (Trinkle-Mulcahy, 2008). Briefly, Hela suspension cells were harvested by centrifugation, washed twice with ice-cold PBS, resuspended in ice-cold hypotonic buffer (10 mM Hepes, pH 7.9, 1.5 mM MgCl, 10 mM KCl, 0.5 mM DTT, and protease inhibitors) and incubated on ice for 15 min. Cells were broken open using Dounce homogenizer with a tight pestle and centrigued at 230 g for 5 min. The supernatant, which was considered a cytoplasmic fraction, was mixed in the SDS-PAGE loading buffer, sonicated and cleared by centrifugation at 16000 g. The crude nuclear pellet was further purified over a sucrose cushion: pellet was resuspended in 0.25 M sucrose, layered over

0.88 M sucrose and centrifuged at 2800 g. The final nuclear pellet was resuspended in the SDS-PAGE loading buffer, sonicated and cleared by centrifugation at 16000 g. Samples were resolved by SDS-PAGE and transfered onto nitrocellulose membrane.

Hypotonic stress survival experiments

KO and WT fibroblasts were seeded at the same density onto a 24-well plate and kept for 24 hrs under normal conditions. Then, the growth medium was discarded, cell washed by PBS and incubated in destile water for 1 to 7 min. After this period, water was removed and cells were allowed to recover for 2 hrs in normal growth medium under standard conditions and counted. The experiment was repeated three times in triplicates and resulting data were statistically evaluated. The same experiment was carried out with the fibroblasts stably expressing GFP or NM1 Flag.

Immunoprecipitations

Cells were extracted either in buffer containing 20 mM Tris pH 7.4, 150 mM NaCl, 1 % Triton X-100, 2 mM EDTA, 10 mM EGTA, 10 mM K2HPO4 (Triton extraction buffer), or 20 mM Tris pH 7.4, 150 mM potassium acetate, 5 mM magnesium acetate, 1 mM DTT, 1 mg/ml digitonin (digitonin buffer) complete protease inhibitors (ROCHE) or 20 mM Tris pH 7.4, 150 mM potassium acetate, 5 mM MgCl2, 1 mM DTT, 0.1 % Tween 20, protease and phophatase inhibitors (Tween buffer). Cells were disrupted by sonication on ice. Lysates were cleared by centrifugation at 14000g for 10min at 4°C. Lysates were incubated with antibodies immobilized on agarose beads for 2 hrs at 4 °C. After 5 washes in 1 ml of lysis buffer beads were washed in 1 ml of 50 mM ammonium bicarbonate pH 7.5 to remove salts and detergent. Bound proteins were eluted twice with 500 µl of 500 mM ammonium hydroxide.

Eluates were evaporated using SpeedVac concentrator (Savant, Holbrook, NY, USA), dry pellets were resuspended in 20 ul of 1x SDS loading buffer, boiled and resolved on 6-20% gradient SDS PAGE.

Microarray gene-expression profiling and data analysis

Lungs and heart was dissected from WT and KO mice, cells were harvested by trypsinization. Preparation of cRNA, hybridization and gene expression profiling was done by an Affymetrix authorized service provider (AROS Applied Biotechnology A/S) using the Affymetrix GeneTitan HT MG-430 PM 24-array plate with the 3' IVT express labeling kit according to the manufacturer´s protocol. Briefly, following fragmentation, 6.5 µg of cRNA were hybridized for 16 h at 45 °C on the Affymetrix array plate using the Affymetrix GeneTitan system. The array plate was washed, stained and scanned using the Affymetrix GeneTitan system with GCOS 1.4 software. Data analysis was carried out by importing raw data CEL files into Genomic Suite Software Partek 6.4 (version 6.09.0602), where the Robust Multichip Analysis was used for background correction.

Immunofluorescence

U2OS cells on coverslips were fixed by 4 % paraformaldehyde for 20 min and permeabilized with 0.05 % Triton X-100 for 10 min. After 30 min blocking with 1 % BSA cells were incubated 1 hr with primary antibody in wet chamber, washed 3 times with PBS-T and incubated 45 min with secondary antibody. Finally, cells were washed 3 times with PBS-T and mounted in Prolong anti-fade agent (Invitrogen).

Antibodies

Following antibodies were used for immunoprecipitations, western blotting and immunostaining: NM1 (M3567, Sigma Aldrich); NM1 - gift from P. Percipalle (Fomproix and Percipalle 2004); NM1/Myo1c - R2652, gift from P. Gillespie (Dumont et al. 2002); lamin A - 133A2, gift from Y. Raymond (Sasseville and Raymond 1995); actin (A2066, Sigma); NM1 - clone #4, (Ye et al. 2008); NM1 (R5, Exbio); Flag (M2, Stratagene); filamin A (MAB1678, Chemicon); alpha-actinin 4 (ab96686, Abcam), myosin 1b (1PB7C2, Sigma Aldrich).

Figure legends

Fig. 1: Domain structure of Myo1c isoforms. The shortest Myo1c isoform c; Myo1c isoform b (NM1) possesing 16 aminoacids at the N-terminus and the longest Myo1c isoform a with 35 amino acids at the N-terminus. Binding sites for ATP, actin, calmodulin and PIP2 are shown.

Fig. 2: NM1 and Myo1c are predominantly localized in the cytoplasm. Suspension Hela cells were fractionated into cytoplasm and nuclei and the same amount of proteins were loaded into each lane. NM1 or both NM1+Myo1c were detected by corresponding antibodies **(A)**. Both isoforms are enriched in the cytoplasm. Bar graph **(B)** is a quantitative representation of the band intensities detected by western blotting. Lamin A is a control of cross-contamination between cytoplasmic and nuclear fractions.

Fig. 3: Knock-out of NM1 causes increased resistency to hypotonic conditions of mouse skin fibroblasts. Mouse skin fibroblasts were derived from WT mouse and KO mouse, which lacks expression of NM1 **(A)**. Both cell lines were subjected to hypotonic conditions (redestilled water) for indicated period of time **(B)** and then let recovered for 2 hr in

complete media. KO fibroblasts show higher ability to resist hypotonic conditions than WT, this behaviour does not change with prolonged incubations.

Fig. 4: Overexpression of NM1 further decreases ability of WT fibroblasts to survive under hypotonic conditions. WT and KO fibroblasts stably expressing NM1-Flag were prepared, KO fibroblasts expressing GFP were used as a control **(A)**. All four cell lines were subjected to a hypotony for 1 min and let recovered in complete media for 2 hrs **(B)**. WT fibroblasts expressing NM1-Fl show lower ability to survive than WT. KO fibroblasts expressing NM1-Flag show similar ability to survive as WT, which correlates with the amount of NM1 expressed by both cell lines.

Fig. 5: Representation of tissue origin and cellular functionality of differentially expressed genes in NM1 KO mouse. Lungs and heart dissected from WT and KO mice as well as skin fibroblast cells were subjected to expression profiling. The micorarray analysis revealed, that most of the differentially expressed genes originates from heart (102) and fibroblast cells (97). Only 23 genes change their expression in lungs **(A)**. Protein products of differentially expressed genes localize and act in various cellular compartments. Mosta abundant are cytoplasmic (57), extracellular (55), nuclear (55) and membrane proteins (40). Shuttling of proteins (if occurs) was taken into account **(B)**.

Fig. 6: NM1 colocalizes with filamin A, annexin A2, alpha-actinin 4 and Myo1b. H1299 cells were fixed by 4 % PFA and permeabilized by 0.1 % Triton X-100. After washes cells were incubated with primary antibodies for 1 hr at room temperature and appropriate secondary antibody coupled to fluorescent dye for 45 min. Cells were imaged at the confocal microscope.

Table 1: Genes differentially expressed in KO mouse tissues in comparison to WT classified according to their functions in cell adhesion, cytoskeletal arrangements and ion channels formation. Mouse lungs, heart and skin fibroblasts from WT and KO mice were subjected to expression profiling. Significantly changed genes were identified and then grouped according to their functions and localization.

Table 2: Proteins interacting with NM1 in lungs and lung cell lines under various conditions. Lung tissues (lungs), lung cell lines (A549) or Hela cells were harvested and lysed in buffers with detergents indicated in the table. Endogenous NM1 was co-immunoprecipitated from the whole cell extracts and its specific interacting partners were identified by mass spectrometry. Mouse monoclonal (*M*, Ye et al. 2008) and rabbit polyclonal (*P*, Exbio) antibodies crosslinked to agarose beads were used **(A)**. Lung A549, H1299 and endothelial HUVEC cell lines expressing stably NM1-Flag were prepared. Cells were extracted using buffers with above indicated detergents and NM1-Flag was co-immunoprecipitated using Flag antibody coupled to agarose beads (M2, Sigma Aldrich). The resulting interacting partners were identified by mass spectrometry **(B)**.

References

Adams RJ, Pollard TD (1989) Binding of myosin I to membrane lipids. Nature 340 (6234):565-568. doi:10.1038/340565a0

Almeida CG, Yamada A, Tenza D, Louvard D, Raposo G, Coudrier E (2011) Myosin 1b promotes the formation of post-Golgi carriers by regulating actin assembly and membrane remodelling at the trans-Golgi network. Nature cell biology 13 (7):779-789. doi:10.1038/ncb2262

Barile M, Pisitkun T, Yu MJ, Chou CL, Verbalis MJ, Shen RF, Knepper MA (2005) Large scale protein identification in intracellular aquaporin-2 vesicles from renal inner medullary collecting duct. Molecular & cellular proteomics : MCP 4 (8):1095-1106. doi:10.1074/mcp.M500049-MCP200

Berg JS, Powell BC, Cheney RE (2001) A millennial myosin census. Molecular biology of the cell 12 (4):780-794

Bose A, Guilherme A, Robida SI, Nicoloro SM, Zhou QL, Jiang ZY, Pomerleau DP, Czech MP (2002) Glucose transporter recycling in response to insulin is facilitated by myosin Myo1c. Nature 420 (6917):821-824. doi:10.1038/nature01246

Bose A, Robida S, Furcinitti PS, Chawla A, Fogarty K, Corvera S, Czech MP (2004) Unconventional myosin Myo1c promotes membrane fusion in a regulated exocytic pathway. Molecular and cellular biology 24 (12):5447-5458. doi:10.1128/MCB.24.12.5447-5458.2004

Brandstaetter H, Kendrick-Jones J, Buss F (2012) Myo1c regulates lipid raft recycling to control cell spreading, migration and Salmonella invasion. Journal of cell science 125 (Pt 8):1991-2003. doi:10.1242/jcs.097212

Cisterna B, Necchi D, Prosperi E, Biggiogera M (2006) Small ribosomal subunits associate with nuclear myosin and actin in transit to the nuclear pores. FASEB journal : official publication of the Federation of American Societies for Experimental Biology 20 (11):1901-1903. doi:10.1096/fj.05-5278fje

Coluccio LM, Geeves MA (1999) Transient kinetic analysis of the 130-kDa myosin I (MYR-1 gene product) from rat liver. A myosin I designed for maintenance of tension? The Journal of biological chemistry 274 (31):21575-21580

Dart AE, Tollis S, Bright MD, Frankel G, Endres RG (2012) The motor protein myosin 1G functions in FcgammaR-mediated phagocytosis. Journal of cell science 125 (Pt 24):6020-6029. doi:10.1242/jcs.109561

Diefenbach TJ, Latham VM, Yimlamai D, Liu CA, Herman IM, Jay DG (2002) Myosin 1c and myosin IIB serve opposing roles in lamellipodial dynamics of the neuronal growth cone. The Journal of cell biology 158 (7):1207-1217

Dumont RA, Zhao YD, Holt JR, Bahler M, Gillespie PG (2002) Myosin-I isozymes in neonatal rodent auditory and vestibular epithelia. Journal of the Association for Research in Otolaryngology : JARO 3 (4):375-389. doi:10.1007/s101620020049

Dzijak R, Yildirim S, Kahle M, Novak P, Hnilicova J, Venit T, Hozak P (2012) Specific nuclear localizing sequence directs two myosin isoforms to the cell nucleus in calmodulin-sensitive manner. PloS one 7 (1):e30529. doi:10.1371/journal.pone.0030529

Fan Y, Eswarappa SM, Hitomi M, Fox PL (2012) Myo1c facilitates G-actin transport to the leading edge of migrating endothelial cells. The Journal of cell biology 198 (1):47-55. doi:10.1083/jcb.201111088

Fomproix N, Percipalle P (2004) An actin-myosin complex on actively transcribing genes. Experimental cell research 294 (1):140-148. doi:10.1016/j.yexcr.2003.10.028

Foth BJ, Goedecke MC, Soldati D (2006) New insights into myosin evolution and classification. Proceedings of the National Academy of Sciences of the United States of America 103 (10):3681-3686. doi:10.1073/pnas.0506307103

Gillespie PG, Cyr JL (2004) Myosin-1c, the hair cell's adaptation motor. Annual review of physiology 66:521-545. doi:10.1146/annurev.physiol.66.032102.112842

Gillespie PG, Muller U (2009) Mechanotransduction by hair cells: models, molecules, and mechanisms. Cell 139 (1):33-44. doi:10.1016/j.cell.2009.09.010

Groth-Pedersen L, Aits S, Corcelle-Termeau E, Petersen NH, Nylandsted J, Jaattela M (2012) Identification of cytoskeleton-associated proteins essential for lysosomal stability and survival of human cancer cells. PloS one 7 (10):e45381. doi:10.1371/journal.pone.0045381

Hagan GN, Lin Y, Magnuson MA, Avruch J, Czech MP (2008) A Rictor-Myo1c complex participates in dynamic cortical actin events in 3T3-L1 adipocytes. Molecular and cellular biology 28 (13):4215-4226. doi:10.1128/MCB.00867-07

Hoffmann EK, Lambert IH, Pedersen SF (2009) Physiology of cell volume regulation in vertebrates. Physiological reviews 89 (1):193-277. doi:10.1152/physrev.00037.2007

Hofmann WA, Vargas GM, Ramchandran R, Stojiljkovic L, Goodrich JA, de Lanerolle P (2006) Nuclear myosin I is necessary for the formation of the first phosphodiester bond during transcription initiation by RNA polymerase II. Journal of cellular biochemistry 99 (4):1001-1009. doi:10.1002/jcb.21035

Hu Q, Kwon YS, Nunez E, Cardamone MD, Hutt KR, Ohgi KA, Garcia-Bassets I, Rose DW, Glass CK, Rosenfeld MG, Fu XD (2008) Enhancing nuclear receptor-induced transcription requires nuclear motor and LSD1-dependent gene networking in interchromatin granules. Proceedings of the National Academy of Sciences of the United States of America 105 (49):19199-19204. doi:10.1073/pnas.0810634105

Huber LA, Fialka I, Paiha K, Hunziker W, Sacks DB, Bahler M, Way M, Gagescu R, Gruenberg J (2000) Both calmodulin and the unconventional myosin Myr4 regulate membrane trafficking along the recycling pathway of MDCK cells. Traffic 1 (6):494-503

Chuang CH, Carpenter AE, Fuchsova B, Johnson T, de Lanerolle P, Belmont AS (2006) Long-range directional movement of an interphase chromosome site. Current biology : CB 16 (8):825-831. doi:10.1016/j.cub.2006.03.059

Ihnatovych I, Migocka-Patrzalek M, Dukh M, Hofmann WA (2012) Identification and characterization of a novel myosin Ic isoform that localizes to the nucleus. Cytoskeleton 69 (8):555-565. doi:10.1002/cm.21040

Kahle M, Pridalova J, Spacek M, Dzijak R, Hozak P (2007) Nuclear myosin is ubiquitously expressed and evolutionary conserved in vertebrates. Histochemistry and cell biology 127 (2):139-148. doi:10.1007/s00418-006-0231-0

Kim SV, Mehal WZ, Dong X, Heinrich V, Pypaert M, Mellman I, Dembo M, Mooseker MS, Wu D, Flavell RA (2006) Modulation of cell adhesion and motility in the immune system by Myo1f. Science 314 (5796):136-139. doi:10.1126/science.1131920

Krendel M, Osterweil EK, Mooseker MS (2007) Myosin 1E interacts with synaptojanin-1 and dynamin and is involved in endocytosis. FEBS letters 581 (4):644-650. doi:10.1016/j.febslet.2007.01.021

Maravillas-Montero JL, Gillespie PG, Patino-Lopez G, Shaw S, Santos-Argumedo L (2011) Myosin 1c participates in B cell cytoskeleton rearrangements, is recruited to the immunologic synapse, and contributes to antigen presentation. Journal of immunology 187 (6):3053-3063. doi:10.4049/jimmunol.1004018

McConnell RE, Higginbotham JN, Shifrin DA, Jr., Tabb DL, Coffey RJ, Tyska MJ (2009) The enterocyte microvillus is a vesicle-generating organelle. The Journal of cell biology 185 (7):1285-1298. doi:10.1083/jcb.200902147

McConnell RE, Tyska MJ (2007) Myosin-1a powers the sliding of apical membrane along microvillar actin bundles. The Journal of cell biology 177 (4):671-681. doi:10.1083/jcb.200701144

Nambiar R, McConnell RE, Tyska MJ (2009) Control of cell membrane tension by myosin-I. Proceedings of the National Academy of Sciences of the United States of America 106 (29):11972-11977. doi:10.1073/pnas.0901641106

Nowak G, Pestic-Dragovich L, Hozak P, Philimonenko A, Simerly C, Schatten G, de Lanerolle P (1997) Evidence for the presence of myosin I in the nucleus. The Journal of biological chemistry 272 (27):17176-17181

Obrdlik A, Louvet E, Kukalev A, Naschekin D, Kiseleva E, Fahrenkrog B, Percipalle P (2010) Nuclear myosin 1 is in complex with mature rRNA transcripts and associates with the nuclear pore basket. FASEB journal : official publication of the Federation of American Societies for Experimental Biology 24 (1):146-157. doi:10.1096/fj.09-135863

Odronitz F, Kollmar M (2007) Drawing the tree of eukaryotic life based on the analysis of 2,269 manually annotated myosins from 328 species. Genome biology 8 (9):R196. doi:10.1186/gb-2007-8-9-r196

Olety B, Walte M, Honnert U, Schillers H, Bahler M (2010) Myosin 1G (Myo1G) is a haematopoietic specific myosin that localises to the plasma membrane and regulates cell elasticity. FEBS letters 584 (3):493-499. doi:10.1016/j.febslet.2009.11.096

Percipalle P, Farrants AK (2006) Chromatin remodelling and transcription: be-WICHed by nuclear myosin 1. Current opinion in cell biology 18 (3):267-274. doi:10.1016/j.ceb.2006.03.001

Pestic-Dragovich L, Stojiljkovic L, Philimonenko AA, Nowak G, Ke Y, Settlage RE, Shabanowitz J, Hunt DF, Hozak P, de Lanerolle P (2000) A myosin I isoform in the nucleus. Science 290 (5490):337-341

Philimonenko VV, Zhao J, Iben S, Dingova H, Kysela K, Kahle M, Zentgraf H, Hofmann WA, de Lanerolle P, Hozak P, Grummt I (2004) Nuclear actin and myosin I are required for RNA polymerase I transcription. Nature cell biology 6 (12):1165-1172. doi:10.1038/ncb1190

Richards TA, Cavalier-Smith T (2005) Myosin domain evolution and the primary divergence of eukaryotes. Nature 436 (7054):1113-1118. doi:10.1038/nature03949

Sasseville AM, Raymond Y (1995) Lamin A precursor is localized to intranuclear foci. Journal of cell science 108 (Pt 1):273-285

Tiwari A, Jung JJ, Inamdar SM, Nihalani D, Choudhury A (2013) The myosin motor Myo1c is required for VEGFR2 delivery to the cell surface and for angiogenic signaling. American journal of physiology Heart and circulatory physiology 304 (5):H687-696. doi:10.1152/ajpheart.00744.2012

Venit T, Dzijak R, Kalendová A, Kahle M, Rohožková J, Schmid tV, Rülicke T, Rathkolb B, Hans V, Bohla A, Eickelberg O, Stoeger T, Wolf E, Yildirim AÖ, Gailus-Durner V, Fuchs H, Hrabě de Angelis M, Hozák P (2013) Mouse nuclear myosin I knock-out shows interchangeability and redundancy of myosin isoforms in the cell nucleus. PloS one in press

Woolner S, Bement WM (2009) Unconventional myosins acting unconventionally. Trends in cell biology 19 (6):245-252. doi:10.1016/j.tcb.2009.03.003

Ye J, Zhao J, Hoffmann-Rohrer U, Grummt I (2008) Nuclear myosin I acts in concert with polymeric actin to drive RNA polymerase I transcription. Genes & development 22 (3):322-330. doi:10.1101/gad.455908

Fig. 1

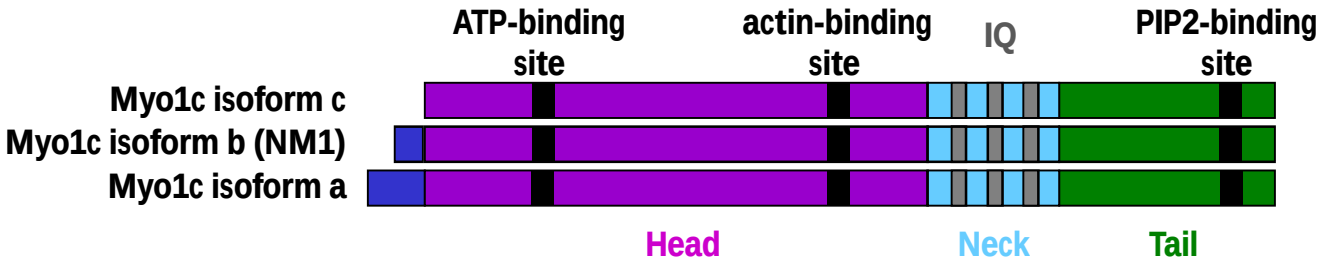
ATP-binding site
actin-binding site
IQ
PIP2-binding site
Myo1c isoform c
Myo1c isoform b (NM1)
Myo1c isoform a
Head
Neck
Tail

Fig. 2

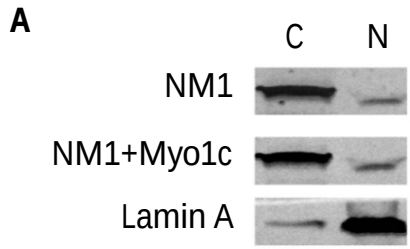
A
C
N
NM1
NM1+Myo1c
Lamin A

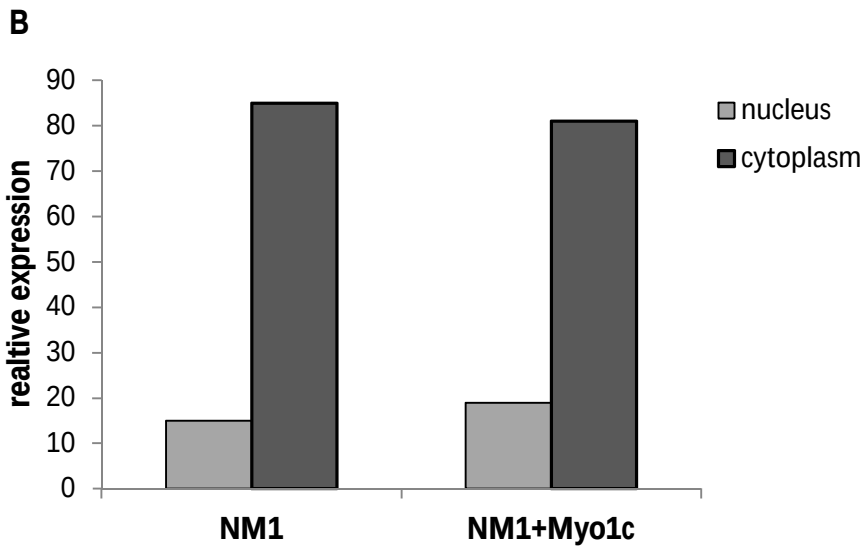
B
realtive expression
90
80
70
60
50
40
30
20
10
0
NM1
NM1+Myo1c
nucleus
cytoplasm

Fig. 3

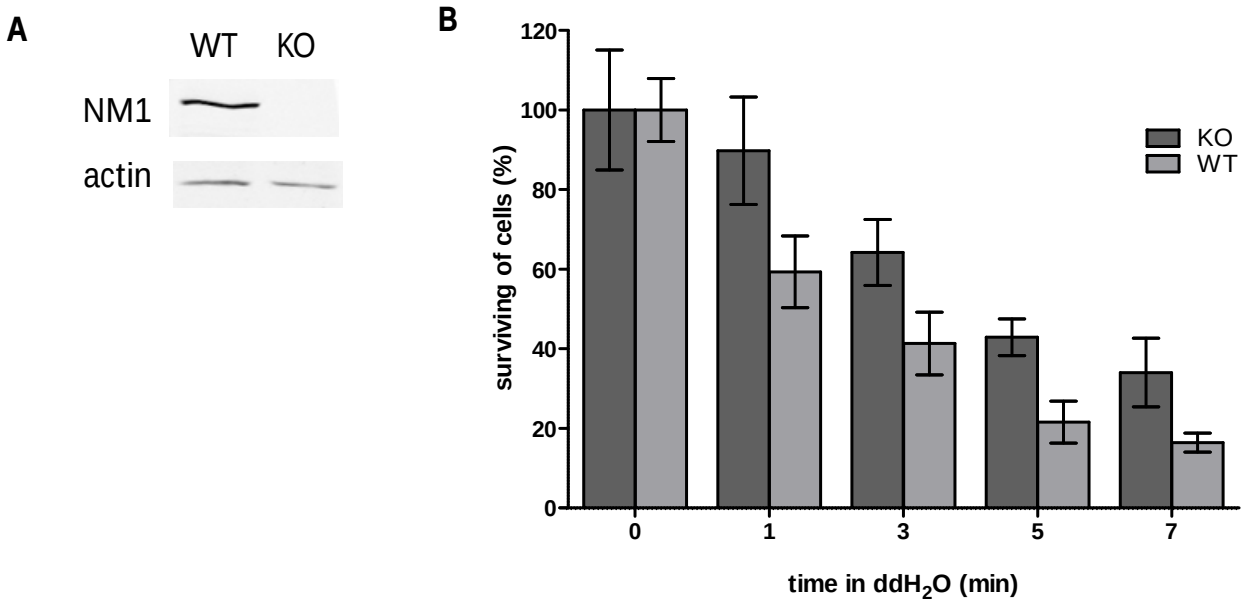
A
WT
KO
NM1
actin
B
surviving of cells (%)
120
100
80
60
40
20
0
0
1
3
5
7
time in ddH2O (min)
KO
WT

Fig. 4

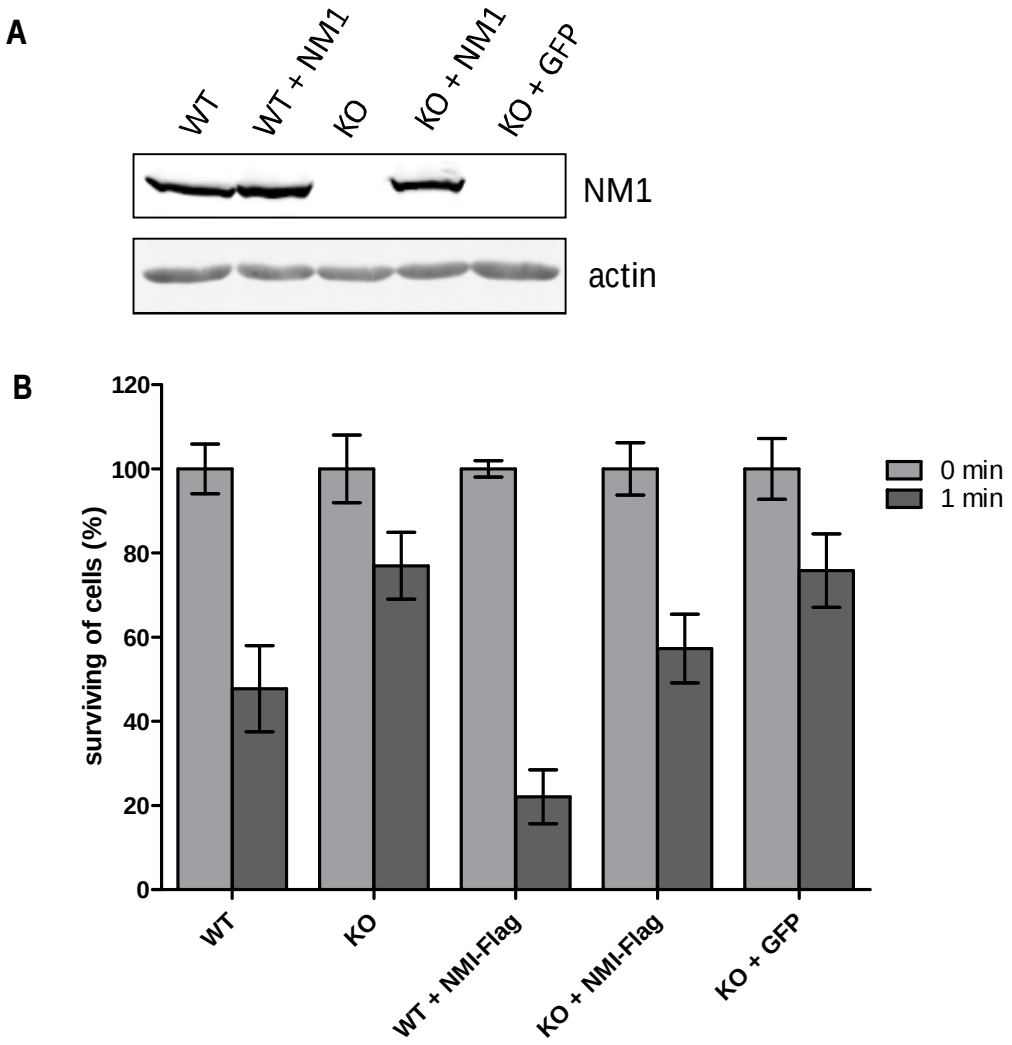
A
WT
WT + NM1
KO
KO + NM1
KO + GFP
NM1
actin
B
surviving of cells (%)
120
100
80
60
40
20
0
0 min
1 min
WT
KO
WT + NMI-Flag
KO + NMI-Flag
KO + GFP

Fig. 5

A

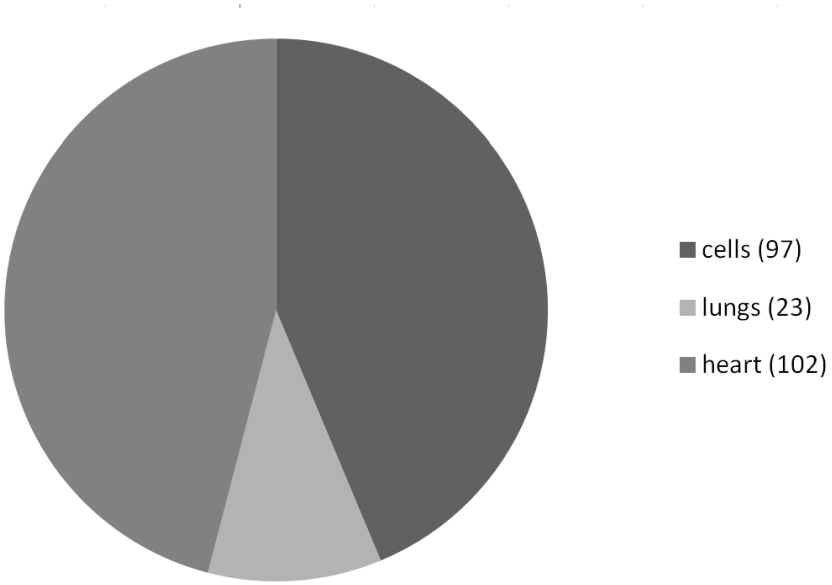
cells (97)
lungs (23)
heart (102)

B

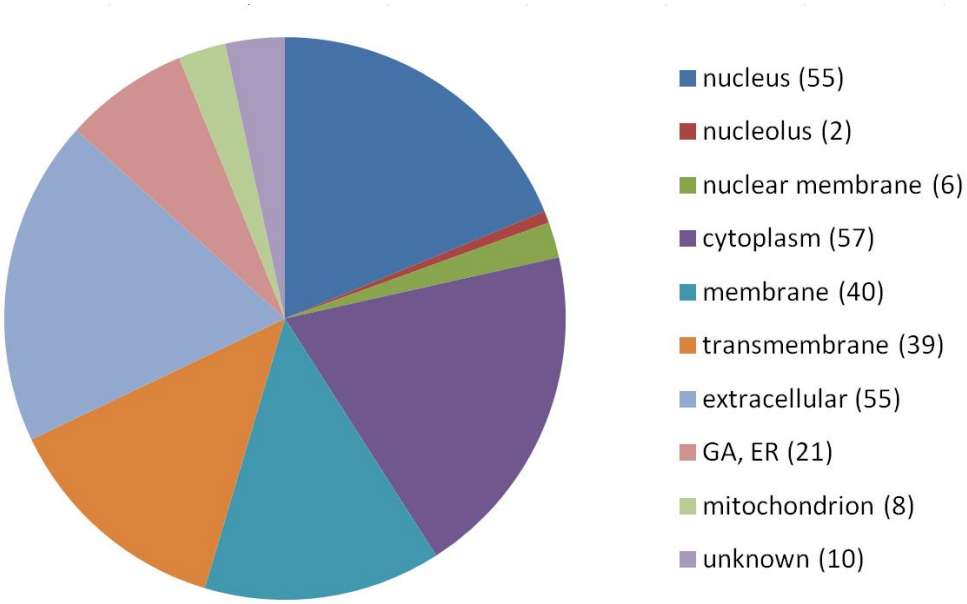
nucleus (55)
nucleolus (2)
nuclear membrane (6)
cytoplasm (57)
membrane (40)
transmembrane (39)
extracellular (55)
GA, ER (21)
mitochondrion (8)
unknown (10)

Fig. 6

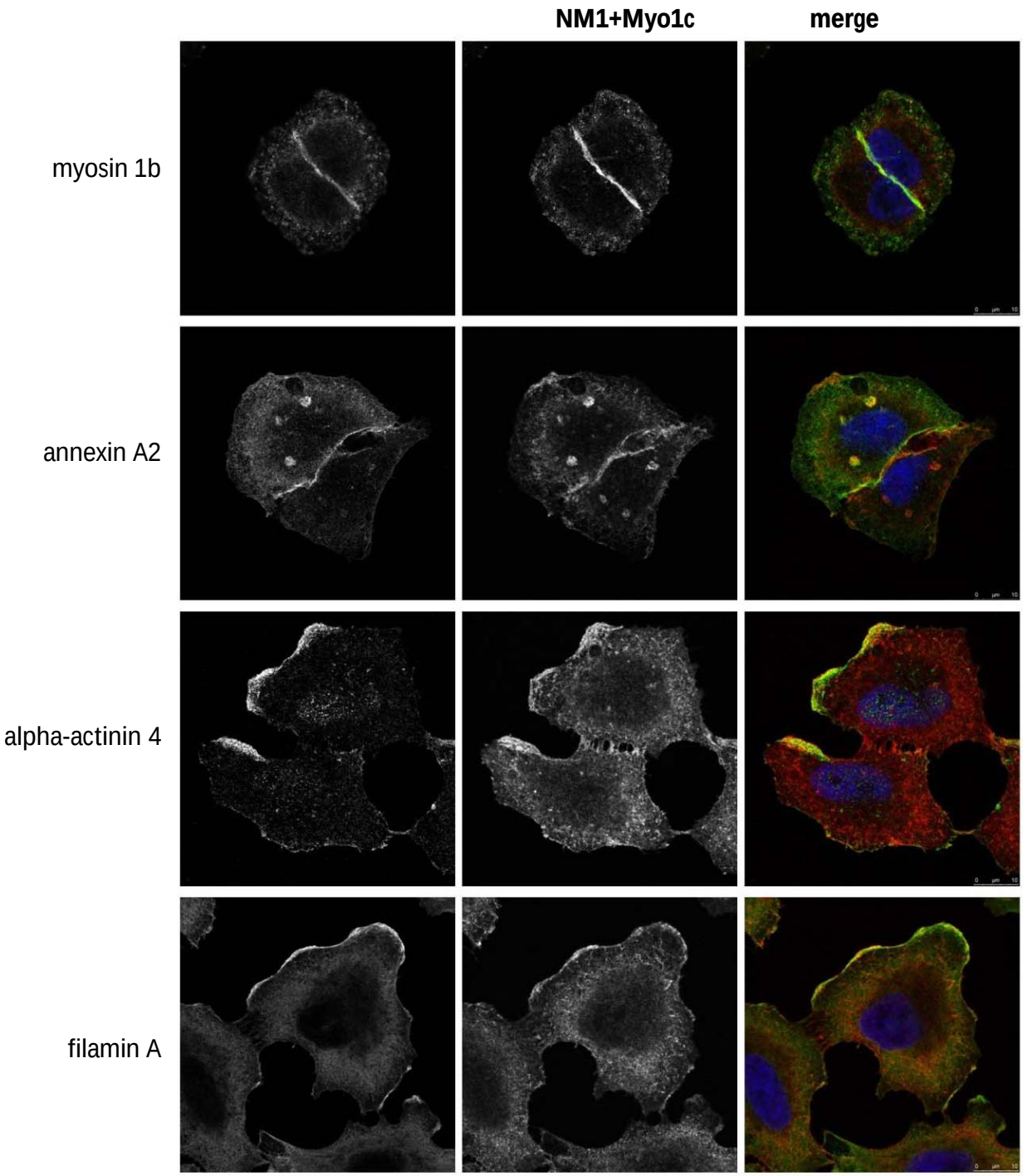
NM1+Myo1c
merge
myosin 1b
annexin A2
alpha-actinin 4
filamin A

Table 1

	Gene symbol	Gene name	Fold change	Tissue	Localization of gene product in cell
Adhesion	Adam22	a disintegrin and metallopeptidase domain 22	2,0	cells	transmembrane
	Agt	angiotensinogen (serpin peptidase inhibitor, clade A, member 8)	-2,3	cells	cytoplasmic, extracellular
	Cdh11	cadherin 11	-2,5	heart	integral to membrane
	Cd24a	CD24a antigen	-3,2	heart	integral to membrane
	Cd34	CD34 antigen	-2,8	cells	integral to membrane, membrane, perinuclear region, cell surface
	Col1a2	collagen, type I, alpha 2	-2,0	heart	ECM, lumen of ER
	Col18a1	collagen, type XVIII, alpha 1	-2,0	heart	ECM
	Entpd1	ectonucleoside triphosphate diphosphohydrolase 1	-2,0	heart	transmembrane
	Itga8	integrin alpha 8	-2,0	lungs	transmembrane
	L1cam	L1 cell adhesion molecule	-2,4	cells	transmembrane
	Ndel1	nuclear distribution gene E-like homolog 1 (A. nidulans)	-2,3	lungs	cytosol, nuclear envelope, centrosome
	Plekha7	pleckstrin homology domain containing, family A member 7	-3,8	heart	cytoplasm, nucleus, cell
	Vcam1	vascular cell adhesion molecule 1	-2,2	heart	transmembrane
	Vasn	vasorin	-2,4	heart	transmembrane,
	Vit	vitrin	-3,4	heart	ECM
	Cd44	CD44 antigen	-2,1	heart	integral to membrane, cell surface
Ion channels	Calhm2	calcium homeostasis modulator 2	-2,2	heart	transmembrane
	Cacna1h	calcium channel, voltage-dependent, T type, alpha 1H subunit	-2,6	heart	transmembrane
	Fxyd6	FXYD domain-containing ion transport regulator 6	2,7	cells	transmembrane
	Chrna7	cholinergic receptor, nicotinic, alpha polypeptide 7	3,5	cells	transmembrane, cell junction
	Kcnk1	potassium channel, subfamily K, member 1	-2,0	lungs	transmembrane
	Kcnj3	potassium inwardly-rectifying channel, subfamily J, member 3	-2,2	heart	transmembrane
	Kcnab1	potassium voltage-gated channel, shaker-related subfamily, beta member 1	2,1	cells	transmembrane
	Kcna1	potassium voltage-gated channel, shaker-related subfamily, member 1	-2,9	heart	transmembrane
	Slc1a6	solute carrier family 1 (high affinity aspartate/glutamate transporter), member	2,3	cells	transmembrane, GA
	Slc38a1	solute carrier family 38, member 1	-2,1	heart	transmembrane
	Slc6a17	solute carrier family 6 (neurotransmitter transporter), member 17	2,7	cells	transmembrane, cell junction
	Slc4a1	solute carrier family 4 (anion exchanger), member 1	-2,4	heart	transmembrane
Cytoskelet	Dmd	dystrophin, muscular dystrophy	2,8	cells	membrane, cytoplasm
	Fblim1	filamin binding LIM protein 1	-2,1	lungs	cytoplasm, cell junction, focal adhesion
	LOC100044570	formin 2 /// similar to formin-2	2,6	cells	cytoplasm
	Gan	giant axonal neuropathy	-2,1	heart	cytoplasm
	Pdlim3	PDZ and LIM domain 3	-2,0	heart	cytoplasm
	Sept4	septin 4	-2,7	cells	cytoplasm

Table 2

A

cell line:	A549		Lungs	Lungs	Hela
detergent/ antibody:	Triton X-100/M	Triton X-100/P	Triton X-100/M	Triton X-100/P	Digitonin/P
	filamin A	α-actinin 4	filamin A	β-actin	PTPRF interacting protein 1
	STAT 1	annexin A2	hnRNP A/B	gamma-tubulin complex component 3 and 2	kinesin 5B
	β-actin	β-actin	β-actin		CTNND1
	calmodulin	calmodulin			U2 small nuclear RNA auxiliary splicing factor
					tRNA splicing endonuclease Sen34

B

cell line:	A549	H1299	HUVEC	A549
detergent:	Triton X-100	Triton X-100	Triton X-100	Tween 20
	spectrin	HSC70	myosin heavy chain 9	gelsolin
	myosin heavy chain 9	β-actin	α-actinin 4	importinβ
	filamin A	calmodulin	β-actin	SLC3A2
	α-actinin 4		calmodulin	protein kinase C alpha
	myosin 1B			EIF4B
	β-actin			HSC70
	calmodulin			GNB2L1 (RACK1)
				β-actin
				γ-actin
				calmodulin

6. Discussion

6.1 Nuclear localization signal of NM1

Nuclear myosin I was described as a nuclear isoform of the well-known “cytoplasmic” myosin 1c protein resulting from an alternative start of transcription of the *MYO1C* gene adding extra 16 amino acids at the N-terminus. Because this is the only difference, the 16 amino-acid N-terminal extension of NM1 protein was thought to be the nuclear localization signal for NM1 (Pestic-Dragovich et al. 2000), but solid data supporting this hypothesis were missing. We therefore prepared different deletion mutants of NM1 fused with GFP thus showing that the nuclear localization signal which directs NM1 to the nucleus is located in the middle part of the molecule within the calmodulin-binding motif of NM1. Moreover, we identified importin beta, importin 5 and importin 7 as nuclear transport receptors that bind NM1; and calmodulin as a negative regulator of nuclear import. This novel calmodulin-dependent NLS is localized in the second of the three IQ domains, and is identical for both isoforms. Therefore, both NM1 and Myo1c translocate into the nucleus. This is in contrary to previous results suggesting a specific cellular compartmentalization of these isoforms. This presumption was based on immunofluorescence detection with antibodies prepared against the N-terminal extension of NM1 which strongly stained the nucleus in comparison to C-terminal antibodies staining both isoforms on plasma membrane (Fomproix and Percipalle 2004). However, by using skin fibroblasts derived from NM1 wild type and knock-out mice, we showed that these antibodies against the N-terminal extension of NM1 give nuclear staining even in NM1 KO cells. This means that these NM1 specific antibodies used previously, cross-reacted with other nuclear protein that was different from NM1. Finally, we confirmed the presence of both isoforms in the nucleus by transfection of tagged NM1 and Myo1c constructs into cultured cells, and also by showing the presence of endogenous Myo1c in purified nuclei of cells derived from NM1 knock-out mice.

6.2 Lipids in the cell nucleus

There has been strong evidence about different lipids in the cell nucleus. However, even after the removal of nuclear envelope by detergents, some portion of these lipids was still present in the nucleus, suggesting their interaction with unknown protein complexes with hydrophobic pockets. PIP_2 is typically localized to the plasma membrane but is also prominent nuclear lipid species. However, in the nucleus no such PIP_2 positive membranous structures can be seen. Because NM1 is known to have the same PH domain as Myo1c, we wanted to know whether NM1 could bind PIP_2 in the cell nucleus. Pull-downs and mobility assays showed that NM1 not only forms a complex with PIP_2 but also that this binding is

antagonistic to PLCδ1 enzyme binding to PIP_2 in the nucleus (Yildirim et al., unpublished data).

Because NM1 has been shown to function in Pol I transcription, we were further interested if PIP_2 also contributes to this process. We found that PIP2 is present on the active ribosomal promoter during transcription and makes a complex with Pol I and with Pol I transcription factor UBF in the nucleolus. Depletion of PIP_2 by PLCδ1 enzyme reduces Pol I transcription. Moreover, PIP_2 colocalizes with nascent transcripts in the nucleolus and binds directly to the pre-rRNA processing factor fibrillarin (Fib). PIP_2 bound UBF and Fib undergo conformational changes that alter their binding to DNA and RNA, respectively. These findings suggest a model in which PIP_2 modulates UBF binding to rDNA, while upon active transcription Fib binds to PIP_2 and associates with nascent rRNA to enforce methylation for further rRNA processing. Taken together, PIP_2 may act as a bridge connecting transcription initiation and early mRNA maturation steps through binding to Po I, UBF and Fib.

6.3 NM1 KO phenotypes

To answer the questions about tissue specific functions of NM1 protein, we prepared mice lacking NM1 isoform without affecting Myo1c expression. Because of high expression of NM1 in different tissues and described function in transcription, chromatin remodeling and chromosomal movements, we expected several severe effects of NM1 KO. Surprisingly, knock-out mice were fully viable and did not show any obvious defects related to previously described functions. One of the possible explanations was that the loss of NM1 protein was compensated by some other protein. We previously showed that Myo1c isoform, which slightly differs from NM1, is also able to enter the nucleus and therefore could be one of the major candidates for replacing NM1 functions in RNA Pol I transcription. Moreover, the ratio between both isoforms in the cell nucleus and in the cytoplasm is nearly equal. We therefore tested ability of Myo1c to function in transcription. We found that Myo1c is able to functionally substitute NM1 in Pol I transcription, and that the deletion of NM1 does not cause any compensatory overexpression of Myo1c. Moreover, Myo1c directly binds to the Pol II CTD domain suggesting a role also in Pol II transcription. In conclusion, we suggest that the two isoforms Myo1c and NM1 (isoforms C and B) are redundant and interchangeable in the general process of transcription. However, as mentioned above, in humans the third Myo1c isoform - isoform A - carrying a different and longer N-terminal extension, has slightly different cytoplasmic and nuclear localization in comparison to NM1 (Ihnatovych et al. 2012). We also noted previously that the localization pattern of exogenously expressed NM1 and Myo1c do not fully overlap (Dzijak et al. 2012). This could suggest different roles for each isoform, dependent on their N-terminal extensions, but most probably without affecting the

general process of transcription by Pol I or Pol II. Because we did not detect changes in Pol I transcription in NM1 KO cells, it is possible that different N-terminal extensions have role in the fine tuning of myosin functions under special conditions or in specialized cell types.

Our studies of NM1 function at the tissue and organism level did not show any obvious deviations in comparison to WT mice. However, we discovered minor differences in bone mineral density of KO mice, and several genes related to lipid metabolism in adipocytes to have changed expression profiles (data not shown). This could relate bone metabolism, insulin signaling and energy metabolism as was suggested previously (Ferron et al. 2010; Fulzele et al. 2010), but NM1 has been never reported in these processes. Obviously, additional studies are needed in this direction.

As a part of physiological examination we also performed hemotogy analysis, that revealed a mild hyperchromic macrocytosis of red blood cells in mutant males characterized by larger red blood cells containing a higher amount of hemoglobin. This phenotype suggests impaired cell division during erythropoiesis (Aslinia et al. 2006). Another possible explanation is that the red blood cells in NM1 knock-out mice have a partially impaired linkage between the plasma membrane and the cytoskeleton, resulting in increased mean corpuscular volume. This is in agreement with previous data on others members of Myosin I family, which have been shown to act as a dynamic link between plasma membrane and cytoskeleton (Nambiar et al. 2009). In particular, class I myosins mediate membrane/cytoskeleton adhesion and thus make a major contribution to membrane tension. The study showed that class I myosins directly control the mechanical properties of the cell membrane and are master regulators of cellular events involving membrane deformation.

6.4 NM1 in the cytoplasm

We described previously that “cytoplasmic” Myo1c can translocate to the nucleus by the same mechanism as NM1, but NM1 functions in the cytoplasm have never been studied before. However, the thorough phenotyping of NM1 KO mice revealed phenotypes in bone mineral density and red blood cells parameters, which are most probably related to cytoplasmic, rather than nuclear processes. NM1 antibodies with predominant nuclear staining which were used previously were shown to be unspecific. Since we lacked the good quality antibodies to NM1, we generated a polyclonal antibody against the N-terminal peptide (AA 1-16) that was affinity purified. Surprisingly, at a steady state, the localization of NM1 visualized by our newly generated antibody was almost exclusively cytoplasmic. This was further proved by biochemical fractionation of cell compartments, which confirmed that in interphase cells the distribution of NM1 was more cytoplasmic than nuclear (80% cytoplasm/20% nucleus). Microarray data from lungs, heart and skin fibroblast revealed 222 genes whose expression was changed more than twice in NM1 knock-out mice. Surprisingly,

only 23 % of the gene products affected by NM1 depletion are nuclear and as much as 60 % are cytosolic, membrane or transmembrane proteins. In agreement with these results, co-immunoprecipitation experiments revealed several NM1 interacting partners on plasma membrane which were further proved by immuno-fluorescence microscopy. This data links NM1 with other myosin I family members which were shown to work as a dynamic link between plasma membrane and cytoskeleton (Nambiar et al. 2009). To test whether NM1 KO has some direct effect on plasma membrane tension, we measured the capability of NM1 WT and KO cells to survive rapid cell swelling caused by hypotonic stress. NM1 KO cells were more resistant to hypotonic stress in comparison to wild type cells. To verify this, the observed phenotype was reverted by exogenous expression of NM1 protein in KO cells. Moreover, wild type cells with overexpression of exogenous NM1 showed increased sensitivity to hypotonic stress. We therefore suggest that NM1, as well as other myosin I family members, functions as a dynamic link between plasma membrane and cytoskeleton. In KO cells, the overall number of myosin molecules on plasma membrane is reduced and the cells are more accessible for cell swelling. In contrary, cells with exogenous over-expression of NM1 have overall higher levels of myosin I molecules in cytoplasm and therefore the link between membrane and cytoskeleton would be more rigid and more sensitive to cell swelling. However, when measuring cell movement, cell size, spreading and adhesion to substrate, no differences between NM1 wild type and knock-out cells were observed. We therefore suggest that in steady state, the overall number of myosin I molecules in the cytoplasm is sufficient for normal proceeding in NM1 knock-out cells. However after the exposure to strong stress conditions, differences in mechanical properties of the cells can be seen. Since NM1 deletion seems to enhance survival in hypotonic conditions, there is also a possibility that NM1 is a negative regulator of regulatory volume decrease, which is the mechanism by which cell tend to balance perturbations in its volume. However, the pathways triggered after cell swelling are quite complex and variable including various ion channels, aquaporins, cell-adhesion molecules, cytoskeletal proteins, growth factor receptors, molecules remodelling membranes and GTP-binding proteins, and therefore NM1 function in these processes will have to be further studied.

7. Summary and conclusions

Nuclear myosin I was the first myosin described in the cell nucleus. Its 16 amino-acid extension was thought to be nuclear localization signal, and as a nuclear protein it was thought to work in Pol I and Pol II transcription. We aimed to extend our knowledge of the properties of NM1 and its functions in nuclear metabolism. Surprisingly, we found that NM1 and Myo1c are located to same cellular compartments and are redundant or overlapping in some functions as Pol I transcription.

Our findings presented in this work can be summarized as follows:

1. Nuclear localization signal directing NM1 to the cell nucleus is localized in the neck part of the myosin molecule. By using GFP-fused constructs, we have shown that the second IQ domain known to bind calmodulin is responsible for nuclear translocation of NM1. Because the domain is localized to the neck region, it has the capacity to direct all myosin1c isoforms to the nucleus. This was further proved by the presence of endogenous Myo1c in purified nuclei of NM1 knock-out mice.

2. NM1 knock-out mice are viable and fertile. NM1 KO mice did not show any defects related to previously described nuclear functions of NM1. Mutant and control animals did not differ in the number of offspring and breeding of heterozygous animals does not deviate from Mendelian laws. Detailed phenotyping however revealed minor changes in bone mineral density and mild hyperchromic macrocytosis in KO mice, but the mechanism is still unknown.

3. Myosin isoforms in the cell nucleus are redundant in the process of Pol I transcription. We have shown that the “cytoplasmic” Myo1c is able to function in transcription in the same manner as NM1. In addition, Myo1c binds to Pol II CTD domain suggesting its role also in Pol II transcription. Moreover, we found that the ratio between both isoforms is similar in the nucleus, and that the knock-out of NM1 does not lead to any compensatory over-expression of Myo1c, suggesting that their roles in transcription are overlapping and/or redundant.

4. PIP_2 is a new key player in the process of Pol I transcription. We found that PIP_2 is present on the active ribosomal promoter during transcription, makes a complex with Pol I and Pol I transcription factor UBF in the nucleolus and depletion of PIP_2 reduces Pol I transcription *in vitro*. In addition, PIP_2 also binds directly to the pre-rRNA processing factor, fibrillarin (Fib), and colocalizes with nascent transcripts in the nucleolus. PIP_2 binding to UBF

and Fib causes conformational changes in these proteins, which alter their binding to DNA and RNA, respectively. Taken together, PIP2 mediates the formation of pre-initiation complex via binding to UBF and Pol I, and acts as a structural platform linking pre-rRNA production and early processing.

5. NM1 contributes to both, cytoplasm and plasma membrane biological processes. Biochemical fractionation of cell compartments revealed that the distribution of NM1 is more cytoplasmic than nuclear (80% cytoplasm, 20% nuclear). In agreement with this, microarray analysis of NM1 KO cells and co-immunoprecipitation experiments showed several cytoplasmic proteins interacting with NM1. Finally, results from rapid cell swelling experiments on NM1 WT and KO skin fibroblasts suggest that NM1 contributes to the plasma membrane tension by linking cell membrane to the cytoskeleton.

8. Prospects

Our results opened some new area in the research of nuclear myosins and phospholipids. Based on these, we plan to address the following questions in a near future:

1. What is the functional difference between NM1 and Myo1c? What are the functions of both proteins in the cell nucleus and the cytoplasm?

We have shown that Myo1c and NM1 contribute to similar processes and knocking-out NM1 does not cause any special strong phenotype. Therefore, we are preparing double knock-out mice which should enable us to study all the different funtions to which both isoforms contribute together. We have found several genes with a changed expression in NM1 KO mice suggesting additional possible roles of NM1 which we will study further. Unfortunately, because of the same DNA sequence of Myo1c and NM1 we cannot prepare single KO of Myo1c to check the expression profile of these mice. Therefore we decided to use Multi Gateway System to prepare double knock-out mice with inducible expression of each isoform in human Nalm-6 cell line. This system will allow us to selectively express each isoform in KO background and to check for differences in expression profiles of these cells. This should help to uncover even minor differences between functioning of both isoforms.

2. How are different lipids distributed in the cell nucleus? What are their binding partners and to which processes do they contribute to?

Although PIP_2 is one of the best described lipids in the cell nucleus, the function and the distribution of other lipids in the nucleus is almost unknown. Determination of lipid localization should be the first step in understanding their functions in the nucleus. Therefore, we prepared different GST-fused lipid binding domains which will be used to visualize the phospholipids by confocal, super-resolution and electron microscopy. We will then use these domains to perform pull down and co-immunoprecipitation experiments to identify the binding partners of phospholipids in the nucleus. To study the contribution of different phospholipids on the nucleoplasm structure, we will use over-expression and down regulation of various phospholipids-affecting enzymes as kinases, lipases and phosphatases and study their impact on nuclear structures and functions.

9. References

Adams RJ, Pollard TD (1989) Binding of myosin I to membrane lipids. Nature 340 (6234):565-568. doi:10.1038/340565a0

Ambrosino C, Tarallo R, Bamundo A, Cuomo D, Franci G, Nassa G, Paris O, Ravo M, Giovane A, Zambrano N, Lepikhova T, Janne OA, Baumann M, Nyman TA, Cicatiello L, Weisz A (2010) Identification of a hormone-regulated dynamic nuclear actin network associated with estrogen receptor alpha in human breast cancer cell nuclei. Molecular & cellular proteomics : MCP 9 (6):1352-1367. doi:10.1074/mcp.M900519-MCP200

Arif E, Wagner MC, Johnstone DB, Wong HN, George B, Pruthi PA, Lazzara MJ, Nihalani D (2011) Motor protein Myo1c is a podocyte protein that facilitates the transport of slit diaphragm protein Neph1 to the podocyte membrane. Molecular and cellular biology 31 (10):2134-2150. doi:10.1128/MCB.05051-11

Aslinia F, Mazza JJ, Yale SH (2006) Megaloblastic anemia and other causes of macrocytosis. Clinical medicine & research 4 (3):236-241

Barylko B, Jung G, Albanesi JP (2005) Structure, function, and regulation of myosin 1C. Acta biochimica Polonica 52 (2):373-380

Boronenkov IV, Loijens JC, Umeda M, Anderson RA (1998) Phosphoinositide signaling pathways in nuclei are associated with nuclear speckles containing pre-mRNA processing factors. Molecular biology of the cell 9 (12):3547-3560

Bose A, Guilherme A, Robida SI, Nicoloro SM, Zhou QL, Jiang ZY, Pomerleau DP, Czech MP (2002) Glucose transporter recycling in response to insulin is facilitated by myosin Myo1c. Nature 420 (6917):821-824. doi:10.1038/nature01246

Bose A, Robida S, Furcinitti PS, Chawla A, Fogarty K, Corvera S, Czech MP (2004) Unconventional myosin Myo1c promotes membrane fusion in a regulated exocytic pathway. Molecular and cellular biology 24 (12):5447-5458. doi:10.1128/MCB.24.12.5447-5458.2004

Bunce MW, Bergendahl K, Anderson RA (2006) Nuclear PI(4,5)P(2): a new place for an old signal. Biochimica et biophysica acta 1761 (5-6):560-569. doi:10.1016/j.bbalip.2006.03.002

Cocco L, Gilmour RS, Ognibene A, Letcher AJ, Manzoli FA, Irvine RF (1987) Synthesis of polyphosphoinositides in nuclei of Friend cells. Evidence for polyphosphoinositide metabolism inside the nucleus which changes with cell differentiation. The Biochemical journal 248 (3):765-770

Cullen PJ, Cozier GE, Banting G, Mellor H (2001) Modular phosphoinositide-binding domains--their role in signalling and membrane trafficking. Current biology : CB 11 (21):R882-893

Di Paolo G, De Camilli P (2006) Phosphoinositides in cell regulation and membrane dynamics. Nature 443 (7112):651-657. doi:10.1038/nature05185

Diefenbach TJ, Latham VM, Yimlamai D, Liu CA, Herman IM, Jay DG (2002) Myosin 1c and myosin IIB serve opposing roles in lamellipodial dynamics of the neuronal growth cone. The Journal of cell biology 158 (7):1207-1217

Divecha N, Banfic H, Irvine RF (1991) The polyphosphoinositide cycle exists in the nuclei of Swiss 3T3 cells under the control of a receptor (for IGF-I) in the plasma membrane, and stimulation of the cycle increases nuclear diacylglycerol and apparently induces translocation of protein kinase C to the nucleus. The EMBO journal 10 (11):3207-3214

Doughman RL, Firestone AJ, Anderson RA (2003) Phosphatidylinositol phosphate kinases put PI4,5P(2) in its place. The Journal of membrane biology 194 (2):77-89. doi:10.1007/s00232-003-2027-7

Dzijak R, Yildirim S, Kahle M, Novak P, Hnilicova J, Venit T, Hozak P (2012) Specific nuclear localizing sequence directs two myosin isoforms to the cell nucleus in calmodulin-sensitive manner. PloS one 7 (1):e30529. doi:10.1371/journal.pone.0030529

Ferron M, Wei J, Yoshizawa T, Del Fattore A, DePinho RA, Teti A, Ducy P, Karsenty G (2010) Insulin signaling in osteoblasts integrates bone remodeling and energy metabolism. Cell 142 (2):296-308. doi:10.1016/j.cell.2010.06.003

Fomproix N, Percipalle P (2004) An actin-myosin complex on actively transcribing genes. Experimental cell research 294 (1):140-148. doi:10.1016/j.yexcr.2003.10.028

Foth BJ, Goedecke MC, Soldati D (2006) New insights into myosin evolution and classification. Proceedings of the National Academy of Sciences of the United States of America 103 (10):3681-3686. doi:10.1073/pnas.0506307103

Fukami K, Furuhashi K, Inagaki M, Endo T, Hatano S, Takenawa T (1992) Requirement of phosphatidylinositol 4,5-bisphosphate for alpha-actinin function. Nature 359 (6391):150-152. doi:10.1038/359150a0

Fulzele K, Riddle RC, DiGirolamo DJ, Cao X, Wan C, Chen D, Faugere MC, Aja S, Hussain MA, Bruning JC, Clemens TL (2010) Insulin receptor signaling in osteoblasts regulates postnatal bone acquisition and body composition. Cell 142 (2):309-319. doi:10.1016/j.cell.2010.06.002

Gillespie PG, Albanesi JP, Bahler M, Bement WM, Berg JS, Burgess DR, Burnside B, Cheney RE, Corey DP, Coudrier E, de Lanerolle P, Hammer JA, Hasson T, Holt JR, Hudspeth AJ, Ikebe M, Kendrick-Jones J, Korn ED, Li R, Mercer JA, Milligan RA, Mooseker MS, Ostap EM, Petit C, Pollard TD, Sellers JR, Soldati T, Titus MA (2001) Myosin-I nomenclature. The Journal of cell biology 155 (5):703-704. doi:10.1083/jcb.200110032

Gillespie PG, Cyr JL (2004) Myosin-1c, the hair cell's adaptation motor. Annual review of physiology 66:521-545. doi:10.1146/annurev.physiol.66.032102.112842

Grummt I (2006) Actin and myosin as transcription factors. Current opinion in genetics & development 16 (2):191-196. doi:10.1016/j.gde.2006.02.001

Harlan JE, Hajduk PJ, Yoon HS, Fesik SW (1994) Pleckstrin homology domains bind to phosphatidylinositol-4,5-bisphosphate. Nature 371 (6493):168-170. doi:10.1038/371168a0

Hartman MA, Spudich JA (2012) The myosin superfamily at a glance. Journal of cell science 125 (Pt 7):1627-1632. doi:10.1242/jcs.094300

Hirai H, Natori S, Sekimizu K (1992) Reversal by phosphatidylglycerol and cardiolipin of inhibition of transcription and replication by histones in vitro. Archives of biochemistry and biophysics 298 (2):458-463

Hoepfner D, van den Berg M, Philippsen P, Tabak HF, Hettema EH (2001) A role for Vps1p, actin, and the Myo2p motor in peroxisome abundance and inheritance in Saccharomyces cerevisiae. The Journal of cell biology 155 (6):979-990. doi:10.1083/jcb.200107028

Hofmann WA, Johnson T, Klapczynski M, Fan JL, de Lanerolle P (2006) From transcription to transport: emerging roles for nuclear myosin I. Biochemistry and cell biology = Biochimie et biologie cellulaire 84 (4):418-426. doi:10.1139/o06-069

Hokanson DE, Laakso JM, Lin T, Sept D, Ostap EM (2006) Myo1c binds phosphoinositides through a putative pleckstrin homology domain. Molecular biology of the cell 17 (11):4856-4865. doi:10.1091/mbc.E06-05-0449

Hokanson DE, Ostap EM (2006) Myo1c binds tightly and specifically to phosphatidylinositol 4,5-bisphosphate and inositol 1,4,5-trisphosphate. Proceedings of the National Academy of Sciences of the United States of America 103 (9):3118-3123. doi:10.1073/pnas.0505685103

Holmes KC, Geeves MA (2000) The structural basis of muscle contraction. Philosophical transactions of the Royal Society of London Series B, Biological sciences 355 (1396):419-431. doi:10.1098/rstb.2000.0583

Holt JR, Gillespie SK, Provance DW, Shah K, Shokat KM, Corey DP, Mercer JA, Gillespie PG (2002) A chemical-genetic strategy implicates myosin-1c in adaptation by hair cells. Cell 108 (3):371-381

Huang FL, Huang KP (1991) Interaction of protein kinase C isozymes with phosphatidylinositol 4,5-bisphosphate. The Journal of biological chemistry 266 (14):8727-8733

Cheney RE, Mooseker MS (1992) Unconventional myosins. Current opinion in cell biology 4 (1):27-35

Cheng MK, Shearn A (2004) The direct interaction between ASH2, a Drosophila trithorax group protein, and SKTL, a nuclear phosphatidylinositol 4-phosphate 5-kinase, implies a role for phosphatidylinositol 4,5-bisphosphate in maintaining transcriptionally active chromatin. Genetics 167 (3):1213-1223. doi:10.1534/genetics.103.018721

Ihnatovych I, Migocka-Patrzalek M, Dukh M, Hofmann WA (2012) Identification and characterization of a novel myosin Ic isoform that localizes to the nucleus. Cytoskeleton 69 (8):555-565. doi:10.1002/cm.21040

Janmey PA, Stossel TP (1987) Modulation of gelsolin function by phosphatidylinositol 4,5-bisphosphate. Nature 325 (6102):362-364. doi:10.1038/325362a0

Kahle M, Pridalova J, Spacek M, Dzijak R, Hozak P (2007) Nuclear myosin is ubiquitously expressed and evolutionary conserved in vertebrates. Histochemistry and cell biology 127 (2):139-148. doi:10.1007/s00418-006-0231-0

Liscovitch M, Chalifa V, Pertile P, Chen CS, Cantley LC (1994) Novel function of phosphatidylinositol 4,5-bisphosphate as a cofactor for brain membrane phospholipase D. The Journal of biological chemistry 269 (34):21403-21406

Martelli AM, Follo MY, Evangelisti C, Fala F, Fiume R, Billi AM, Cocco L (2005) Nuclear inositol lipid metabolism: more than just second messenger generation? Journal of cellular biochemistry 96 (2):285-292. doi:10.1002/jcb.20527

Mellman DL, Gonzales ML, Song C, Barlow CA, Wang P, Kendziorski C, Anderson RA (2008) A PtdIns4,5P2-regulated nuclear poly(A) polymerase controls expression of select mRNAs. Nature 451 (7181):1013-1017. doi:10.1038/nature06666

Nambiar R, McConnell RE, Tyska MJ (2009) Control of cell membrane tension by myosin-I. Proceedings of the National Academy of Sciences of the United States of America 106 (29):11972-11977. doi:10.1073/pnas.0901641106

Nowak G, Pestic-Dragovich L, Hozak P, Philimonenko A, Simerly C, Schatten G, de Lanerolle P (1997) Evidence for the presence of myosin I in the nucleus. The Journal of biological chemistry 272 (27):17176-17181

Obrdlik A, Louvet E, Kukalev A, Naschekin D, Kiseleva E, Fahrenkrog B, Percipalle P (2010) Nuclear myosin 1 is in complex with mature rRNA transcripts and associates with the nuclear pore basket. FASEB journal : official publication of the Federation of American Societies for Experimental Biology 24 (1):146-157. doi:10.1096/fj.09-135863

Osborne SL, Thomas CL, Gschmeissner S, Schiavo G (2001) Nuclear PtdIns(4,5)P2 assembles in a mitotically regulated particle involved in pre-mRNA splicing. Journal of cell science 114 (Pt 13):2501-2511

Percipalle P, Fomproix N, Cavellan E, Voit R, Reimer G, Kruger T, Thyberg J, Scheer U, Grummt I, Farrants AK (2006) The chromatin remodelling complex WSTF-SNF2h interacts with nuclear myosin 1 and has a role in RNA polymerase I transcription. EMBO reports 7 (5):525-530. doi:10.1038/sj.embor.7400657

Pestic-Dragovich L, Stojiljkovic L, Philimonenko AA, Nowak G, Ke Y, Settlage RE, Shabanowitz J, Hunt DF, Hozak P, de Lanerolle P (2000) A myosin I isoform in the nucleus. Science 290 (5490):337-341

Philimonenko VV, Zhao J, Iben S, Dingova H, Kysela K, Kahle M, Zentgraf H, Hofmann WA, de Lanerolle P, Hozak P, Grummt I (2004) Nuclear actin and myosin I are required for RNA polymerase I transcription. Nature cell biology 6 (12):1165-1172. doi:10.1038/ncb1190

Pollard TD, Korn ED (1973) Acanthamoeba myosin. I. Isolation from Acanthamoeba castellanii of an enzyme similar to muscle myosin. The Journal of biological chemistry 248 (13):4682-4690

Randazzo PA, Kahn RA (1994) GTP hydrolysis by ADP-ribosylation factor is dependent on both an ADP-ribosylation factor GTPase-activating protein and acid phospholipids. The Journal of biological chemistry 269 (14):10758-10763

Rando OJ, Zhao K, Janmey P, Crabtree GR (2002) Phosphatidylinositol-dependent actin filament binding by the SWI/SNF-like BAF chromatin remodeling complex. Proceedings of the National

Academy of Sciences of the United States of America 99 (5):2824-2829. doi:10.1073/pnas.032662899

Reizes O, Barylko B, Li C, Sudhof TC, Albanesi JP (1994) Domain structure of a mammalian myosin I beta. Proceedings of the National Academy of Sciences of the United States of America 91 (14):6349-6353

Sellers JR (2000) Myosins: a diverse superfamily. Biochimica et biophysica acta 1496 (1):3-22

Smith CD, Wells WW (1983) Phosphorylation of rat liver nuclear envelopes. II. Characterization of in vitro lipid phosphorylation. The Journal of biological chemistry 258 (15):9368-9373

Sokac AM, Schietroma C, Gundersen CB, Bement WM (2006) Myosin-1c couples assembling actin to membranes to drive compensatory endocytosis. Developmental cell 11 (5):629-640. doi:10.1016/j.devcel.2006.09.002

Stauffer EA, Scarborough JD, Hirono M, Miller ED, Shah K, Mercer JA, Holt JR, Gillespie PG (2005) Fast adaptation in vestibular hair cells requires myosin-1c activity. Neuron 47 (4):541-553. doi:10.1016/j.neuron.2005.07.024

Syamaladevi DP, Spudich JA, Sowdhamini R (2012) Structural and functional insights on the Myosin superfamily. Bioinformatics and biology insights 6:11-21. doi:10.4137/BBI.S8451

Thompson RF, Langford GM (2002) Myosin superfamily evolutionary history. The Anatomical record 268 (3):276-289. doi:10.1002/ar.10160

Toker A (1998) The synthesis and cellular roles of phosphatidylinositol 4,5-bisphosphate. Current opinion in cell biology 10 (2):254-261

Vann LR, Wooding FB, Irvine RF, Divecha N (1997) Metabolism and possible compartmentalization of inositol lipids in isolated rat-liver nuclei. The Biochemical journal 327 (Pt 2):569-576

Wagner MC, Barylko B, Albanesi JP (1992) Tissue distribution and subcellular localization of mammalian myosin I. The Journal of cell biology 119 (1):163-170

Wang FS, Wolenski JS, Cheney RE, Mooseker MS, Jay DG (1996) Function of myosin-V in filopodial extension of neuronal growth cones. Science 273 (5275):660-663

Waterman-Storer C, Duey DY, Weber KL, Keech J, Cheney RE, Salmon ED, Bement WM (2000) Microtubules remodel actomyosin networks in Xenopus egg extracts via two mechanisms of F-actin transport. The Journal of cell biology 150 (2):361-376

Ye J, Zhao J, Hoffmann-Rohrer U, Grummt I (2008) Nuclear myosin I acts in concert with polymeric actin to drive RNA polymerase I transcription. Genes & development 22 (3):322-330. doi:10.1101/gad.455908

Yonezawa N, Homma Y, Yahara I, Sakai H, Nishida E (1991) A short sequence responsible for both phosphoinositide binding and actin binding activities of cofilin. The Journal of biological chemistry 266 (26):17218-17221

Yoshida S, Tamiya-Koizumi K, Kojima K (1989) Interaction of DNA polymerases with phospholipids. Biochimica et biophysica acta 1007 (1):61-66

Yu H, Fukami K, Watanabe Y, Ozaki C, Takenawa T (1998) Phosphatidylinositol 4,5-bisphosphate reverses the inhibition of RNA transcription caused by histone H1. European journal of biochemistry / FEBS 251 (1-2):281-287

Zadro C, Alemanno MS, Bellacchio E, Ficarella R, Donaudy F, Melchionda S, Zelante L, Rabionet R, Hilgert N, Estivill X, Van Camp G, Gasparini P, Carella M (2009) Are MYO1C and MYO1F associated with hearing loss? Biochimica et biophysica acta 1792 (1):27-32. doi:10.1016/j.bbadis.2008.10.017

Zhao K, Wang W, Rando OJ, Xue Y, Swiderek K, Kuo A, Crabtree GR (1998) Rapid and phosphoinositol-dependent binding of the SWI/SNF-like BAF complex to chromatin after T lymphocyte receptor signaling. Cell 95 (5):625-636

Zhou MM, Ravichandran KS, Olejniczak EF, Petros AM, Meadows RP, Sattler M, Harlan JE, Wade WS, Burakoff SJ, Fesik SW (1995) Structure and ligand recognition of the phosphotyrosine binding domain of Shc. Nature 378 (6557):584-592. doi:10.1038/378584a0